

# Rozprawa doktorska



Uniwersytet Rolniczy im. Hugona Kołłątaja w Krakowie

Wydział Leśny

**Piotr Janiec**

## **Wykorzystanie danych z lotniczego skanowania laserowego i cyfrowej fotogrametrii lotniczej do kalibracji i aktualizacji modeli wzrostu wysokości drzewostanów**

The use of airborne lasers canning and digital aerial  
photogrammetry data for the calibration and updating of stand  
height growth models

Promotor rozprawy doktorskiej

**Prof. dr hab. inż. Jarosław Socha**

Promotor pomocnicza rozprawy doktorskiej

**dr inż. Luiza Tymińska Czabańska**

Uniwersytet Rolniczy im. Hugona Kołłątaja w Krakowie

Wydział Leśny, Katedra Zarządzania Zasobami Leśnymi

Kraków, kwiecień 2025

## ***Podziękowania***

*Pragnę złożyć serdeczne podziękowania wszystkim osobom, które przyczyniły się do powstania niniejszej rozprawy doktorskiej.*

*Na szczególne wyrazy wdzięczności zasługuje mój promotor, **Prof. dr hab. inż. Jarosławowi Socha**, za nieocenione wsparcie, cenne wskazówki oraz inspirujące rozmowy, które miały kluczowe znaczenie dla rozwoju mojej pracy badawczej.*

*Dziękuję również mojej promotor pomocniczej, **dr inż. Luizie Tymińskiej Czabańskiej**, za jej zaangażowanie, merytoryczną pomoc i nieustanne wsparcie na każdym etapie realizacji rozprawy.*

*Słowa uznania i wdzięczności kieruję również do **Pracowników Katedry Zarządzania Zasobami Leśnymi**, a w szczególności do **dr inż. Pawła Hawryło**, za cenne uwagi, pomoc w analizach oraz motywację do dalszej pracy.*

*Dziękuję pracownikom **Biura Urządzania Lasu, Oddział w Krakowie**, za wsparcie merytoryczne, które miały istotne znaczenie dla realizacji badań.*

*Największe podziękowania kieruję jednak do moich najbliższych, których obecność i wsparcie były dla mnie nieocenione. Szczególnie dziękuję mojej żonie, **Natalii**, za jej cierpliwość, wyrozumiałość oraz nieustanne wsparcie w momentach zwątpienia. Bez Ciebie ta praca nie byłaby możliwa.*

*Dziękuję wszystkim, którzy w jakikolwiek sposób przyczynili się do powstania tej rozprawy.*

## **Streszczenie**

Modele wzrostu drzewostanów umożliwiają ocenę produkcyjności siedliska oraz prognozowanie zmian zachodzących w drzewostanie. W obliczu zmieniającego się klimatu monitoring wzrostu drzewostanów staje się kluczowym zadaniem w gospodarce leśnej. Niezbędne jest również opracowanie metod aktualizacji tych modeli w zmieniających się warunkach środowiskowych. Celem niniejszej rozprawy było opracowanie metod kalibracji oraz aktualizacji modeli wzrostu wysokości drzewostanów sosny zwyczajnej, wykorzystujących dane teledetekcyjne z lotniczego skanowania laserowego (ALS) i cyfrowej fotogrametrii lotniczej (DAP). Badania miały na celu wykazanie, że dane te mogą zastąpić tradycyjne metody pomiarowe, oferując wyższą dokładność oraz efektywność. Wykazano, że dane ALS pozwalają na kalibrację regionalnych modeli wzrostu z wysoką dokładnością, przewyższającą modele oparte na pomiarach naziemnych. Jednocześnie udowodniono, że dane DAP, mimo występowania systematycznych błędów pomiarowych, po odpowiedniej korekcie mogą stanowić tańszą i równie skuteczną alternatywę dla ALS. W pracy opracowano metody korekty błędów DAP, wykorzystujące dane referencyjne z ALS lub pomiarów terenowych, nawet z różnych lat, co umożliwia wykorzystanie archiwalnych zbiorów danych. Dokładność korekty zależy od liczby założonych powierzchni próbnich, a ich wymagana ilość może zostać obliczona na podstawie błędu standardowego danych DAP. Wykazano, że modele wzrostu skalibrowane na podstawie skorygowanych danych DAP charakteryzują się dokładnością porównywalną do modeli opartych na ALS. Wyniki badań mają istotne znaczenie praktyczne, oferując narzędzia do efektywnego monitorowania i prognozowania wzrostu drzewostanów, co jest kluczowe dla zrównoważonej gospodarki leśnej w warunkach zmian klimatycznych. Praca wnosi nowe podejście do wykorzystania teledetekcji w leśnictwie, wskazując na możliwość szerokiego zastosowania danych DAP oraz ALS w kalibracji i aktualizacji modeli wzrostu drzewostanów.

**Słowa kluczowe:** LiDAR, DAP, ALS, modele wzrostu drzewostanów, wskaźnik bonitacji

## **Summary**

Stands growth models enable the assessment of site productivity and the forecasting of changes occurring within the stand. In the face of a changing climate, monitoring the stands growth becomes a crucial task in forest management. It is also essential to develop methods for updating these models under evolving environmental conditions. The aim of this dissertation was to develop calibration and updating methods for height growth models of Scots pine stands, utilizing remote sensing data from airborne laser scanning (ALS) and digital aerial photogrammetry (DAP). The research aimed to demonstrate that these data can replace traditional measurement methods, offering higher accuracy and efficiency. It was shown that ALS data allow for the calibration of regional growth models with high accuracy, surpassing models based on ground measurements. At the same time, it was proven that DAP data, despite the presence of systematic measurement errors, after appropriate correction, can serve as a cheaper and equally effective alternative to ALS. The study developed methods for correcting DAP errors, utilizing reference data from ALS or field measurements, even from different years, enabling the use of archival data sets. The accuracy of the correction depends on the number of established sample plots, and their required quantity can be calculated based on the standard error of the DAP data. It was demonstrated that growth models calibrated on the basis of corrected DAP data exhibit accuracy comparable to models based on ALS. The research findings have significant practical implications, providing tools for effective monitoring and forecasting of forest stand growth, which is crucial for sustainable forest management under climate change conditions. The dissertation introduces a new approach to the use of remote sensing in forestry, indicating the potential for widespread application of DAP and ALS data in the calibration and updating of forest stand growth models.

**Slowa kluczowe:** LiDAR, DAP, ALS, stand height growth models, site index

## **Spis treści**

|           |   |           |
|-----------|---|-----------|
| <b>1.</b> | <b>Struktura pracy .....</b>                                      | <b>6</b>  |
| <b>2.</b> | <b>Wprowadzenie .....</b>   | <b>7</b>  |
| <b>3.</b> | <b>Uzasadnienie wyboru tematu badawczego.....</b>                 | <b>11</b> |
| <b>4.</b> | <b>Cel pracy .....</b>  | <b>14</b> |
| <b>5.</b> | <b>Metodyka .....</b>   | <b>15</b> |
| <b>a.</b> | <b>Obszar badań .....</b>   | <b>15</b> |
| <b>b.</b> | <b>Materiał badawczy.....</b>                                     | <b>17</b> |
| <b>c.</b> | <b>Modelowanie i walidacja zbudowanych modeli .....</b>           | <b>20</b> |
| <b>6.</b> | <b>Najważniejsze wyniki badań .....</b>                           | <b>22</b> |
| <b>7.</b> | <b>Podsumowanie wyników i wnioski .....</b>                       | <b>24</b> |
| <b>8.</b> | <b>Literatura.....</b>  | <b>25</b> |
| <b>9.</b> | <b>Prace naukowe wchodzące w skład rozprawy doktorskiej .....</b> | <b>33</b> |

## **1. Struktura pracy**

Przygotowana rozprawa doktorska ma formę spójnego tematycznie zbioru trzech prac opublikowanych w czasopismach naukowych:

### **Publikacja nr 1**

Janiec, P., Tymińska-Czabańska, L., Hawryło, P., & Socha, J. (2023). Development of regional height growth model for Scots pine using repeated airborne laser scanning data. *Frontiers in Environmental Science*, 11, 1260725. <https://doi.org/10.3389/fenvs.2023.1260725>  
(Lista MEiN **100 pkt., IF 3.3**)

### **Publikacja nr 2**

Janiec, P., Hawryło, P., Tymińska-Czabańska, L., Miszczyaszyn, J., & Socha, J. (2024). A low-cost alternative to LiDAR for site index models: applying repeated digital aerial photogrammetry data in the modelling of forest top height growth. *Forestry: An International Journal of Forest Research*, cpae047. <https://doi.org/10.1093/forestry/cpae047>  
(Lista MEiN **140 pkt., IF 3.0**)

### **Publikacja nr 3**

Janiec, P., Hawryło, P., Tymińska-Czabańska, L., Polak, M., & Socha, J. (2024). Digital aerial photogrammetry as a spatial and temporal extension of ALS in forest height growth modeling. *International Journal of Digital Earth*, 17(1), 2418879.  
<https://doi.org/10.1080/17538947.2024.2418879>  
(Lista MEiN **100 pkt., IF 3.7**)

## 2. Wprowadzenie

W ostatnich latach obserwujemy dynamiczne zmiany w ekosystemach leśnych, szczególnie w zakresie ich wzrostu oraz produkcyjności (Mensah i in., 2021; Pretzsch, 2021; Pretzsch i in., 2014). Zmiany te mają istotny wpływ na odporność lasów oraz ich zdolność do adaptacji na zmiany klimatu (Pretzsch, 2009). W obliczu zmieniających się warunków wzrostu kluczowa staje się monitorowanie charakterystyk lasu w czasie rzeczywistym lub zbliżonym do rzeczywistego (Achim i in., 2022). Równie ważna jest aktualizacja modeli wzrostu drzewostanów, która uwzględnia lokalne warunki siedliskowe i rzeczywiste wzorce rozwoju lasów. Takie modele mogą stanowić istotne narzędzie wspierające monitoring ekosystemów leśnych (Achim i in., 2022; Blanco Vaca & Lo Wong, 2023; Bontemps & Bouriaud, 2014). Postęp technologiczny, w szczególności rozwój teledetekcji, dostarcza niespotykanej dotąd ilości danych o lasach, co umożliwia tworzenie nowoczesnych modeli wzrostu, przekraczających ograniczenia wynikające z wcześniejszej niedostępności danych (Tompalski i in., 2021). W kontekście obecnych zmian środowiskowych niezwykle istotne jest połączenie tradycyjnych metod monitorowania i modelowania wzrostu lasu z wykorzystaniem danych teledetekcyjnych. Tego rodzaju zintegrowane podejście pozwala lepiej reagować na pojawiające się wyzwania i wspierać zrównoważone zarządzanie lasami.

Wysokość drzewostanu stanowi jedną z kluczowych zmiennych stosowaną w ramach monitoringu ekosystemów leśnych, jednocześnie odgrywając kluczową rolę jako zmienna wejściowa w modelowaniu wzrostu drzewostanów (António i in., 2007; Bastin i in., 2018; Bi i in., 2010; Sharma i in., 2002; Vanninen i in., 1996). Szczególne znaczenie ma wysokość górna (TH), która jest podstawową cechą drzewostanu. Dostarcza ona bezpośrednich informacji o dynamice wzrostu lasu, który ma pośredni wpływ na magazynowanie węgla w biomasie (Zhou i in., 2019). TH najczęściej definiowana jest jako średnia wysokość 100 najgrubszystch drzew na 1 ha (Sharma i in., 2002). Takie podejście ma pewne ograniczenia, ponieważ wyniki szacowania zależą od wielkości powierzchni próbnej oraz liczby drzew na powierzchni (Magnussen i in., 1999). W konsekwencji określanie TH jako 100 najgrubszystch drzew na 1 ha może znacznie zawyjaździć jej rzeczywistą wartość (Garcia & Batho, 2005). Dlatego coraz częściej nawiązuje się do definicji TH zaproponowanej przez Rennolla (1978). Według tej definicji TH definiowana jest jako średnia wysokość 100 najgrubszystch drzew na ha oszacowaną dla wszystkich niepustych podpowierzchni o wielkości 0,01 ha. Hawryło i in. (2024), zmodyfikował tą definicję tak, aby mogła być zastosowana do użycia z danymi Light

Deception and Ranging (LIDaR). Podejście to zostało zweryfikowane w badaniach dotyczących określania TH przy użyciu lotniczego skanowania laserowego (ALS) (Socha i in., 2017; Tymińska-Czabańska i in., 2021, 2022). Ostatnie badania wskazują, że wysokość drzewostanu, a w szczególności szacunki TH uzyskane z wysokiej jakości danych teledetekcyjnych, są dokładniejsze niż pomiary terenowe (Hawryło i in., 2024; Jurjević i in., 2020; Sibona i in., 2017; Wang i in., 2019), dlatego rozwijanie metod modelowania i analizy na podstawie danych z teledetekcji, zwłaszcza z ALS, staje się kluczowe dla poprawy dokładności inwentaryzacji zasobów leśnych i modelowania dynamiki drzewostanów.

Posiadając dokładne dane dotyczące TH drzewostanu jesteśmy w stanie precyzyjnie modelować jego wzrost (Socha i in., 2017; Tompalski i in., 2015). W leśnictwie wykorzystuje się różnorodne dane do modelowania wzrostu wysokości, co pozwala na oszacowanie produkcyjności danego drzewostanu, która najczęściej wyrażana jest klasą bonitacji lub wskaźnikiem bonitacji (SI) (Bravo-Oviedo i in., 2010). Tego rodzaju wskaźniki są szeroko wykorzystywane w zarządzaniu zasobami leśnymi. Najczęściej wskaźniki produkcyjności, takie jak SI, opierają się na modelowaniu wysokości drzewostanu w określonym wieku. Wskaźniki te odzwierciedlają również jakość drzewostanu, ponieważ produkcyjność, czyli możliwa do wykorzystania część potencjału wzrostowego drzewostanu, może być powiązana z jego jakością (Skovsgaard & Vanclay, 2008). W modelowaniu produkcyjności drzewostanu najczęściej wykorzystuje się krzywe wzrostu. Tradycyjnie były one konstruowane przy użyciu metod opartych na określonym wieku bazowym, jednak ich istotną wadą jest zależność parametrów od przyjętego wieku (Cieszewski, 2000). Współcześnie powszechnie stosuje się metodę uogólnionych różnic algebraicznych (GADA), która pozwala na konstruowanie modeli wzrostu niezależnych od wyboru wieku bazowego (Cieszewski, 2000, 2004). Dzięki temu możliwe jest bardziej elastyczne modelowanie zarówno anamorficznych krzywych wzrostu (charakteryzujących się pojedynczymi asymptotami), jak i polimorficznych krzywych wzrostu ze zmiennymi asymptotami, które lepiej oddają przebieg wzrostu drzewostanów.

Dane z jakich najczęściej korzysta się opracowywania modeli wzrostu wysokości drzewostanów to dane uzyskane na podstawie analizy strzały lub powtarzalnych pomiarów prowadzonych na stałych bądź tymczasowych powierzchniach próbnych (Raulier i in., 2003). Pozyskanie danych tego typu jest czasochłonne, kosztowne i zazwyczaj ograniczone do niewielkich, lokalnych obszarów. Modele oparte na analizie strzały mogą prowadzić do przeszacowania wzrostu TH (Marziliano i in., 2019; Raulier i in., 2003). Dodatkowo, ze

względzie na skupienie się na pojedynczym drzewie i założenie jego dominującej pozycji, modele te nie uwzględniają śmiertelności drzew ani zmian w ich pozycji biosocjalnej, co wpływa na dynamikę zmiany TH (Raulier i in., 2003). Z kolei wykorzystanie z danych z tymczasowych powierzchni próbnych może skutkować niedoszacowaniem wzrostu TH drzewostanu (Raulier i in., 2003). Aby prawidłowo modelować na podstawie tego źródła danych, próba musi być duża i pozbawiona błędów systematycznych w całym zakresie wieku drzewostanów. Warto również zauważyć, że tradycyjne modele wzrostu wysokości drzew, bazujące na długich szeregach czasowych, mogą być niewystarczające do prognozowania przyszłych zmian w dynamice wzrostu drzewostanów. Wynika to z wpływu zmieniających się warunków klimatycznych, które w istotny sposób kształtują tempo i charakter wzrostu lasów.

Potencjalnym czwartym źródłem danych do modelowania wzrostu i produkcyjności drzewostanów są dane teledetekcyjne. W ciągu ostatnich kilku dekad wykorzystanie danych teledetekcyjnych było czynnikiem, który zrewolucjonizował inwentaryzację lasów. W szczególności ALS odegrał znaczącą rolę w rozwoju modelowania wzrostu lasów na podstawie danych teledetekcyjnych (Vauhkonen i in., 2014). Do tej pory dane ALS najczęściej wykorzystywano do oceny produkcyjności siedlisk przy użyciu istniejących modeli wzrostu wysokości. Holopainen i in. (2010) zastosowali te dane do wyznaczania SI dla sosny zwyczajnej i świerka pospolitego. Noordermeer i in. (2018, 2020) wykorzystali dane ALS do oszacowania SI, a Solberg i in. (2019) określali SI, dla pojedynczego drzewa, na podstawie danych ALS. Dane ALS wykorzystuje się już do kalibracji modeli wzrostu i produkcyjności drzewostanów (Socha i in., 2017; Tompalski i in., 2015; Tymińska-Czabańska i in., 2021, 2022). Modele powstałe do tej pory zostały jednak opracowane dla relatywnie niewielkich obszarów w skali lokalnej, przy stosunkowo niskim stopniu zmienności warunków panujących w danym miejscu. Rosnąca dostępność danych z powtarzających się akwizycji ALS umożliwia monitorowanie wzrostu i opracowywanie modeli dla coraz większych obszarów.

Oprócz rosnącego zainteresowania wykorzystaniem chmur punktów pochodzących z ALS w leśnictwie, chmury punktów z ukośnych zdjęć lotniczych o wysokiej rozdzielcości (DAP) są coraz częściej wykorzystywane ze względu na niższe koszty ich pozyskania (Fassnacht i in., 2016; Hawryło i in., 2017, p. 20; Igihaut i in., 2019; Tompalski i in., 2021; White i in., 2013). Chmury punktów DAP okazały się przydatne do oceny podstawowych charakterystyk drzewostanów, takich jak wysokość (Guerra-Hernández i in., 2018), pierśnicowe pole przekroju (White i in., 2015), czy miąższość (Hawryło i in., 2017; Straub i

in., 2013). Przeprowadzono także badania, w których porównano inwentaryzacje drzewostanów przy użyciu chmur punktów pochodzących z DAP i ALS (Guerra-Hernández i in., 2018; Hartley i in., 2020; Hawryło i in., 2017; Mielcarek i in., 2020; Wallace i in., 2016). We wszystkich tych badaniach wartości TH pochodzące z ALS charakteryzują się mniejszymi błędami niż te pochodzące z DAP. Jednocześnie większość z wyżej wymienionych badań wykazuje bardzo silną korelację między DAP, ALS i danymi terenowymi. Wciąż jednak nie dysponujemy badaniami, dotyczącymi możliwości modelowania wzrostu i produkcyjności drzewostanów przy użyciu danych DAP.

### **3. Uzasadnienie wyboru tematu badawczego**

Dokładna ocena produkcyjności siedliska ma kluczowe znaczenie dla zrównoważonej gospodarki leśnej. Znajomość potencjalnej oraz aktualnej produkcyjności odgrywa istotną rolę w podejmowaniu świadomych decyzji dotyczących składu gatunkowego, praktyk hodowli lasu, dopuszczalnych poziomów pozyskania drewna, długości rotacji oraz prognoz związanych z jego pozyskaniem (Pretzsch, 2009). Do tej pory monitorowanie i modelowanie wzrostu drzewostanów opierało się głównie na danych z powtarzanych pomiarów na stałych powierzchniach próbnych lub danych z krajowych inwentaryzacji lasów (NFI). Metody te wymagają jednak długoterminowych pomiarów na dużej liczbie powierzchni, co stanowi ich główne ograniczenie (Perin i in., 2013; Raulier i in., 2003). Ponadto stałe powierzchnie próbne są zwykle zakładane do celów eksperymentalnych, głównie w miejscach o lepszych warunkach dla wzrostu drzew, co ogranicza zakres warunków siedliskowych reprezentowanych przez dane. Podobnie, w przypadku danych NFI, wyniki nie zapewniają reprezentacji rzadkich miejsc. Dlatego modelowanie na dużych obszarach przy użyciu tradycyjnych pomiarów terenowych często nie uwzględnia pełnej zmienności warunków wzrostu i prowadzi do uproszczeń, skutkujących przeszacowaniem lub niedoszacowaniem wzrostu drzewostanów (Marziliano i in., 2019; Raulier i in., 2003). Innym ważnym wyzwaniem jest uchwycenie krótkoterminowych wahań wzrostu spowodowanych zmianami klimatycznymi we wzorcach wzrostu drzew, co jest szczególnie trudne w przypadku korzystania z danych z inwentaryzacji terenowej. Ponadto korzystanie z tych źródeł danych wiąże się z dużą pracochłonnością i czasochłonnością (Noordermeer i in., 2018).

Większość wyżej opisanych problemów można rozwiązać dzięki wykorzystaniu danych teledetekcyjnych do inwentaryzacji i monitoringu obszarów leśnych. Rozdzielcość przestrzenna i czasowa oferowana przez te technologie pozwala przezwyciężyć ograniczenia związane z tradycyjnymi metodami (White i in., 2016). Wykorzystując dane ALS jesteśmy w stanie pozyskać informację dotyczącą TH drzewostanu, które charakteryzują całkowitą zmienność badanego obszaru.

Modelowanie wzrostu drzewostanów przy użyciu danych ALS jest stosunkowo nowym zagadnieniem ze względu na dopiero niedawne pojawienie się obszarów, z dostępnością danych z co najmniej dwóch akwizycji. W rezultacie opracowane modele mają charakter lokalny, co nie pozwala w pełni wykorzystać potencjału technologii teledetekcyjnych. Tradycyjne metody

modelowania mają charakter jedynie punktowy, więc niezbędne jest opracowanie metodyki modelowania, która sprawdzi się na większych obszarach.

Znacznie bardziej dostępny, ale mniej powszechnym źródłem danych o wysokości drzewostanu przydatnych do modelowania wzrostu są wieloczasowe dane DAP. Do tej pory nie kalibrowano modeli wzrostu przy użyciu chmur punktów pochodzących z DAP. Jednocześnie chmury punktów DAP mogą stanowić stosunkowo łatwo dostępne i tańsze źródło danych do kalibracji modeli wzrostu. Dane te można pozyskać za pomocą samolotów lub dronów w ramach inwentaryzacji lasu. Archiwalne dane DAP są znacznie szerzej dostępne niż dane LiDAR, dzięki temu umożliwiają modelowanie z wykorzystaniem znacznie dłuższych szeregów czasowych. Technika Structure from Motion (SfM) pozwala na łatwe generowanie chmur punktów bez konieczności stosowania ścisłej jednorodności, poprzez nakładanie obrazów, pozycjonowanie oraz kalibrację kamery co znacznie przyspiesza, do tej pory bardzo żmudną obróbkę danych tego typu (Iglhaut i in., 2019). Możliwość wykorzystania danych DAP do pomiaru TH i modelowania wzrostu może pozwolić na szerokie zastosowanie tej techniki na dużych przestrzennych i czasowych skalach, dzięki obniżeniu kosztów pozyskania danych w porównaniu do danych ALS. Ponadto, wykorzystanie danych DAP umożliwioby analizę archiwalnych zbiorów danych obrazów cyfrowych w badaniach retrospektywnych dotyczących zmian w strukturze wysokościowej drzewostanów.

Kolejnym krokiem w rozwoju wykorzystania danych teledetekcyjnych w modelowaniu wzrostu drzewostanów jest fuzja różnych typów danych. Dane DAP reprezentują głównie górną warstwę drzewostanu co może prowadzić do błędów określania wysokości (White i in., 2013). Badania porównujące metody określania wysokości drzewostanu oparte na danych ALS i DAP wykazały, że dane ALS charakteryzują się mniejszym błędem (Guerra-Hernández i in., 2018; Hartley i in., 2020; Hawryło i in., 2017; Mielcarek i in., 2020). Wartości wysokości drzewostanu określone za pomocą DAP mają systematyczne błędy specyficzne dla każdego pozyskania, a jednocześnie są silnie skorelowane z rzeczywistymi wartościami wysokości drzewostanu (Jensen & Mathews, 2016). Można, więc założyć, że możliwa jest korekta tego systematycznego błędu na podstawie innego typu danych np. ALS lub powierzchni próbnych.

Założeniem opisanej wyżej hipotezy jest to, że dane referencyjne z pomiarów terenowych lub danych ALS są dostępne dla badanego obszaru w latach pozyskania danych DAP. Wtedy możliwe jest bezpośrednie określenie błędu systematycznego w określaniu wysokości drzewostanu i przeprowadzenie korekty. To założenie jest zarazem pewnym ograniczeniem tej metody korekty; podczas gdy dane DAP są ogólnie łatwo dostępne, to dane

ALS lub referencyjne dane z pomiarów terenowych dla określonego obszaru są czasami trudniej dostępne. W związku z tym często trudno jest zastosować tę metodę, a ogromny potencjał wykorzystania danych DAP pozostaje ograniczony. Odpowiedzią na to ograniczenie jest opracowanie metody korygowania danych DAP w oparciu o dane ALS lub dane z pomiarów powierzchni próbnych odnoszące się do innego roku niż rok pozyskania danych DAP.

Fakt,

że nie tylko dane ALS, ale także dane z pomiarów terenowych z lat poprzedzających pozyskanie danych DAP mogą być wykorzystane jako odniesienie, sprawia, że opracowane podejście jest elastyczne i może przyczynić się do pełnego wykorzystania potencjału danych DAP.

Szersze wykorzystanie danych pochodzących z technologii ALS oraz DAP w procesie inwentaryzacji lasów oraz modelowania wzrostu drzewostanów pozwala na eliminację problemu ograniczonej dostępności informacji. Możliwość monitorowania dużych obszarów leśnych stwarza także szansę na weryfikację dotychczasowych założeń i teorii dotyczących dynamiki wzrostu lasów. Wykorzystanie nowych, wcześniej niedostępnych źródeł danych teledetekcyjnych, w postaci długoterminowych szeregów czasowych, stanowi dodatkową motywację do podjęcia prób zastosowania technologii ALS oraz DAP w procesie kalibracji modeli wzrostu drzewostanów.

## 4. Cel pracy

Celem pracy było opracowanie nowoczesnych metod budowy modeli wzrostu wysokości drzewostanów, umożliwiających ich efektywną kalibrację na rozległych obszarach z wykorzystaniem szeregow czasowych danych teledetekcyjnych.

Postawiono dwie główne tezy pracy:

1. Dane ALS pozwalają na kalibrację modeli wzrostu drzewostanów na dużych obszarach, uwzględniając całą zmienność wysokości drzewostanów i uzyskując dokładność większą lub porównywalną do tradycyjnych modeli.
2. Wykorzystanie danych DAP może być alternatywą dla danych ALS w modelowaniu wzrostu drzewostanów, jeśli zastosujemy poprawkę redukującą błąd pomiaru wysokości.

Zdefiniowano również szereg pytań badawczych, na które udzielono odpowiedzi w cyklu trzech publikacji naukowych składających się na dysertację:

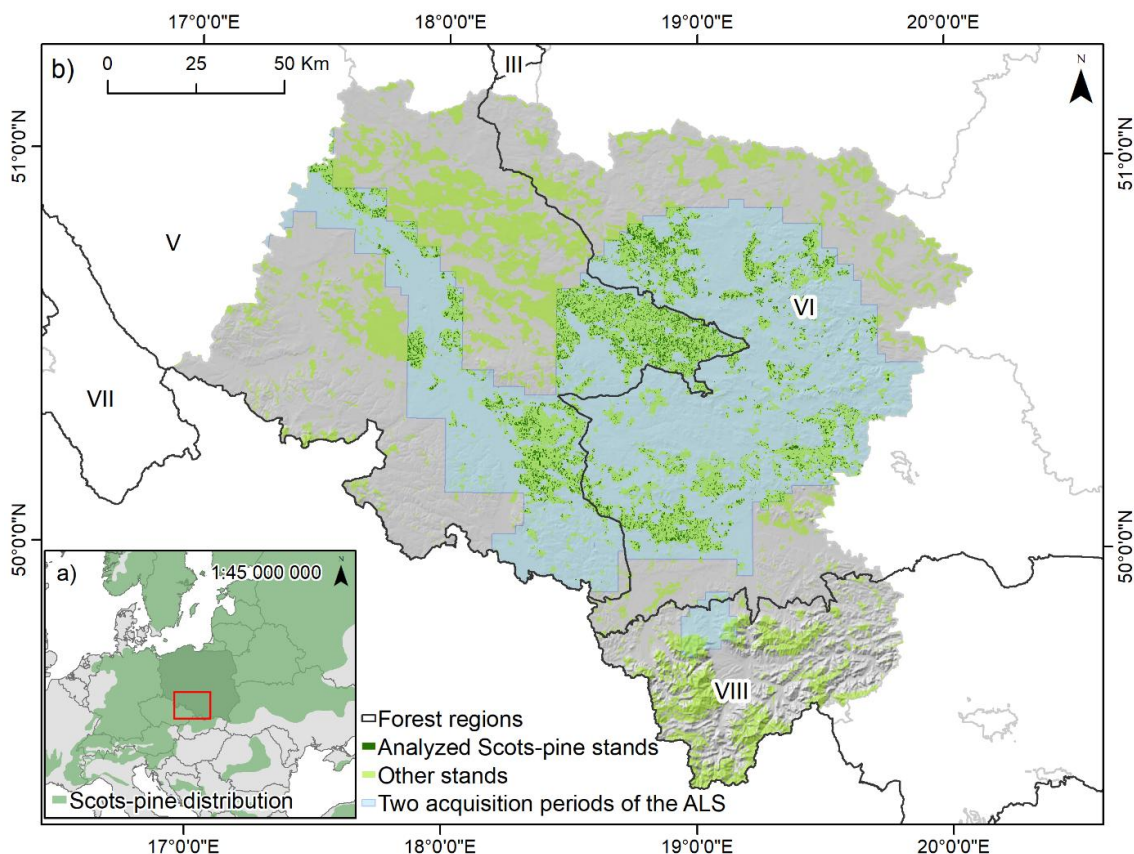
- Czy dane ALS z pochodzące z dużego obszaru (niejednorodna chmura punktów, różne okresy skanowania) mogą służyć do opracowania modeli wzrostu drzewostanów (**Publikacja nr 1**)?
- Czy wyniki kalibracji regionalnych modeli wzrostu na podstawie danych ALS są porównywalne do tradycyjnych modeli regionalnych (**Publikacja nr 1**)?
- Czy dane DAP charakteryzują się błędem pomiaru wysokości, a jeśli tak to, czy jest on stały i nie zależy od charakterystyk pozyskanych zdjęć (**Publikacja nr 2**)?
- Czy jest możliwa korekta danych DAP na podstawie danych referencyjnych wykonanych w roku pozyskania danych DAP (**Publikacja nr 2**)?
- Jak wielka musi być wielkość próby danych referencyjnych, aby skorygować błąd pomiaru wysokości danych DAP (**Publikacja nr 2**)?
- Czy jest możliwa korekta danych DAP na podstawie danych referencyjnych wykonanych w roku innym niż rok pozyskania danych DAP (**Publikacja nr 3**)?
- Czy na podstawie danych DAP możliwe jest kalibrowanie modeli wzrostu drzewostanów, które charakteryzują się dokładnością porównywalną do modeli na podstawie ALS oraz tradycyjnych danych (**Publikacja nr 3**)?

## 5. Metodyka

### a. Obszar badań

Badania opisane w niniejszej pracy dotyczą obszaru Polski. W zależności od zagadnienia i dostępności danych obszar objęty analizami był jednak różny.

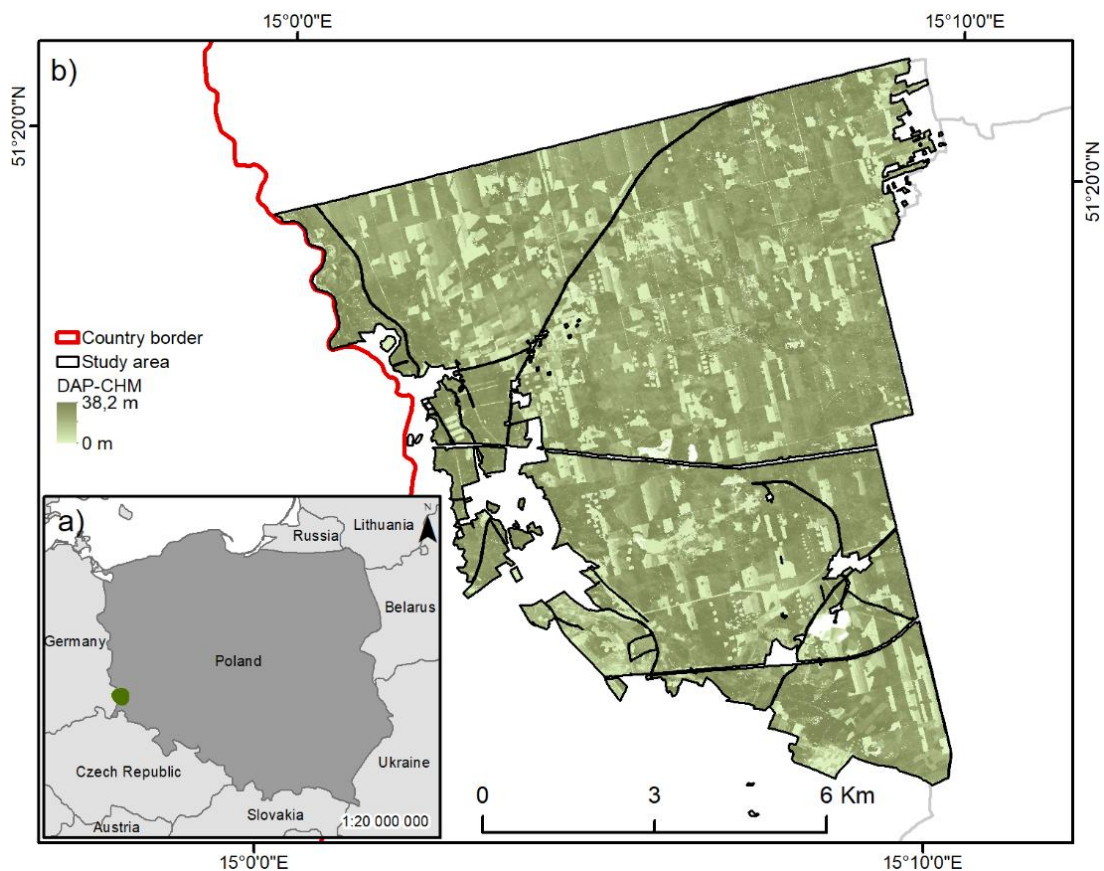
W publikacji nr 1 obszar badań obejmuje drzewostany sosnowe na terenie Regionalnej Dyrekcji Lasów Państwowych w Katowicach, położone w trzech krainach przyrodniczo-leśnych południowo-zachodniej Polski (Zielony & Kliczkowska, 2012) (Rycina 1a, b). Głównym gatunkiem na badanym obszarze jest sosna zwyczajna (około 66%) o średnim wieku drzewostanów 56 lat. Do kalibracji modelu wybrano drzewostany sosnowe, dla których dostępne były dane ALS dla dwóch różnych lat. Wybrane drzewostany miały ponad 70% udział sosny zwyczajnej i były w wieku od 10 do 140 lat.



Rycina 1. Lokalizacja obszaru badań w Europie Środkowej (a). Rozmieszczenie drzewostanów na obszarze badań, dla których dostępne były dane z dwóch okresów pozyskania danych ALS (b).

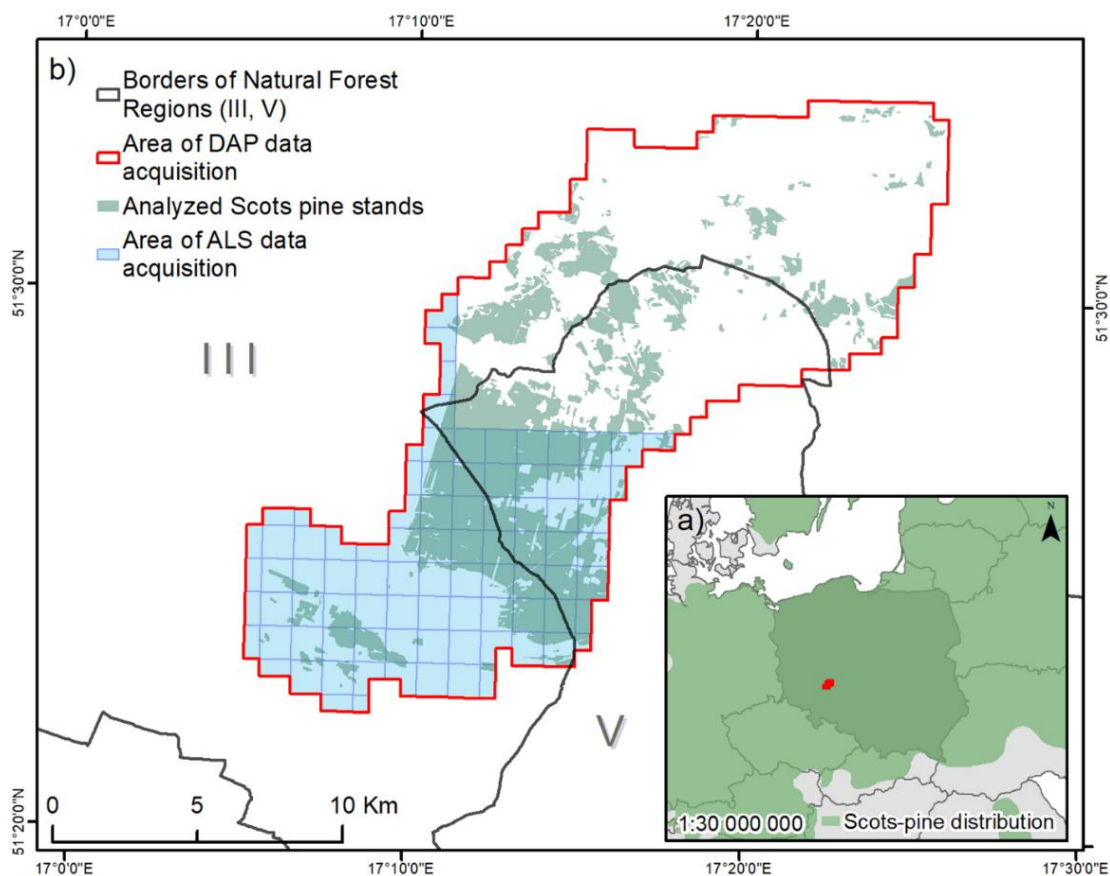
W publikacji nr 2 obszar badań obejmuje 8000 hektarów i znajduje się w Nadleśnictwie Pieńsk (Rycina 2). Jest on zdominowany przez sosnę zwyczajną o udziale 80%, wraz z niewielkim udziałem brzozy brodawkowej (9%), dębu (2%) i olszy czarnej (2%). Wiek drzewostanów na

badanym obszarze wahał się od 1 do 205 lat. Do analizy wybrano drzewostany starsze niż 5 lat i z udziałem sosny zwyczajnej przekraczającym 90%.



Rycina 2. Lokalizacja obszaru badań w Polsce (a); (b) Numeryczny model pokrycia terenu na podstawie zdjęć lotniczych w oparciu o chmurę punktów DAP pozyskaną w 2021 r.

**W publikacji nr 3** obszar badań obejmował drzewostany sosnowe w Nadleśnictwie Milicz (Rycina 3). Cały obszar badań obejmował prawie 23 600 ha, z czego drzewostany sosnowe zajmowały prawie 6 400 ha. Obszar ten znajdował się częściowo w III i V krainie przyrodniczo-leśnej (Zielony & Kliczkowska, 2012). Drzewostany na badanym obszarze to głównie sosna zwyczajna (75%), z udziałem dębu (10%), buka (6%), olszy czarnej (5%) i brzozy brodawkowej (2%). Wiek drzewostanów sosnowych waha się od 1 do 160 lat, jednak w analizie wykluczyliśmy drzewostany młodsze niż 10 lat i starsze niż 120 lat. Wykluczono również drzewostany z udziałem sosny niższym niż 80%. Dane ALS z dwóch okresów (2012 i 2019) obejmowały tylko południową część badanego obszaru (Rycina 3), podczas gdy dane DAP z dwóch innych okresów (2013 i 2020) obejmowały cały badany obszar.



Rycina 3. Obszar badań w Polsce (a) oraz w nadleśnictwie Milicz (b).

## b. Materiał badawczy

W publikacji nr 1 dane ALS zostały pozyskane z repozytorium Głównego Urzędu Geodezji i Kartografii (GUGiK). Dane ALS zostały pozyskane w warunkach bezlistnych (Leaf off). Średnia gęstość chmury punktów wynosiła 4 punkty/m<sup>2</sup>, a dokładność pozycjonowania danych ALS nie przekraczała 0,5 m. Dane pozyskiwano w latach 2011–2019, przy czym większość zbiorów przypada na lata 2011 i 2019 (Tabela 1).

Tabela 1. Lata pozyskania danych ALS w analizowanych drzewostanach.

| Lata pozyskania par danych ALS | Udział analizowanych drzewostanów (%) |
|--------------------------------|---------------------------------------|
| 2011-2019                      | 59.40                                 |
| 2012-2019                      | 22.77                                 |
| 2013-2019                      | 13.17                                 |
| 2014-2019                      | 4.62                                  |
| 2015-2019                      | 0.04                                  |

W publikacji nr 2 dane ALS i DAP z 2015 r. zostały pozyskane w ramach projektu REMBIOFOR. Dane ALS i DAP dla roku 2021 pozyskano z repozytorium GUGiK (Tabela 2).

Tabela 2. Parametry danych DAP (cyfrowe zdjęcia lotnicze) i ALS (lotniczy skaning laserowy) dla dwóch akwizycji z 2015 i 2021 roku.

| <b>Źródło danych</b> | <b>Rok pozyskania</b> | <b>Gęstość chmury punktów (punkty/m<sup>2</sup>)</b> | <b>Dokładność pozycjonowania (m)</b> | <b>Rozdzielcość przestrzenna (m)</b> |
|----------------------|-----------------------|--|--------------------------------------|--------------------------------------|
| <b>ALS</b>           | 2015                  | 7,3  | 0,2                                  | -                                    |
|                      | 2021                  | 4  | 0,5                                  | -                                    |
| <b>DAP</b>           | 2015                  | 9  | -                                    | 0,2                                  |
|                      | 2021                  | 7  | -                                    | 0.25                                 |

W publikacji nr 3 dane ALS i DAP zostały pozyskane z repozytorium GUGiK. Dane DAP pochodziły z lat 2013 oraz 2020, natomiast ALS z 2012 i 2019 roku (Tabela 3).

Tabela 3. Parametry danych DAP (cyfrowe zdjęcia lotnicze) i ALS (lotniczy skaning laserowy) dla akwizycji z lat 2012, 2013, 2019 oraz 2020.

| <b>Źródło danych</b> | <b>Rok pozyskania</b> | <b>Gęstość chmury punktów (punkty/m<sup>2</sup>)</b> | <b>Dokładność pozycjonowania (m)</b> | <b>Rozdzielcość przestrzenna (m)</b> |
|----------------------|-----------------------|--|--------------------------------------|--------------------------------------|
| <b>ALS</b>           | 2012                  | 4  | 0.15                                 | -                                    |
|                      | 2019                  | 4  | 0.15                                 | -                                    |
| <b>DAP</b>           | 2013                  | 4.3  | -                                    | 0.25                                 |
|                      | 2020                  | 4.5  | -                                    | 0.25                                 |

W każdej z trzech publikacji skład gatunkowy, udział poszczególnych gatunków oraz wiek drzewostanów pochodzą z Systemu Informacyjnego Lasów Państwowych (SILP).

Chmury punktów z danych DAP zostały wygenerowane przy użyciu oprogramowania Agisoft PhotoScan Professional. Do przetwarzania danych zastosowano metodykę opisaną przez Dandois & Ellis (2013) oraz Turner i in. (2012). Użyto parametru wysokiej dokładności do wyrównania zdjęć, z limitem 1000 punktów kluczowych na Mpx i limitem 10000 punktów wiązania. Zostały wykorzystane punkty kontrolne dostarczone przez wykonawcę zdjęć lub punkty wygenerowane manualnie na podstawie ortofotomapy oraz cyfrowego modelu terenu.

Chmury punktów przetwarzano przy użyciu pakietu lidR w środowisku R (Roussel i in. 2020). Każda z pozyskanych chmur punktów została znormalizowana. Do normalizacji danych ALS wykorzystano funkcję *normalize\_height* i algorytm *knnidw* z jego domyślnymi parametrami. W przypadku danych DAP, znormalizowano je poprzez odjęcie numerycznego modelu terenu od każdego punktu chmury DAP. Wykorzystane numeryczne modele terenu pochodziły z GUGiK. W kolejnym etapie utworzono modele koron drzew (CHM). Wszystkie CHM zostały utworzone z rozdzielczością przestrzenną 1 m. W tym celu wykorzystano algorytm *p2r* z podokręgiem o rozmiarze 0,3 m.

W każdej z publikacji została obliczona TH dla każdego wygenerowanego CHM. CHM został zagregowany do rozdzielczości 10 m (Rycina 4a). Przy agregacji przyjęto wartości maksymalne. Wszystkie wydzielania na badanych obszarach zostały podzielone na siatkę o rozmiarze oczka  $50 \times 50$  m, która została uzyskana z agregacji 25 oczek  $10 \times 10$  m. W tym celu, obliczono wysokość drzewostanu dla oczek siatki  $50 \times 50$  m jako średnią z 25 maksymalnych wartości CHM z oczek  $10 \times 10$  m (Rycina 4b). Przy obliczaniu średnich, oczka siatki  $10 \times 10$  m z maksymalnymi wartościami CHM niższymi niż  $2/3$  TH oczek siatki  $50 \times 50$  m, które uznano za puste, zostały usunięte, aby uchwycić tylko wysokości najwyższych drzew. Aby wyeliminować efekt brzegowy sąsiednich wydzielień w każdym wydzielaniu, zastosowano wewnętrzny bufor o szerokości 15 m, a do obliczeń włączono oczka siatki  $50 \times 50$  m, które znajdowały się całkowicie w wydzielaniu bez wchodzenia w granice bufora (Rycina 4c). Ta metoda określania wysokości została zastosowana zarówno do danych DAP, jak i ALS dla poszczególnych lat pozyskania, na każdym z badanych obszarów. Wartości TH obliczone dla komórek siatki  $50 \times 50$  m były traktowane jako pojedyncze obserwacje w dalszych etapach.



Rycina 4. Metodyka obliczania wysokości górnej (TH): a) wysokość maksymalna w oczkach  $10 \times 10$  m; b) utworzenie siatki  $50 \times 50$  m poprzez agregację 25 oczek  $10 \times 10$  m; c) włączenie oczek siatki  $50 \times 50$  m, które nie znajdowały się całkowicie w wydzielaniu, bez wchodzenia w granice bufora.

### c. Modelowanie i walidacja zbudowanych modeli

W każdej z omawianych publikacji, najważniejszym etapem było opracowanie modelu wzrostu wysokości. Przyjmując wyniki wcześniejszych badań dotyczących wzrostu wysokości oraz modelowania produkcyjności drzewostanów (Socha i in., 2020; Socha & Orzeł, 2013), jako funkcję bazową przyjęto równanie dynamiczne (1) opracowane przy użyciu metody GADA (Cieszewski, 2000):

$$TH = TH_1 \frac{T^{\beta_1} (T_1^{\beta_1} R + \beta_2)}{T_1^{\beta_1} (T^{\beta_1} R + \beta_2)} \quad (1)$$

gdzie:

$$R = Z_0 + (Z_0^2 + \frac{2\beta_2 TH_1}{T_1^{\beta_1}})^{0.5} \quad (1.1)$$

$$Z_0 = TH_1 - \beta_3 \quad (1.2)$$

$\beta_1$ ,  $\beta_2$ , i  $\beta_3$  to szacowane parametry modelu; TH to wysokość górna w wieku T; a  $TH_1$  to wysokość górna w wieku T1. R jest wyrażeniem opisującym tempo wzrostu, natomiast  $Z_0$  jest wyrażeniem dostosowującym.

W publikacji nr 1 do kalibracji modeli użyto danych ALS. Skalibrowano 3 modele globalny oraz modele lokalne dla krajów przyrodniczo-leśnych V i VI. Aby oszacować istotność modelu dla skalibrowanych parametrów, przeprowadzono test t-Studenta oraz obliczono błąd standardowy (SE), wartość statystyki t (t-value) i wartość p (p-value). W ramach walidacji, porównano otrzymane modele z modelami wzrostu wysokości dla sosny zwyczajnej opracowanymi na podstawie analizy strzały (Socha i in., 2021). Dla każdego z porównywanych modeli obliczono średni błąd bezwzględny (MAE) oraz błąd średniokwadratowy (RMSE).

W publikacji nr 2 do kalibracji modeli użyto danych DAP, które zostały skorygowane na podstawie symulowanych powierzchni próbnich z danych ALS. Zaproponowano prostą metodę korekcji błędu oszacowań TH opartych na danych DAP. Poprzez iteracyjne losowe próbkowanie określono minimalną liczbę pomiarów referencyjnych niezbędnych do wyznaczenia korekty TH na podstawie obliczonego SE danych DAP.

Skalibrowano 3 modele wzrostu:  $DAP_M$  – model na podstawie surowych danych DAP ,  $DAP_{M-corr}$  – model na podstawie skorygowanych danych DAP oraz  $ALS_M$  – model na

podstawie danych ALS. Dla każdego z porównywanych modeli obliczono MAE, RMSE oraz skorygowany współczynnik korelacji ( $R_{adj}^2$ ).

**W publikacji nr 3** do kalibracji modeli, również użyto danych z DAP. Zostały one jednak skorygowane na podstawie referencji z roku innego niż ten w którym zostały pozyskane dane DAP. W opracowanym podejściu, referencyjna TH została zaktualizowana do roku w którym pozyskano dane DAP, przy użyciu istniejących modeli wzrostu. W aktualizacji porównano trzy modele wzrostu M1 – model ogólnopolski, M2 – model dla krainy III oraz M3 model dla krainy V (Socha i in., 2021). W celu zweryfikowania, czy TH zaktualizowana przy użyciu tych modeli różni się istotnie statystycznie przeprowadzono test t-Studenta.

W kolejnym kroku skorygowano dane DAP przy użyciu 3 zaktualizowanych wartości TH. Obliczono 3 wartości błędu (bias) na podstawie 3 zaktualizowanych TH referencyjnych. Wartości bias dodano do TH obliczonego na podstawie DAP, dzięki czemu otrzymano trzy wartości skorygowanego TH na podstawie danych DAP. W ostatnim etapie skalibrowano 3 modele wzrostu i obliczono dla nich SE, t-value, p-value, RMSE oraz MAE. Modele porównano z modelami wzrostu wysokości dla sosny zwyczajnej opracowanymi na podstawie analizy strzały (Socha i in., 2021).

## **6. Najważniejsze wyniki badań**

**W publikacji nr 1** wykazano, że dane ALS mogą być wykorzystywane do modelowania przyrostu wysokości drzewostanów na skalę regionalną. W oparciu o czasowe pomiary ALS skalibrowano model wzrostu wysokości drzewostanów sosny zwyczajnej na obszarze Regionalnej Dyrekcji Lasów Państwowych w Katowicach. Wyniki wskazują, że model skalibrowany z wykorzystaniem danych teledetekcyjnych nie wykazuje istotnych różnic w porównaniu do modelu opartego na tradycyjnych pomiarach terenowych uzyskanych z analizy strzały. Co więcej, zastosowanie modelu opracowanego na podstawie danych ALS zapewnia nawet wyższą dokładność modelowania przyrostu wysokości niż model tradycyjny oparty na danych naziemnych. Uzyskane wyniki potwierdzają potencjał powtarzalnych pomiarów ALS do konstrukcji regionalnych modeli przyrostu wysokości, umożliwiając długoterminową prognozę wzrostu drzew w zmieniających się warunkach klimatycznych.

**W publikacji nr 2** wykazano przydatność chmur punktów pozyskanych metodą DAP do opracowania lokalnych modeli wzrostu wysokości TH. W związku z identyfikacją systematycznych błędów w wartościach TH wyznaczonych na podstawie danych DAP, opracowano prostą metodę korekty tych błędów. W analizach wykorzystano dane ALS do korekty błędu TH obliczonego z danych DAP, jednak zaproponowane podejście może zostać zastosowane również w oparciu o naziemne dane pomiarowe (np. z powierzchni próbnych 10×10 m lub pomiarach pojedynczego drzewa). Dodatkowo zaproponowano prosty algorytm określania wielkości próby niezbędnej do dokładnej korekty wartości TH pochodzących z DAP. Po korekcie, wartości TH wyznaczone z danych DAP wykorzystano do opracowania modelu wzrostu wysokości TH dla sosny zwyczajnej. Opracowany model charakteryzuje się parametrami dopasowania zbliżonymi do modelu referencyjnego opartego na danych ALS, a także analogicznymi zdolnościami predykcyjnymi. Badanie potwierdza, że dane DAP stanowią rzetelną podstawę do tworzenia modeli wzrostu TH i mogą być szeroko stosowane w skali lokalnej i regionalnej, znacznie obniżając koszty pozyskania danych w porównaniu z danymi ALS.

**W publikacji nr 3** opracowano nową metodę wykorzystania danych DAP w modelowaniu wzrostu drzewostanów, polegającą na korekcie wartości TH pochodzących z DAP przy użyciu referencyjnych wartości TH. Nowatorskość tego podejścia wynika z faktu, że dane referencyjne mogą być pozyskane w innym okresie niż dane DAP. Opracowana metoda zakłada aktualizację wartości referencyjnych TH pochodzących z danych archiwalnych (ALS lub pomiarów terenowych) do roku pozyskania danych DAP z wykorzystaniem istniejących modeli wzrostu TH.

Takie podejście umożliwia wykorzystanie danych ALS lub danych z pomiarów naziemnych pochodzących z dowolnego roku jako danych referencyjnych służących do korekty TH wyznaczonej na podstawie danych DAP. Przeprowadzono testy przydatności różnych modeli wzrostu TH do aktualizacji wartości TH z ALS na rok pozyskania danych DAP. Ponieważ skuteczność tej aktualizacji TH jest niemal niezależna od zastosowanego modelu wzrostu, proces aktualizacji może być realizowany nawet przy użyciu modeli niedostosowanych do lokalnych warunków wzrostu. Dodatkowo wykazano, że wartości TH uzyskane z danych DAP po zastosowaniu proponowanej korekty stanowią użyteczne dane wejściowe do opracowania wiarygodnych lokalnych modeli wzrostu wysokości TH drzewostanu.

## **7. Podsumowanie wyników i wnioski**

1. Dane ALS z pochodzące z dużego obszaru mogą służyć do opracowania modeli wzrostu drzewostanów na skalę regionalną.
2. Zastosowanie modelu opracowanego na danych ALS zapewnia wyższą dokładność modelowania przyrostu wysokości niż modelowanie na danych tradycyjnych.
3. Dane DAP charakteryzują się błędem systematycznym błędem, przez co pomiar wysokości jest drzewostanu jest zniżany. Błąd ten nie jest stały, co znacznie utrudnia korektę danych.
4. Korekta błędu systematycznego danych DAP jest możliwa przez zastosowanie danych referencyjnych w postaci danych ALS lub danych z pomiarów terenowych powierzchni próbnych. Dokładność korekty zależy od wielkości obszaru, dla którego dostępne są referencyjne dane ALS lub liczby referencyjnych powierzchni próbnych.
5. Liczba powierzchni próbnych potrzebnych do uzyskania wymaganej dokładności może zostać obliczona na podstawie błędu standardowego (SE) danych DAP.
6. Możliwa jest korekta błędu systematycznego danych DAP na podstawie danych referencyjnych pozyskanych w roku innym niż rok pozyskania danych DAP. W takim przypadku konieczna jest jednak aktualizacja wysokości z danych referencyjnych do roku pozyskania danych DAP.
7. Dokładność aktualizacji wysokości referencyjnych wykorzystywanych do korekty błędu systematycznego danych DAP jest niezależna od zastosowanego w tym celu modelu wzrostu.
8. Modele wzrostu drzewostanów skalibrowane na podstawie skorygowanych danych DAP charakteryzują się dokładnością porównywalną do modeli wzrostu skalibrowanych na podstawie danych ALS oraz danych z analiz strzał.

## 8. Literatura

- Achim, A., Moreau, G., Coops, N. C., Axelson, J. N., Barrette, J., Bédard, S., Byrne, K. E., Caspersen, J., Dick, A. R., D'Orangeville, L., Drolet, G., Eskelson, B. N. I., Filipescu, C. N., Flamand-Hubert, M., Goodbody, T. R. H., Griess, V. C., Hagerman, S. M., Keys, K., Lafleur, B., ... White, J. C. (2022). The changing culture of silviculture. *Forestry*, 95(2), 143–152. <https://doi.org/10.1093/forestry/cpab047>
- António, N., Tomé, M., Tomé, J., Soares, P., & Fontes, L. (2007). Effect of tree, stand, and site variables on the allometry of *Eucalyptus globulus* tree biomass. *Canadian Journal of Forest Research*, 37(5), 895–906. <https://doi.org/10.1139/X06-276>
- Bastin, J.-F., Rutishauser, E., Kellner, J. R., Saatchi, S., Pélassier, R., Hérault, B., Slik, F., Bogaert, J., De Cannière, C., Marshall, A. R., Poulsen, J., Alvarez-Loyayza, P., Andrade, A., Angbonga-Basia, A., Araujo-Murakami, A., Arroyo, L., Ayyappan, N., de Azevedo, C. P., Banki, O., ... Zebaze, D. (2018). Pan-tropical prediction of forest structure from the largest trees. *Global Ecology and Biogeography*, 27(11), 1366–1383. <https://doi.org/10.1111/geb.12803>
- Bi, H., Long, Y., Turner, J., Lei, Y., Snowdon, P., Li, Y., Harper, R., Zerihun, A., & Ximenes, F. (2010). Additive prediction of aboveground biomass for *Pinus radiata* (D. Don) plantations. *Forest Ecology and Management*, 259(12), 2301–2314. <https://doi.org/10.1016/j.foreco.2010.03.003>
- Blanco Vaca, J. A., & Lo Wong, Y.-H. (2023). *Latest trends in modelling forest ecosystems: New approaches or just new methods?* <https://doi.org/10.1007/s40725-023-00189-y>
- BonTEMPS, J.-D., & Bouriaud, O. (2014). Predictive approaches to forest site productivity: Recent trends, challenges and future perspectives. *Forestry*, 87(1), 109–128.

- Bravo-Oviedo, A., Gallardo-Andrés, C., Río, M. del, & Montero, G. (2010). Regional changes of *Pinus pinaster* site index in Spain using a climate-based dominant height model. *Canadian Journal of Forest Research*, 40(10), 2036–2048.  
<https://doi.org/10.1139/X10-143>
- Cieszewski, C. J. (2000). Generalized Algebraic Difference Approach: Theory Based Derivation. *Forest Science*, 46(1).
- Cieszewski, C. J. (2004). *GADA derivation of dynamic site equations with polymorphism and variable asymptotes from Richards to Weibull and other exponential functions* (p. PMRC Tech. Rep.).
- Dandois, J. P., & Ellis, E. C. (2013). High spatial resolution three-dimensional mapping of vegetation spectral dynamics using computer vision. *Remote Sensing of Environment*, 136, 259–276.
- Fassnacht, F. E., Latifi, H., Stereńczak, K., Modzelewska, A., Lefsky, M., Waser, L. T., Straub, C., & Ghosh, A. (2016). Review of studies on tree species classification from remotely sensed data. *Remote Sensing of Environment*, 186, 64–87.
- Garcia, O., & Batho, A. (2005). Top Height Estimation in Lodgepole Pine. *Western Journal of Applied Forestry*, 20(1), 64–68.
- Guerra-Hernández, J., Cosenza, D. N., Rodriguez, L. C. E., Silva, M., Tomé, M., Díaz-Varela, R. A., & González-Ferreiro, E. (2018). Comparison of ALS-and UAV (SfM)-derived high-density point clouds for individual tree detection in Eucalyptus plantations. *International Journal of Remote Sensing*, 39(15–16), 5211–5235.
- Hartley, R. J., Leonardo, E. M., Massam, P., Watt, M. S., Estarija, H. J., Wright, L., Melia, N., & Pearse, G. D. (2020). An assessment of high-density UAV point clouds for the measurement of young forestry trials. *Remote Sensing*, 12(24), 4039.

- Hawryło, P., Socha, J., Węzyk, P., Ochał, W., Krawczyk, W., Miszczyszyn, J., & Tymińska-Czabańska, L. (2024). How to adequately determine the top height of forest stands based on airborne laser scanning point clouds? *Forest Ecology and Management*, 551, 121528. <https://doi.org/10.1016/j.foreco.2023.121528>
- Hawryło, P., Tompalski, P., & Węzyk, P. (2017). Area-based estimation of growing stock volume in Scots pine stands using ALS and airborne image-based point clouds. *Forestry: An International Journal of Forest Research*, 90(5), 686–696. <https://doi.org/10.1093/forestry/cpx026>
- Holopainen, M., Vastaranta, M., Haapanen, R., Yu, X., Hyppä, J., Kaartinen, H., Viitala, R., & Hyppä, H. (2010). Site-Type Estimation Using Airborne Laser Scanning and Stand Register Data. *The Photogrammetric Journal of Finland*, 22(1), 16–32.
- Iglhaut, J., Cabo, C., Puliti, S., Piermattei, L., O'Connor, J., & Rosette, J. (2019). Structure from Motion Photogrammetry in Forestry: A Review. *Current Forestry Reports*, 5(3), 155–168. <https://doi.org/10.1007/s40725-019-00094-3>
- Jensen, J. L. R., & Mathews, A. J. (2016). Assessment of Image-Based Point Cloud Products to Generate a Bare Earth Surface and Estimate Canopy Heights in a Woodland Ecosystem. *Remote Sensing*, 8(1), Article 1. <https://doi.org/10.3390/rs8010050>
- Magnussen, S., Gougeon, F., Leckie, D., & Wulder, M. (1999). Predicting tree heights from a combination of Lidar canopy heights and digital stem counts. *Proceedings of IUFRO Conference on Remote Sensing and Forest Monitoring, June 1-3, 1999, Rogow, Poland*, 498–513.

- Marziliano, P. A., Tognetti, R., & Lombardi, F. (2019). Is tree age or tree size reducing height increment in *Abies alba* Mill. At its southernmost distribution limit? *Annals of Forest Science*, 76(1), Article 1. <https://doi.org/10.1007/s13595-019-0803-5>
- Mensah, A. A., Holmström, E., Petersson, H., Nyström, K., Mason, E. G., & Nilsson, U. (2021). The millennium shift: Investigating the relationship between environment and growth trends of Norway spruce and Scots pine in northern Europe. *Forest Ecology and Management*, 481, 118727.
- Mielcarek, M., Kamińska, A., & Stereńczak, K. (2020). Digital Aerial Photogrammetry (DAP) and Airborne Laser Scanning (ALS) as Sources of Information about Tree Height: Comparisons of the Accuracy of Remote Sensing Methods for Tree Height Estimation. *Remote Sensing*, 12(11), Article 11. <https://doi.org/10.3390/rs12111808>
- Noordermeer, L., Bollandsås, O. M., Gobakken, T., & Næsset, E. (2018). Direct and indirect site index determination for Norway spruce and Scots pine using bitemporal airborne laser scanner data. *Forest Ecology and Management*, 428, 104–114.
- Noordermeer, L., Gobakken, T., Næsset, E., & Bollandsås, O. M. (2020). Predicting and mapping site index in operational forest inventories using bitemporal airborne laser scanner data. *Forest Ecology and Management*, 457, 117768.
- Perin, J., Hébert, J., Brostaux, Y., Lejeune, P., & Claessens, H. (2013). Modelling the top-height growth and site index of Norway spruce in Southern Belgium. *Forest Ecology and Management*, 298, 62–70.

Pretzsch, H. (2009). Forest Dynamics, Growth, and Yield. In H. Pretzsch (Ed.), *Forest Dynamics, Growth and Yield: From Measurement to Model* (pp. 1–39). Springer.  
[https://doi.org/10.1007/978-3-540-88307-4\\_1](https://doi.org/10.1007/978-3-540-88307-4_1)

Pretzsch, H. (2021). Trees grow modulated by the ecological memory of their past growth. Consequences for monitoring, modelling, and silvicultural treatment. *Forest Ecology and Management*, 487(January), 118982.  
<https://doi.org/10.1016/j.foreco.2021.118982>

Pretzsch, H., Biber, P., Schütze, G., Uhl, E., & Rötzer, T. (2014). Forest stand growth dynamics in Central Europe have accelerated since 1870. *Nature Communications*, 5(1), 4967.

Raulier, F., Lambert, M.-C., Pothier, D., & Ung, C.-H. (2003). Impact of dominant tree dynamics on site index curves. *Forest Ecology and Management*, 184(1–3), 65–78.

Rennolls, K. (1978). ‘Top Height’; Its Definition and Estimation. *The Commonwealth Forestry Review*, 57(3 (173)), 215–219.

Sharma, M., Amateis, R. L., & Burkhart, H. E. (2002). Top height definition and its effect on site index determination in thinned and unthinned loblolly pine plantations. *Forest Ecology and Management*, 168(1), 163–175.

[https://doi.org/10.1016/S0378-1127\(01\)00737-X](https://doi.org/10.1016/S0378-1127(01)00737-X)

Skovsgaard, J. P., & Vanclay, J. K. (2008). Forest site productivity: A review of the evolution of dendrometric concepts for even-aged stands. *Forestry: An International Journal of Forest Research*, 81(1), 13–31.

<https://doi.org/10.1093/forestry/cpm041>

- Socha, J., Hawryło, P., Stereńczak, K., Miśicki, S., Tymińska-Czabańska, L., Młoczek, W., & Gruba, P. (2020). Assessing the sensitivity of site index models developed using bi-temporal airborne laser scanning data to different top height estimates and grid cell sizes. *International Journal of Applied Earth Observation and Geoinformation*, 91, 102129. <https://doi.org/10.1016/j.jag.2020.102129>
- Socha, J., & Orzeł, S. (2013). Dynamic site index curves for Scots pine (*Pinus sylvestris* L.) in southern Poland. *Sylwan*, 157(1).
- Socha, J., Pierzchalski, M., Bałazy, R., & Ciesielski, M. (2017). Modelling top height growth and site index using repeated laser scanning data. *Forest Ecology and Management*, 406, 307–317.
- Socha, J., Tymińska-Czabańska, L., Bronisz, K., Zięba, S., & Hawryło, P. (2021). Regional height growth models for Scots pine in Poland. *Scientific Reports*, 11(1), 1–14. <https://doi.org/10.1038/s41598-021-89826-9>
- Solberg, S., Kvaalen, H., & Puliti, S. (2019). Age-independent site index mapping with repeated single-tree airborne laser scanning. *Scandinavian Journal of Forest Research*, 34(8), 763–770.
- Straub, C., Stepper, C., Seitz, R., & Waser, L. T. (2013). Potential of UltraCamX stereo images for estimating timber volume and basal area at the plot level in mixed European forests. *Canadian Journal of Forest Research*, 43(8), 731–741. <https://doi.org/10.1139/cjfr-2013-0125>
- Tompalski, P., Coops, N. C., White, J. C., Goodbody, T. R., Hennigar, C. R., Wulder, M. A., Socha, J., & Woods, M. E. (2021). Estimating changes in forest attributes and enhancing growth projections: A review of existing approaches and future

directions using airborne 3D point cloud data. *Current Forestry Reports*, 7(1), 1–24.

Tompalski, P., Coops, N. C., White, J. C., & Wulder, M. A. (2015). Augmenting site index estimation with airborne laser scanning data. *Forest Science*, 61(5), 861–873.

Turner, D., Lucieer, A., & Watson, C. (2012). An automated technique for generating georectified mosaics from ultra-high resolution unmanned aerial vehicle (UAV) imagery, based on structure from motion (SfM) point clouds. *Remote Sensing*, 4(5), 1392–1410.

Tymińska-Czabańska, L., Hawryło, P., & Socha, J. (2022). Assessment of the effect of stand density on the height growth of Scots pine using repeated ALS data. *International Journal of Applied Earth Observation and Geoinformation*, 108, 102763.

Tymińska-Czabańska, L., Socha, J., Hawryło, P., Bałazy, R., Ciesielski, M., Grabska-Szwagrzyk, E., & Netzel, P. (2021). Weather-sensitive height growth modelling of Norway spruce using repeated airborne laser scanning data. *Agricultural and Forest Meteorology*, 308, 108568.

Vanninen, P., Ylitalo, H., Sievänen, R., & Mäkelä, A. (1996). Effects of age and site quality on the distribution of biomass in Scots pine (*Pinus sylvestris* L.). *Trees*, 10(4), 231–238. <https://doi.org/10.1007/BF02185674>

Vauhkonen, J., Maltamo, M., McRoberts, R. E., & Næsset, E. (2014). Introduction to Forestry Applications of Airborne Laser Scanning. In M. Maltamo, E. Næsset, & J. Vauhkonen (Eds.), *Forestry Applications of Airborne Laser Scanning: Concepts and Case Studies* (pp. 1–16). Springer Netherlands. [https://doi.org/10.1007/978-94-017-8663-8\\_1](https://doi.org/10.1007/978-94-017-8663-8_1)

Wallace, L., Lucieer, A., Malenovský, Z., Turner, D., & Vopěnka, P. (2016). Assessment of Forest Structure Using Two UAV Techniques: A Comparison of Airborne Laser Scanning and Structure from Motion (SfM) Point Clouds. *Forests*, 7(3), Article 3.

<https://doi.org/10.3390/f7030062>

White, J. C., Coops, N. C., Wulder, M. A., Vastaranta, M., Hilker, T., & Tompalski, P. (2016). Remote sensing technologies for enhancing forest inventories: A review. *Canadian Journal of Remote Sensing*, 42(5), 619–641.

White, J. C., Stepper, C., Tompalski, P., Coops, N. C., & Wulder, M. A. (2015). Comparing ALS and Image-Based Point Cloud Metrics and Modelled Forest Inventory Attributes in a Complex Coastal Forest Environment. *Forests*, 6(10), Article 10.

<https://doi.org/10.3390/f6103704>

White, J. C., Wulder, M. A., Vastaranta, M., Coops, N. C., Pitt, D., & Woods, M. (2013). The Utility of Image-Based Point Clouds for Forest Inventory: A Comparison with Airborne Laser Scanning. *Forests*, 4(3), Article 3.

<https://doi.org/10.3390/f4030518>

Zhou, M., Lei, X., Duan, G., Lu, J., & Zhang, H. (2019). The effect of the calculation method, plot size, and stand density on the top height estimation in natural spruce-fir-broadleaf mixed forests. *Forest Ecology and Management*, 453, 117574. <https://doi.org/10.1016/j.foreco.2019.117574>

Zielony, R., & Kliczkowska, A. (2012). *Regionalizacja Przyrodniczo-Leśna Polski 2010*.

## **9. Prace naukowe wchodzące w skład rozprawy doktorskiej**



## OPEN ACCESS

## EDITED BY

Qingwang Liu,  
Chinese Academy of Forestry, China

## REVIEWED BY

Lin Zhang,  
Chinese Academy of Sciences (CAS),  
China  
Xueqian Hu,  
China Agricultural University, China

## \*CORRESPONDENCE

Piotr Janiec,  
piotrjaniec2@gmail.com

RECEIVED 18 July 2023

ACCEPTED 28 September 2023

PUBLISHED 12 October 2023

## CITATION

Janiec P, Tymińska-Czabańska L, Hawryło P and Socha J (2023). Development of regional height growth model for Scots pine using repeated airborne laser scanning data. *Front. Environ. Sci.* 11:1260725. doi: 10.3389/fenvs.2023.1260725

## COPYRIGHT

© 2023 Janiec, Tymińska-Czabańska, Hawryło and Socha. This is an open-access article distributed under the terms of the [Creative Commons Attribution License \(CC BY\)](#). The use, distribution or reproduction in other forums is permitted, provided the original author(s) and the copyright owner(s) are credited and that the original publication in this journal is cited, in accordance with accepted academic practice. No use, distribution or reproduction is permitted which does not comply with these terms.

# Development of regional height growth model for Scots pine using repeated airborne laser scanning data

Piotr Janiec<sup>1,2\*</sup>, Luiza Tymińska-Czabańska<sup>1</sup>, Paweł Hawryło<sup>1</sup> and Jarosław Socha<sup>1</sup>

<sup>1</sup>Department of Forest Resources Management, Faculty of Forestry, University of Agriculture in Krakow, Kraków, Poland, <sup>2</sup>Forest Management and Geodesy Bureau, Sekocin Stary, Poland

The rapid development of remote sensing technologies is creating unprecedented opportunities for monitoring and inventorying forest ecosystems. One advantage of remote sensing data is that it can be used to monitor and measure tree growth in near real-time, providing extremely useful data for growth modelling. This study used Aerial Laser Scanning (ALS) data from 14,920 Scots pine stands for the Katowice Regional Directorate of State Forests in southwestern Poland. We tested the possibility of calibrating a regional height growth model for Scots pine for a study area covering 754 thousands of hectares of forests. The model was validated with models developed for Scots pine using the traditional approach based on field data. Our results show that the model calibrated using remote sensing data does not differ significantly from the model calibrated using traditional field measurements from stem analysis. What is more, using a model developed from ALS data gives even better accuracy in modelling height growth than a traditional model calibrated with ground data. Our results are promising for the application of repeated ALS data to the development of regional height growth models, allowing long-term prediction of tree growth under current climatic conditions.

## KEYWORDS

ALS, height growth increment, growth dynamic, ecosystem modelling, site productivity

## 1 Introduction

Forest ecosystems play a key role in the Earth system, thus monitoring and modelling the dynamics of forest growth is of great importance. Many recent studies (Pretzsch et al., 2014; Socha et al., 2020a; Mensah et al., 2021) provided evidence of changing growth patterns in the Northern Hemisphere as a result of climate and anthropogenic pressures. Therefore, near real-time monitoring of forest is needed to understand and model current growth dynamics.

To date, monitoring and modelling of forest growth has mostly been based on data from repeated measurements of permanent sample plots or data from National Forest Inventories (NFIs). However, these approaches require long-term measurements on a large number of plots, which is a major limitation of them (Perin et al., 2013; Raulier et al., 2003). In addition, permanent sample plots are usually established for experimental purposes, mainly at sites with better conditions for tree growth, which limits the range of site conditions represented by the data. Similarly, for NFIs data, results from permanent sample plots are usually representative of large areas and do not ensure representation of rare sites. Therefore,

modelling over large areas using traditional field measurements often doesn't take into account the full variability of growing conditions and leads to simplifications, resulting in over- or underestimation of tree growth (Marziliano et al., 2019; Raulier et al., 2003; Socha and Tymińska-Czabańska, 2019). Another important challenge is to capture short-term growth fluctuations due to climate change on tree growth patterns, which is particularly difficult when using field inventory data. Furthermore, the use of these data sources is associated with high labour and time intensity (Noordermeer et al., 2018). Most of the problems associated with field inventories can be addressed by inventory and monitoring using remote sensing technologies. The spatial and temporal resolution of these technologies overcomes the limitations of the sample plots available from traditional NFI or long-term experimental networks (White et al., 2016).

Unprecedented opportunities for monitoring and inventorying forest ecosystems are arising from the rapid development of remote sensing technologies. One advantage of remote sensing data is that it can be used to monitor and measure tree growth in near real time, providing extremely useful data for growth modelling. One of the main technologies is Light Detection and Ranging (LiDAR). It has been proven useful in measuring forest structure characteristics due to its speed, coverage, and ability in describing 3D attributes (Beland et al., 2019). LiDAR is an accurate tool for measuring topography, but also more complex attributes of the structure of the forests (Jurjević et al., 2020; Lefsky et al., 2002; Wang et al., 2019). LiDAR data have a great capacity to be a tool for the estimation of tree and forest height (Næsset et al., 2004; Holmes et al., 2015). The results of measurements of the height of trees from the upper storey of a stand using the ALS are even much more accurate than the ground measurements that are traditionally used (Jurjević et al., 2020; Wang et al., 2019). LiDAR data are particularly effective in measuring tree height increment (Hopkinson et al., 2008).

Due to its close correlation with timber and biomass increment, tree height is an indirect proxy for estimating forest productivity, so measuring height and growth is important for both forest research and management. Monitoring and assessment of the impact of climate change on site productivity by measuring changes in height growth rate can be extremely useful in assisting researchers and forest managers to develop effective adaptation strategies for sustainable forest management.

The first attempts to use ALS data to calibrate height growth models have been made in recent years (Socha et al., 2017; Tompalski et al., 2015; Tymińska-Czabańska et al., 2021). However, these models have been developed for relatively small areas at a local scale, with a relatively low degree of variation in site conditions. Increasing availability of data from repeated ALS acquisitions enables growth monitoring and model development for increasingly larger areas. Spreading the data allows calibrating growth models for whole regions or even countries. Therefore, this study aims to test and demonstrate that bi-temporal ALS height growth data collected at an unprecedented quantitative and spatial scale from 16 688 232 trees growing in 27 753 stands are robust for modelling height growth.

The study was carried out for Scots pine, which is one of the most important European forest tree species. In Poland, it is the most widespread and most important species in both ecological and economic terms (Zajęczkowski et al., 2018). Thus, the ability to

monitor increment and develop growth models for Scots pine using repeated ALS data may be of interest to forest science and has great practical importance for forest management. To achieve our objectives, we tested the possibility of calibrating a height growth model for Scots pine using wall-to-wall data from the entire Katowice Regional Directorate of State Forests in southern Poland covering 754 thousands of hectares of forests. In addition to demonstrating the ability to calibrate the height growth model for the study area, the developed model was tested against models developed for Scots pine using the traditional approach based on field data.

## 2 Materials and methods

### 2.1 Study area description

The study area covers Scots pine stands in the Katowice Regional Directorate of State Forests located in three natural forest regions of southwestern Poland (Figure 1). The main species within the study area is Scots pine (about 66%) with a mean age of stands 56 years. For model calibration, pine stands for which ALS data were available for two different years were selected. The selected stands had a Scots pine share of more than 70% from Scots pine and were aged between 10 and 140 years.

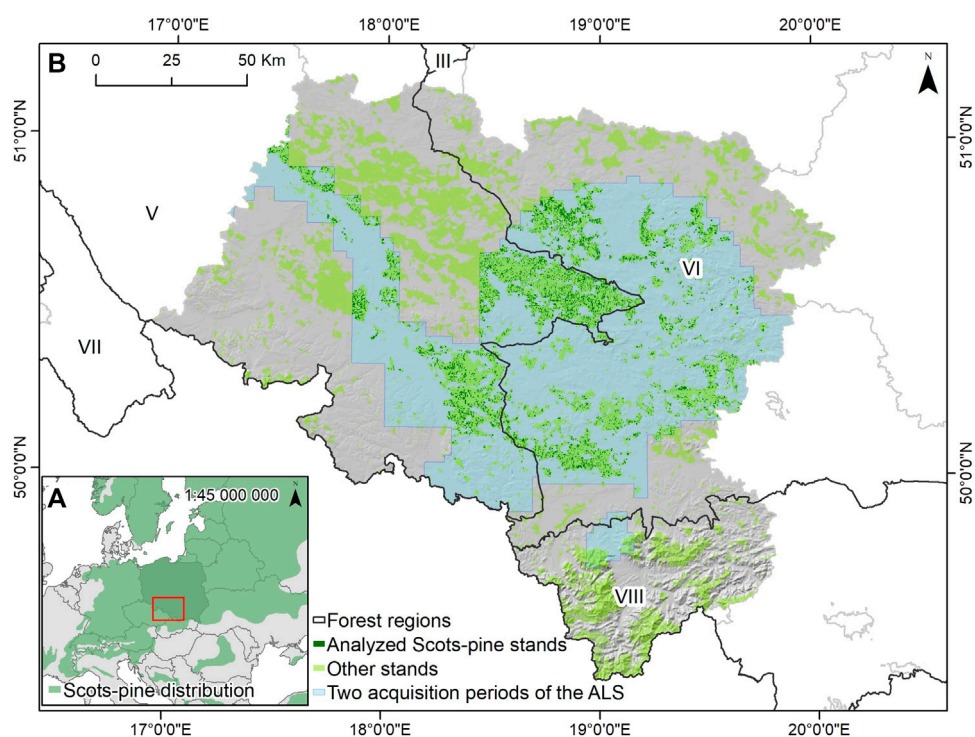
The study area is located within two natural forest regions. 14 920 stands were located in Region V (14 920) and 12 833 were located in region VI. Natural forest regions in Poland are adopted as regionalisation units. They are characterised by high natural diversity, especially in terms of climatic and geological conditions, naturally occurring ranges of the main forest-forming tree species, the presence and distribution of natural landscapes, and the distribution of primary units of potential natural vegetation (Zielony and Kliczkowska, 2012).

### 2.2 TH estimation from repeated ALS data

The ALS data were collected from the General Office of Geodesy and Cartography (GUGiK) repository and are publicly available on the Geoportal webpage (<https://mapy.geoportal.gov.pl/>). The ALS data were acquired in leaf-off conditions which is significant in the tree stands with well-developed deciduous undergrowth during the classification of ground points and therefore determination of the top height. The mean density of the data was 4 points/m<sup>2</sup>. The positional accuracy of the ALS was not worse than 0.5 m. The acquisition period is between 2011–2019 years however most of the data were acquired in the 2011 and 2019 years (Table 1).

We used the lidR package in the R environment (Computing, 2013) for point cloud processing (Roussel et al., 2020). We used the “normalize\_height” algorithm to preprocess the point cloud for each date and normalize it. The canopy height models (CHMs) have been created with the “p2r” algorithm. The spatial resolution of the CHMs was 1.0 m.

For the TH (top height) estimation we used the modified approach proposed by Socha et al. (2020a) (Figure 2). To avoid the edge effect we have created, an internal buffer (15 m) for each forest stand. The CHMs were resampled into 10 × 10 grid cells. For

**FIGURE 1**

(A) Location of the study area within the distribution of Scots pine in Central Europe. (B) Distribution of the tree stands within the study area, where two periods ALS data were available (light blue). Analyzed tree stands (share of Scots pine above 70%) are in dark green other stands are in light green.

**TABLE 1 Time and percentage of the bi-temporal aerial laser scanning (ALS) data acquisition in the analyzed tree stands.**

| First ALS acquisition year | Second ALS acquisition year | Percentage of the analyzed stands [%] |
|----------------------------|-----------------------------|---------------------------------------|
| 2011                       | 2019                        | 59.40                                 |
| 2012                       |                             | 22.77                                 |
| 2013                       |                             | 13.17                                 |
| 2014                       |                             | 4.62                                  |
| 2015                       |                             | 0.04                                  |

each year in each forest subdivision, the TH has been calculated as the average of two-thirds of the highest values in the  $10 \times 10$  grid. We excluded tree stands with the TH variance in the forest subdivision higher than 2 and the percentage of no data higher than 0.5. We assumed that these tree stands are in the process of reconstruction or there are outliers caused by tilting the top of the tree to another cell.

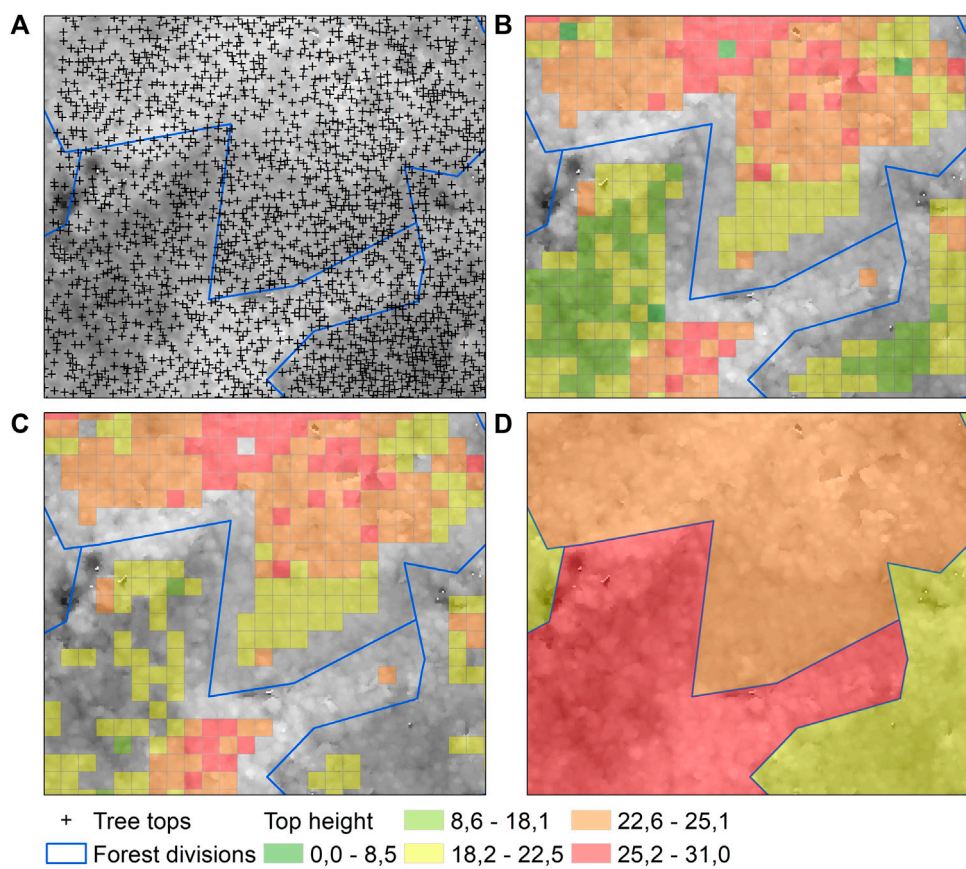
To remove the outliers we have applied the standard outlier elimination proposed by Tukey (1977) and used by Socha et al. (2017) for the TH estimation based on the ALS data. We calculated differences between TH in two subsequent periods for each grid cell. Outliers were separated using lower and upper quartiles (Q1–Q3), and the interquartile range (IQ) was calculated. We defined extreme values in the tails of the distribution by the lower inner bound  $Q_1 - 1.5 \times IQ$  and the upper inner bound  $Q_3 + 1.5 \times IQ$  according to Tukey (1977), which picked  $1.5 \times IQ$  as the demarcation line for

outliers. The reasonableness of this measure for bell-curve-shaped data means that usually, about one percent of the data will ever be outliers. The outliers elimination has been performed for age classes based on the 20 years interval.

### 2.3 Height growth models calibration

For the height growth model calibration we have used the dynamic equation based on the Bertalanffy–Richards function using the generalized algebraic difference approach (GADA), proposed by (Cieszewski, 2001):

$$TH = TH_1 \frac{T_1^{\beta_1} (T_1^{\beta_1} R + \beta_2)}{T_1^{\beta_1} (T_1^{\beta_1} R + \beta_2)}$$

**FIGURE 2**

(A) Tree tops detected based on the canopy height model (CHM) generated from the ALS data. (B) Top height (TH) calculated in the  $10 \times 10$  grid cells, with the consideration of an internal buffer (15 m) for each forest stand. (C) Grid cells after the exclusion of cells with the TH lower than two-thirds of the highest values in each subdivision. (D) TH calculated for each subdivision.

**TABLE 2** The number of growth series and the parameters of the global and regional height growth models used for the validation of the aerial laser scanning (ALS) models (Socha et al., 2021b).

| Model     | Number of growth series | b1      | b2       | b3      |
|-----------|-------------------------|---------|----------|---------|
| SA-GLOBAL | 855                     | 1.363   | 5920.904 | 30.443  |
| SA-V      | 39                      | 1.39    | 3325.004 | 36.6838 |
| SA-VI     | 311                     | 1.44385 | 21667.2  | -9.1771 |

where

$$R = Z_0 + \left( Z_0^2 + \frac{2\beta_2 TH_1}{T_1^{\beta_1}} \right)^{0.5}$$

$$Z_0 = TH_1 - \beta_3$$

and  $\beta_1$ ,  $\beta_2$ , and  $\beta_3$  are global model parameters, TH is the top height at age T and  $TH_1$  is the top height at age  $T_1$ .

We have used all prepared and filtered earlier data. We fitted the global parameters and site-specific parameters simultaneously using the nonlinear least-squares optimization and the Levenberg-Marquardt algorithm (Moré, 2006) in the R environment (Computing, 2013) using the gsnls library. Levenberg-Marquardt algorithm, attempt to find a local minimum of the objective function

by making iterative steps in the direction of the solution informed by the gradient of a first- or second-order Taylor approximation of the nonlinear objective function (Moré, 2006). As starting parameters we choose  $b1 = 1$ ,  $b2 = 10000$ , and  $b3 = 28$ , according to (Socha et al., 2017).

Due to the significant variation in growth conditions within the study area, we decided to develop three height growth models using ALS data. The first model has been developed for the entire study area, while the other two models have been developed for areas located in the natural forest region V and VI respectively. For each model, we used the maximum number of iterations. To estimate the model significance of the calibrated parameters we performed a t-test and calculated Standard Error (SE), t-value and p-value.

**TABLE 3** Parameters and fit characteristics of the regional top height growth models for the Scots pine for Katowice Regional Directorate of State Forests based on the bi-temporal aerial laser scanning (ALS) data.

| Model       | Parameter | Estimate     | Standard error | t-value      | p-value     |
|-------------|-----------|--------------|----------------|--------------|-------------|
| ALS- Global | $b_1$     | 1.14711      | 0.01518        | 75.571       | <2e-16      |
|             | $b_2$     | 372.63998    | 245.73587      | 1.516        | 0.129       |
|             | $b_3$     | 51.61396     | 1.09208        | 47.262       | <2e-16      |
| ALS -V      | $b_1$     | 1.166513208  | 0.016104574    | 72.43365792  | <2e-16      |
|             | $b_2$     | 2748.341304  | 347.4405851    | 7.910248318  | 2.93773E-15 |
|             | $b_3$     | 35.49450202  | 1.472985185    | 24.09698507  | 1.255E-123  |
| ALS -VI     | $b_1$     | 1.305076733  | 0.017488256    | 74.62589279  | <2e-16      |
|             | $b_2$     | -778.7063391 | 248.7820607    | -3.130074318 | 0.001756058 |
|             | $b_3$     | 53.85751441  | 0.832881799    | 64.66405494  | <2e-16      |

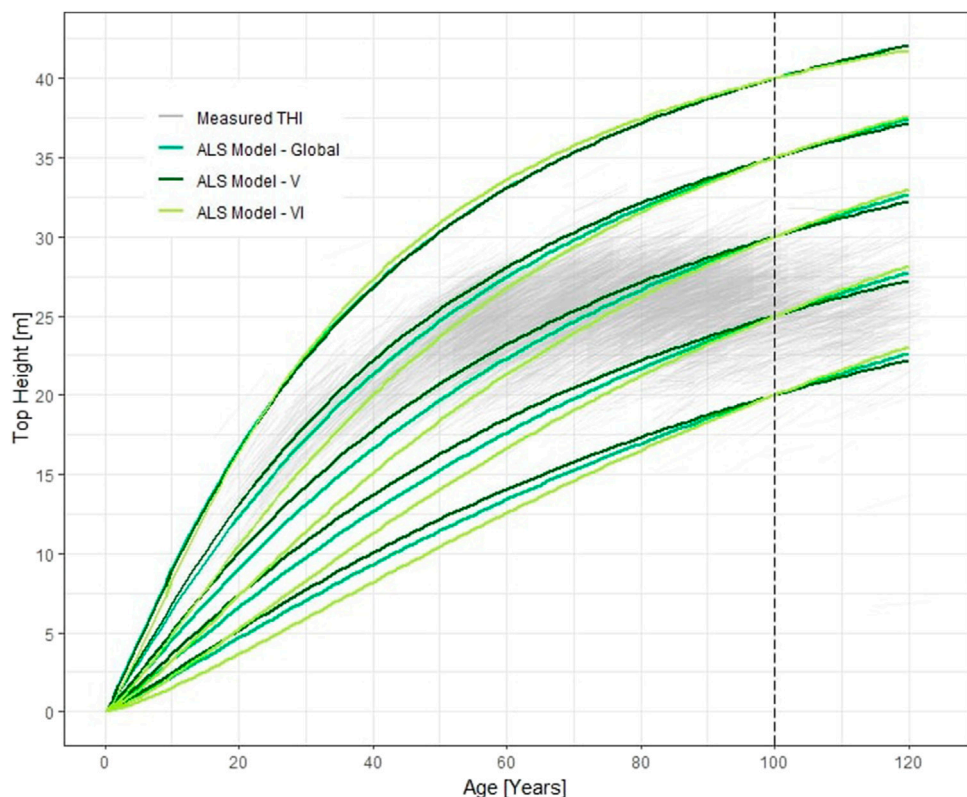


**FIGURE 3**

Growth trajectories of three top height growth models developed using aerial laser scanning (ALS) data against the observed top height increment (THI) values from ALS measurements over two periods (thin grey), black dashed line represent base age.

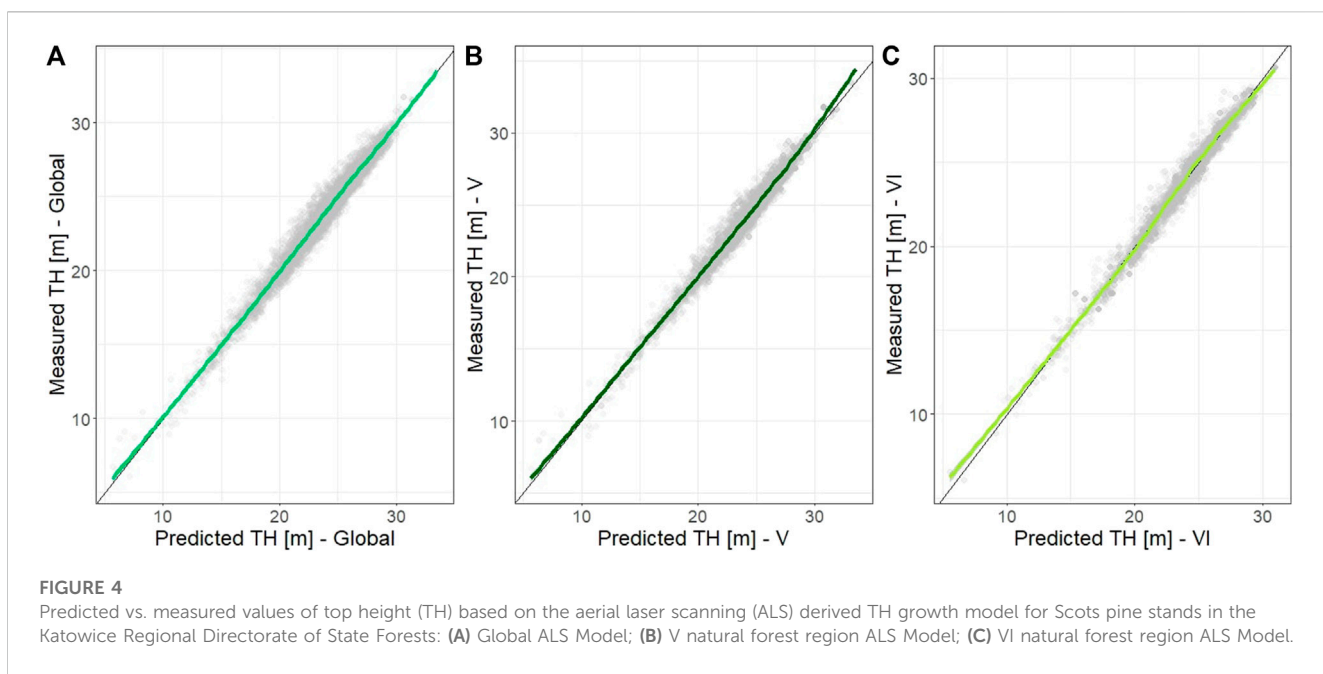
## 2.4 Models validation

We compared the obtained models with the height growth models for Scots pine in Poland developed based on Stem Analysis (SA) data (Socha et al., 2021a) (Table 2). Models calibrated on SA data were used as a reference. Model developed using repeated ALS data for whole study area was compared with global height growth models for Scots pine for Poland. Models

developed for areas located in the natural forest regions V and VI was compared with SA regional models.

For each model we have calculated mean absolute error (MAE) and RMSE (root mean squared error) based on the equations:

$$RMSE(y, \hat{y}) = \sqrt{\frac{\sum_{i=0}^{N-1} (y_i - \hat{y}_i)^2}{N}}$$



$$\text{MAE}(y, \hat{y}) = \frac{\sum_{i=0}^{N-1} |y_i - \hat{y}_i|}{N}$$

where,  $y_i$  is the measured value;  $\hat{y}_i$  is the predicted value; i is the summation index; N is the number of cases. We also calculated and adjusted  $R^2$  as a measure of model fit.

## 3 Results

### 3.1 ALS-derived TH growth model

By estimating the parameters of the growth function, we developed three TH growth models for the Scots pine stands based on the bi-temporal ALS data (Table 3).

The parameters fitted based on the ALS data differ from regional and global parameters for the models developed from SA. Across the range of site conditions, the developed global ALS model demonstrate a good fitting to the data (Figure 3). For the sites with the highest productivity, the course of the model curves is almost identical. Some slight differences are visible in the younger stands growing on more poor site conditions.

The modeled TH values did not differ significantly from the reference data (Figure 4). The smooth lines were well fitted across most of the TH observation distributions, only on the edge of the distribution slight differences were visible.

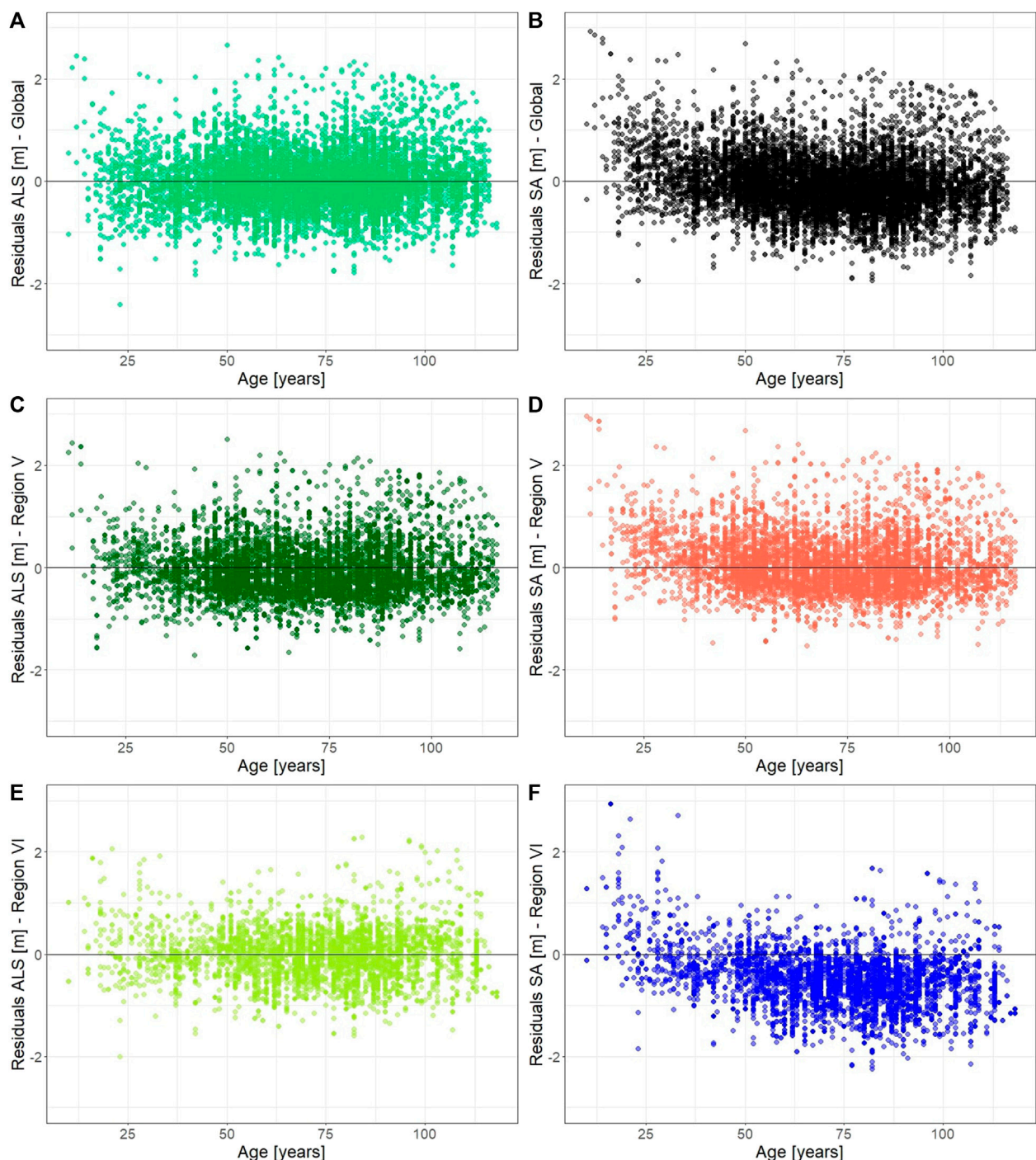
Errors in TH estimation for the ALS-derived models were not correlated with stand age (Figure 5). In most cases the errors in TH estimation are within about 1 m. The ALS models were characterized by lower error values, comparing to the SA models. The residuals are evenly distributed across the Global and V region models. For the model from the VI region, more residuals have negative values, especially for the SA model, where majority of the residuals are below 0.

Using the global ALS model, a site index map was produced for the study area (Figure 6). As the site productivity indicator we used the site index (SI), which is commonly used indicator of the site productivity assessment in the forestry (Hägglund and Lundmark, 1977). We calculated the SI as the height that the tree stand will reach at the base age of 100 years. Our results show large variation in site conditions throughout the study area. These differences are also visible within the forest regions. The V-forest region is characterized by higher SI, especially in the north-western part, while Scots pine stands in the central part of Region V and most stands in Region VI are characterized by substantially lower site productivity. The majority of the stands in Region VI are characterized by an SI of between 20 and 35 m.

### 3.2 Models validation

In the first step, we compared the ALS-derived global model with the global model developed by Socha et al. (2021b) for Scots pine in Poland based on SA data. We found that the model TH growth trajectories developed from the ALS data do not differ significantly from the global model developed from the SA data (Figure 7). Compared to the global model for Poland developed from SA data, the model calibrated with ALS data showed only slightly higher values of height increment for younger stands from the most productive sites.

Next, we compared the regional ALS-derived model with models built from SA data for natural forest region V and VI (Figure 8). The ALS model curves for stands located in V Natural forest region was compared with SA model for region V. Models show a high similarity, only in the younger stands especially growing on poor site conditions slight differences are noticeable (Figure 8A). Larger differences are evident when comparing the ALS model with the model-based SA data from natural forest region VI (Figure 8B).

**FIGURE 5**

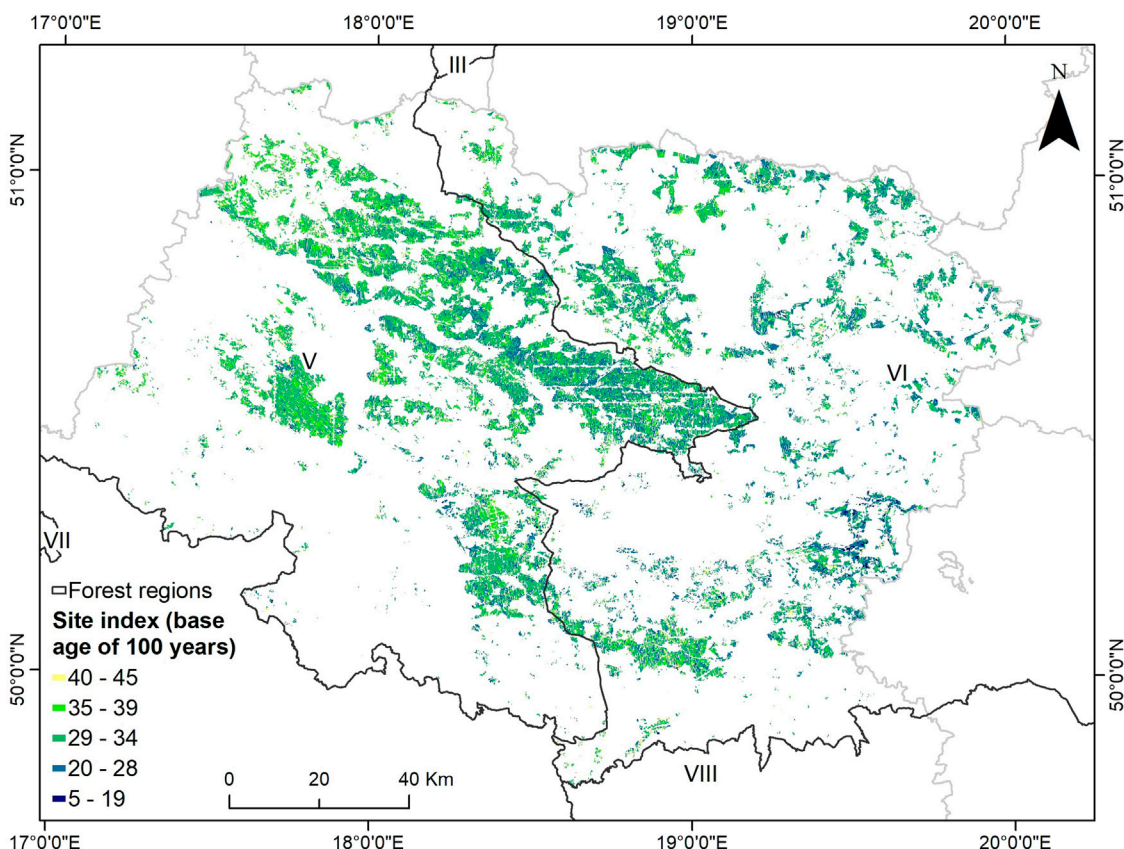
Residual top height versus age and aerial laser scanning (ALS) derived top height based on bi-temporal ALS data for the Katowice Regional Directorate of State Forests Scots pine stands: Global ALS (A) and Stem Analysis (SA) Models (B); V natural forest region ALS (C) and SA Models (D); VI natural forest region ALS (E) and SA Models (F).

While, for the most productive sites the model curves for these models are very similar, for the poorest sites, the TH growth model developed from ALS data shows an overall lower increment than the model developed from SA data.

Despite satisfactory model-fitting results, the THI trajectories for the V (Figure 8C) and VI (Figure 8D) natural forest regions

developed with the use of ALS data slightly differed from the SA model THI trajectories. According to the THI from ALS data, the culmination of growth occurs faster and THI is slight higher, especially in the stands with the higher SI.

Finally, we compared the fit statistics for three ALS-derived models with the two regional models and the global model



developed on SA data (Table 4). The ALS-derived TH was taken as reference data. All models are characterized by the similar  $R^2$ . However, the all ALS models have lower RMSE and MAE errors. The highest RMSE and MAE (0.645 m, 0.519 m) have a regional model for natural forest region VI developed using SA. In comparison the ALS model for the VI natural forest region has lowest RMSE (0.48 m) and MAE (0.36 m) errors.

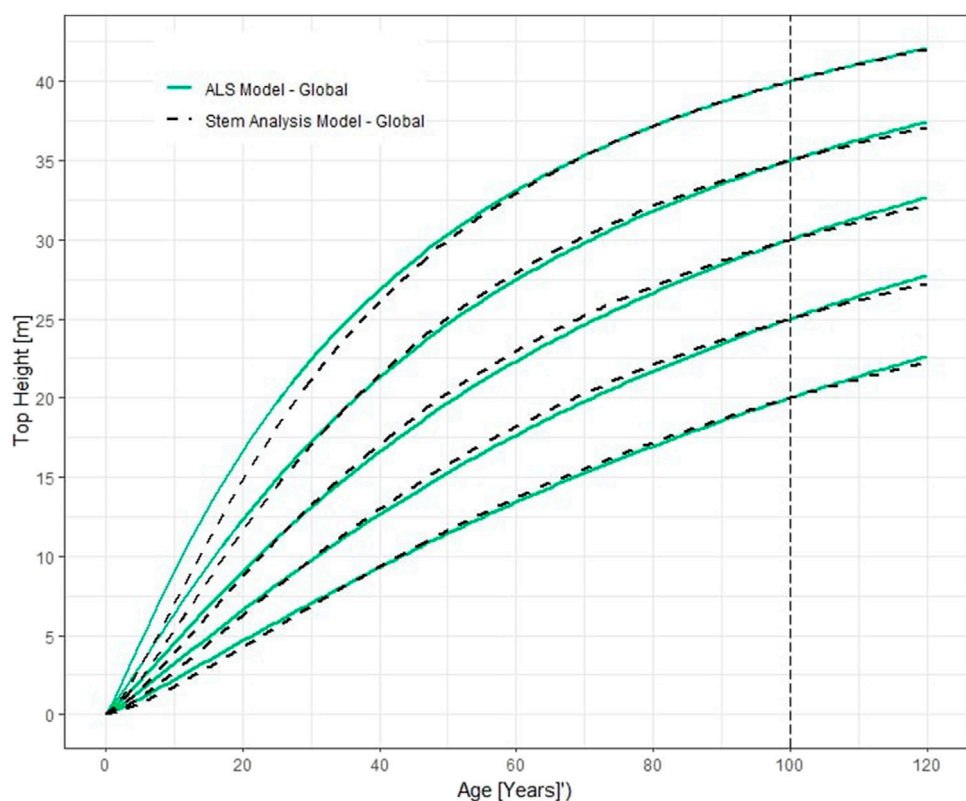
The residual distribution is quite similar for all models (Figure 9). However, it can be seen that the SA models have higher errors, especially for the natural forest region VI. Both positive and negative residuals are evenly distributed across the models, except the SA model from the VI natural forest region. In all the models we can see that the outliers are higher in the lower stands where there are a smaller number of observations.

## 4 Discussion

Our study demonstrate the usefulness of ALS data for calibration height growth models for large areas. We calibrated the height growth model of Scots pine stands in the Katowice Regional Directorate of State Forests based on the bi-temporal ALS measurements. Our results show that the model calibrated using remote sensing data does not differ substantially from the model calibrated using

traditional field measurements from SA. Bi-temporal ALS data have been used previously to calibrate growth models, but for relatively small areas (Socha et al., 2017; Socha et al., 2020b; Tompalski et al., 2015; Tymińska-Czabańska et al., 2021). The growth trajectories obtained from models developed on ALS data are similar to those obtained from models calibrated on SA data.

We found that model curves constructed from ALS data for entire study area were almost identical to model curves derived from SA data. Very slight differences can be observed in the younger and middle age classes (Figure 5). However, the ALS model was developed based on data from 27 753 stands while the SA model was based on data from 855 trees. Therefore, the model developed from ALS data may even better reflect the growth patterns currently observed for Scots pine on the most productive sites of the study area. ALS models developed for stands located in natural forest region V and VI are characterised by slightly different model curves, but also show a very high similarity to the models developed on the basis of data from SA. The model developed on the basis of the ALS for natural region VI shows larger differences in the course of growth trajectories, especially in the lowest productivity areas, compared to the SA model. This is most likely due to the local specificity of the site conditions. We also found that the model calibrated with ALS data has better accuracy in the prediction of height growth than the traditional model calibrated with field data.

**FIGURE 7**

Comparison of growth curves for top height global model calibrated with aerial laser scanning (ALS) derived point cloud (green, thick lines) and global Stem Analysis model (dashed, black line).

Compared to the SA data, the period of availability of the ALS data is relatively short, which is one of the limitations in modelling forest growth (Coops, 2015). Moreover, in the case of growth models developed using data from a short observation period, height growth trajectories may be affected by weather conditions between ALS acquisitions (Tymińska-Czabańska et al., 2021). However, Hopkinson et al. (2008) observed that after the 5-year ALS observation period the uncertainties in the THI decreased to 6%. Furthermore, the advantage of the ALS data on height growth over a short period of time is that they reflect the actual growth trends. In addition, the ALS makes it possible to collect data from the entire region, which makes it possible to cover the whole distribution of forest age and site conditions. By calibrating the growth model using SA data, we are able to capture long-term trends. However, due to climate change, such models may reflect historical growth patterns that are not necessarily observed under current climate conditions. Moreover, Raulier et al. (2003) claim that SA models often overestimate the TH increment when compared to the permanent sample plots. In contrast, ALS data reflect current growth trends. ALS data allow to observe changes in the height of individual stands and trees for the whole area of interest, and therefore may better represent height growth trends compared to sample plot data or growth trajectory reconstructions from SA traditionally used in forestry research. In addition, a major advantage of remote sensing data is that it can be collected using a consistent methodology. Remote sensing provides a standardized

way of collecting data, reducing the risk of human error and bias (Jurjević et al., 2020). This allows more reliable comparisons to be made over time and between regions.

Currently, the main limitation related to the applicability of multi-temporal ALS data in monitoring and modelling forest growth is connected with the availability of repeated ALS data (Tompalski et al., 2021). Another limitation is the need for data from a specific point in the growing season. If ALS is acquired during the height growth period, there is no certainty that growth from a given year is already included in the measurement. For this reason, data collected outside the height growth period is preferable. Remote sensing can also be used to accurately measure the height of trees in the upper canopy layer. Trees growing below the canopy are more difficult to detect and the accuracy of the measurement is much lower due to the number of individual laser beams (Xu et al., 2021). However, over time, as ALS becomes more widely used, it may become an alternative to traditional data collection methods, especially for measuring forest height and growth increment (Tompalski et al., 2021). Another limitation of ALS data to date has been its accuracy with respect to point cloud density (Nilsson et al., 2017). However, developments in remote sensing technologies are increasing the availability of dense point clouds covering entire countries (Kurczyński and Bakula, 2013). The use of multi-temporal data appears to be very promising, as it avoids the problems associated with short-term growth fluctuations driven by weather conditions, while at the same time exploiting the advantage of

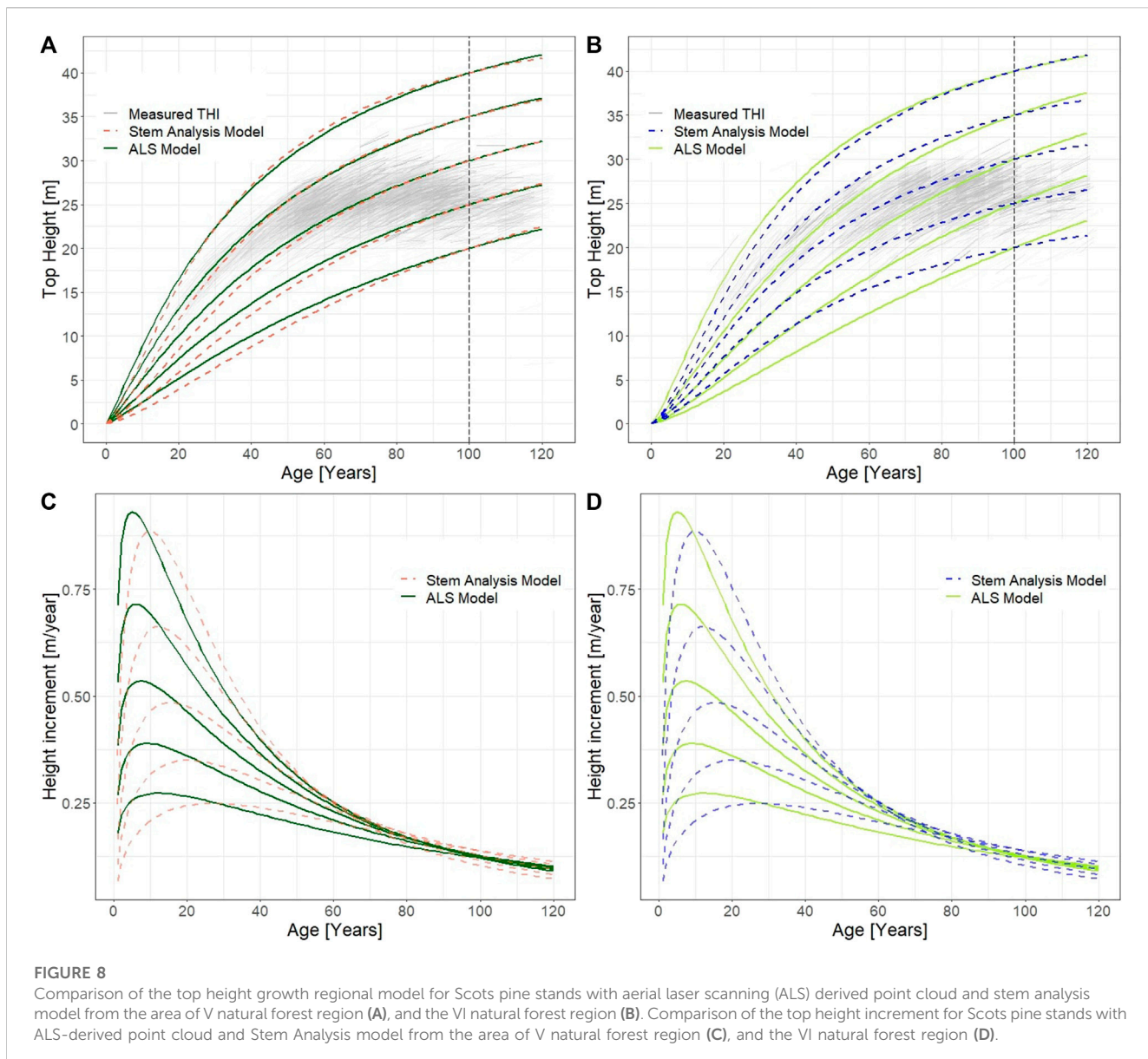


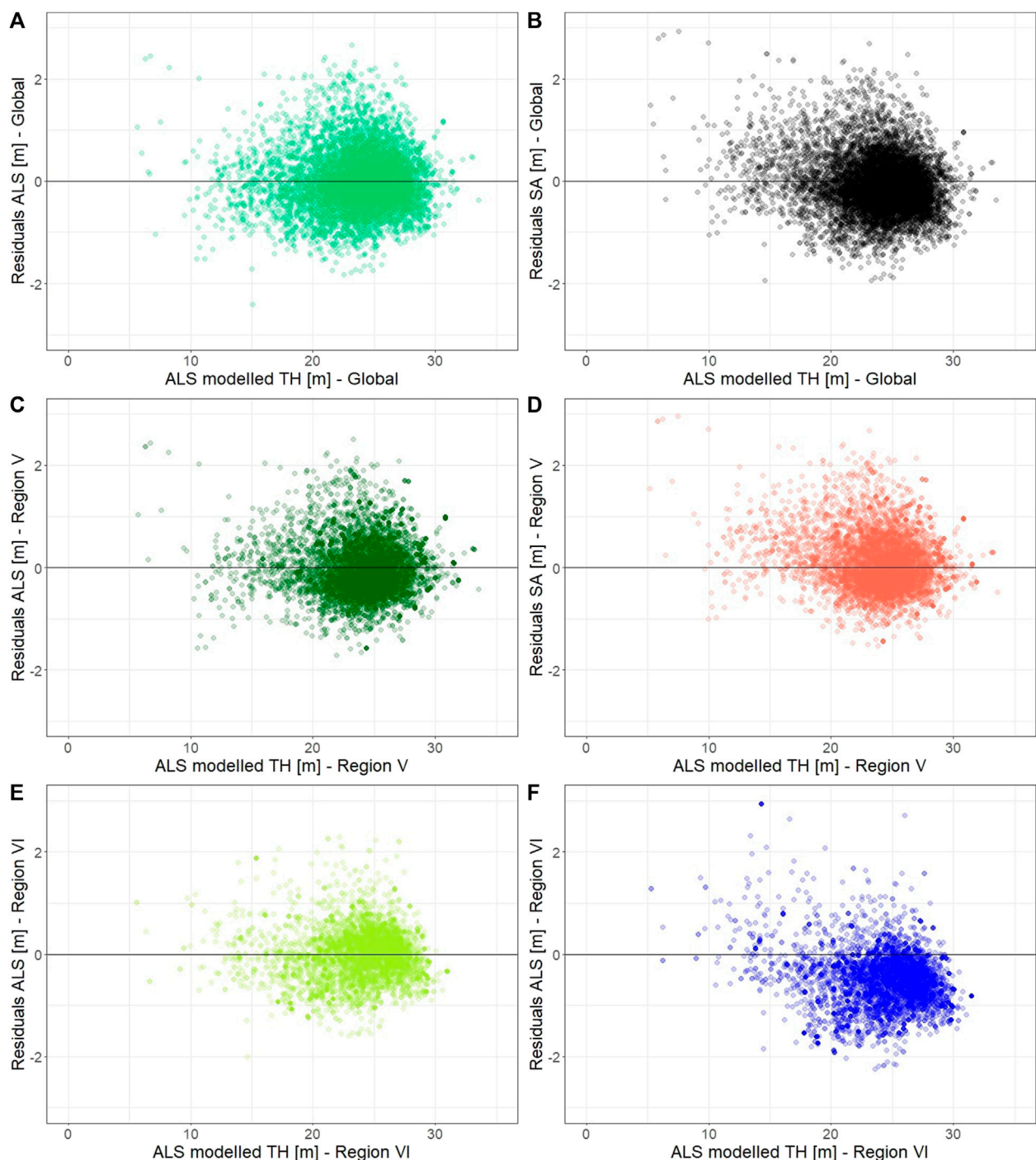
**TABLE 4** Fit statistics of the top height growth models developed on the basis of aerial laser scanning (ALS) data and of the top height growth models developed on the basis of Stem Analysis (SA) data.

|       | ALS—global | ALS—V | ALS—VI | SA—V | SA—VI | SA—global |
|-------|------------|-------|--------|------|-------|-----------|
| RMSE  | 0.54       | 0.53  | 0.48   | 0.56 | 0.65  | 0.57      |
| MAE   | 0.41       | 0.41  | 0.36   | 0.43 | 0.52  | 0.43      |
| $R^2$ | 0.97       | 0.97  | 0.98   | 0.97 | 0.97  | 0.97      |

models that capture current growth trends. Therefore, ALS appears to be a promising source of data for height growth modelling. It is expected that repeated ALS will become increasingly important and a common data source in forestry (Socha et al., 2020a; Tompalski et al., 2021). The biggest advantage of remote sensing is its ability to cover large geographical areas, allowing us to monitor forest growth on a global scale (Tompalski et al., 2021). It would be incredibly time-consuming and costly to collect data on a similar scale using

field measurements. In addition, remote sensing data can be collected repeatedly over the same area, allowing time-series analysis. This allows scientists to track changes in forest growth and health status over time, which can provide important insights about the effects of climate change, pest outbreaks or other disturbances (Tymińska-Czabańska et al., 2022).

What is important, some remote sensing technologies can provide near real-time data, making it possible, for example, to

**FIGURE 9**

Top height residuals against values predicted from aerial laser scanning (ALS) derived models and three models based on the Stem Analysis (SA) for Scots pine stands in Katowice Regional Directorate of State Forests: Global ALS (A) and Stem Analysis (SA) Models (B); V natural forest region ALS (C) and SA Models (D); VI natural forest region ALS (E) and SA Models (F).

track the response of forests to changing climatic conditions. A model developed using the most up-to-date data provides a reliable prediction of forest growth under currently observed climatic conditions, which may differ significantly from those observed in the past (Socha et al., 2021a; Mensah et al., 2021). In the future, different remote sensing data fusion should be utilized. The use of

machine learning methods allows to implementation of robust models for the site productivity assessment (Bomburun et al., 2020). The implementation of optical remote sensing data and climatic variables could substantially increase the results of the ALS model (Rahimzadeh-Bajiran et al., 2020; Schneider et al., 2023; Tymińska-Czabańska et al., 2021). The data fusion

approach could help us to create and integrate the forest productivity and forest growth models from local to global scale (Schneider et al., 2023). This is particularly important for both the adaptation of forests to climate change and the provision of ecosystem services. For example, it can help identify areas of environmental stress (Tymińska-Czabańska et al., 2022) or assess the effectiveness of forest management and adaptation efforts. In this context, regional height growth models can be a tool to predict the future role of forest tree species under changing climatic conditions, which can help to select appropriate forest management strategies.

Numerous studies have shown that growth modelling, especially on a regional scale, provides information for a more accurate assessment of forest growth and should be an important component of regional forest planning and management (Coops et al., 2007; Coops et al., 2010; Socha et al., 2020b). Variability in growth dynamics can lead to differences in height growth trajectories due to local variations in climate, soils and genotype-environment interactions (Viet et al., 2022). Thus, regional variation in growth trajectories can lead to inappropriate estimates of site productivity (Socha et al., 2021b). This can result in under- or overestimation of growth potential at a given site (Monserud and Rehfeldt, 1990; González et al., 2005). Research results indicate that variability due to environmental factors is the main reason why a more flexible approach should be used in the development of height growth models in order to accurately reflect height growth variability at the regional scale (Bravo-Oviedo et al., 2008). Therefore, more reliable predictions of stand growth and more accurate forest management decisions can be made by taking into account the local specificity of site conditions through the construction of regional growth models. Both biomass production and carbon sequestration are closely linked to the dynamics of height growth. Furthermore, one of the most important demands of modern forestry is to determine the global CO<sub>2</sub> sequestration capacity of forests (Smith et al., 2014; Shukla et al., 2019). A reliable assessment of the biomass production and carbon sequestration capacity of forest ecosystems therefore depends on the ability to adequately estimate forest growth (Pretzsch, 2009; Bontemps and Bouriaud, 2014; Coops, 2015). Therefore, monitoring regional forest growth helps scientists understand the role of forests in the global carbon cycle, which is crucial for climate change research and mitigation strategies.

Research aimed at developing forest growth models is of great importance both for the development of forest science and for forest management practice. Further research into remote sensing data processing methods and their application in forestry can contribute to the scientific understanding of many forest ecosystem processes, which is particularly important in an era of climate change and anthropopression. Previous studies have demonstrated the feasibility of developing local height growth models using ALS data. Our study demonstrates the high suitability of bi-temporal ALS data for the development of regional models. The regional variability in site conditions and most recent data should be taken into account when modelling height growth, especially if up-to-date models are desired. The longer observation period with multi-temporal ALS data collections and the extension of the study

area to the country level may allow further development of the proposed approach.

## 5 Conclusion

We have demonstrated that ALS data can be used for height growth modelling on a regional scale. We developed three TH growth models for the Scots pine stands based on the bi-temporal ALS data and validated them with models developed for Scots pine using the traditional approach based on field data. Our results show that the model calibrated with remote sensing data does not differ significantly from the model calibrated with traditional field measurements from stem analysis, and that the model calibrated with ALS data has better accuracy than the traditional model calibrated with field data. Our study highlights that modelling height growth for regions allows local patterns of growth to be captured. This may be important for determining forest productivity at the scale of regions, as well as having implications for regional forest management. Our results are also promising for long-term prediction of tree growth under current climatic conditions using repeated ALS data for the development of regional height growth models.

## Data availability statement

Publicly available datasets were analyzed in this study. This data can be found here: [https://mapy.geoportal.gov.pl/imap/Imgp\\_2.html?gmap=gp0](https://mapy.geoportal.gov.pl/imap/Imgp_2.html?gmap=gp0).

## Author contributions

PJ: Conceptualization, Data curation, Formal Analysis, Methodology, Validation, Writing—original draft. LT-C: Conceptualization, Writing—original draft. PH: Conceptualization, Writing—review and editing. JS: Conceptualization, Funding acquisition, Writing—review and editing.

## Funding

The authors declare financial support was received for the research, authorship, and/or publication of this article. This research was funded by General Directorate of State Forests in Poland under the project entitled: Modele przyrostu miąższości głównych gatunków lasotwórczych Polski (Volume increment models for the main forest-forming species of Poland), contract no. EZ.271.3.20.2021.

## Conflict of interest

The authors declare that the research was conducted in the absence of any commercial or financial relationships that could be construed as a potential conflict of interest.

## Publisher's note

All claims expressed in this article are solely those of the authors and do not necessarily represent those of their affiliated

organizations, or those of the publisher, the editors and the reviewers. Any product that may be evaluated in this article, or claim that may be made by its manufacturer, is not guaranteed or endorsed by the publisher.

## References

- Beland, M., Parker, G., Sparrow, B., Harding, D., Chasmer, L., Phinn, S., et al. (2019). On promoting the use of lidar systems in forest ecosystem research. *For. Ecol. Manag.* 450, 117484. doi:10.1016/j.foreco.2019.117484
- Bombrun, M., Dash, J. P., Pont, D., Watt, M. S., Pearse, G. D., and Dungey, H. S. (2020). Forest-Scale Phenotyping: Productivity Characterisation Through Machine Learning. *Front. Plant Sci.* 11, 99. doi:10.3389/fpls.2020.00099
- Bontemps, J.-D., and Bouriaud, O. (2014). Predictive approaches to forest site productivity: Recent trends, challenges and future perspectives. *Forestry* 87 (1), 109–128. doi:10.1093/forestry/cpt034
- Bravo-Oviedo, A., Tomé, M., Bravo, F., Montero, G., and del Río, M. (2008). Dominant height growth equations including site attributes in the generalized algebraic difference approach. *Can. J. For. Res.* 38 (9), 2348–2358. doi:10.1139/X08-077
- Ciesewski, C. J. (2001). Three methods of deriving advanced dynamic site equations demonstrated on inland Douglas-fir site curves. *Can. J. For. Res.* 31 (1), 165–173. doi:10.1139/x00-132
- Computing, Rf. (2013). *R: a language and environment for statistical computing*. Vienna: R Core Team.
- Coops, N. C. (2015). Characterizing forest growth and productivity using remotely sensed data. *Curr. For. Rep.* 1, 195–205. doi:10.1007/s40725-015-0020-x
- Coops, N. C., Gillanders, S. N., Wulder, M. A., Gergel, S. E., Nelson, T., and Goodwin, N. R. (2010). Assessing changes in forest fragmentation following infestation using time series Landsat imagery. *For. Ecol. Manag.* 259 (12), 2355–2365. doi:10.1016/j.foreco.2010.03.008
- Coops, N. C., Hilker, T., Wulder, M. A., St-Onge, B., Newnham, G., Siggins, A., et al. (2007). Estimating canopy structure of Douglas-fir forest stands from discrete-return LiDAR. *Trees* 21, 295–310. doi:10.1007/s00468-006-0119-6
- González, J. G. Á., González, A. D. R., Soalleiro, R. R., and Anta, M. B. (2005). Ecoregional site index models for *Pinus pinaster* in Galicia (northwestern Spain). *Ann. For. Sci.* 62 (2), 115–127. doi:10.1051/forest:2005003
- Hägglund, B., and Lundmark, J.-E. (1977). *Site index estimation by means of site properties*.
- Holmes, K. R., Coops, N. C., Nelson, T. A., Fontana, F. M., and Wulder, M. A. (2015). Indicators of vegetation productivity under a changing climate in British Columbia, Canada. *Appl. Geogr.* 56, 135–144. doi:10.1016/j.apgeog.2014.11.020
- Hopkinson, C., Chasmer, L., and Hall, R. J. (2008). The uncertainty in conifer plantation growth prediction from multi-temporal lidar datasets. *Remote Sens. Environ.* 112 (3), 1168–1180. doi:10.1016/j.rse.2007.07.020
- Jurčević, L., Liang, X., Gašparović, M., and Balenović, I. (2020). Is field-measured tree height as reliable as believed – Part II, A comparison study of tree height estimates from conventional field measurement and low-cost close-range remote sensing in a deciduous forest. *ISPRS J. Photogrammetry Remote Sens.* 169, 227–241. doi:10.1016/j.isprsjprs.2020.09.014
- Kurczyński, Z., and Bakula, K. (2013). Generowanie referencyjnego numerycznego modelu terenu o zasięgu krajowym w oparciu o lotnicze skanowanie laserowe w projekcji ISOK. *Arch. Fotogram. Kartogr. i Teledetekcji*, 59–68.
- Lefsky, M. A., Cohen, W. B., Parker, G. G., and Harding, D. J. (2002). Lidar Remote Sensing for Ecosystem Studies: Lidar, an emerging remote sensing technology that directly measures the three-dimensional distribution of plant canopies, can accurately estimate vegetation structural attributes and should be of particular interest to forest, landscape, and global ecologists. *BioScience* 52 (1), 19–30. doi:10.1641/0006-3568(2002)052[0019:LRSSES]2.0.CO;2
- Marziliano, P. A., Tognetti, R., and Lombardi, F. (2019). Is tree age or tree size reducing height increment in *Abies alba* Mill. At its southernmost distribution limit? *Ann. For. Sci.* 76 (1), 17. Article 1. doi:10.1007/s13595-019-0803-5
- Mensah, A. A., Holmström, E., Petersson, H., Nyström, K., Mason, E. G., and Nilsson, U. (2021). The millennium shift: Investigating the relationship between environment and growth trends of Norway spruce and Scots pine in northern Europe. *For. Ecol. Manag.* 481, 118727. doi:10.1016/j.foreco.2020.118727
- Monserud, R. A., and Rehfeldt, G. E. (1990). Genetic and environmental components of variation of site index in inland Douglas-fir. *For. Sci.* 36 (1), 1–9.
- Moré, J. J. (2006). The Levenberg-Marquardt algorithm: Implementation and theory, Numerical Analysis: Proceedings of the Biennial Conference Held at Dundee, June 28–July 1, USA. IEEE, 105.
- Næsset, E., Gobakken, T., Holmgren, J., Hyppä, H., Hyppä, J., Maltamo, M., et al. (2004). Laser scanning of forest resources: The Nordic experience. *Scand. J. For. Res.* 19 (6), 482–499. doi:10.1080/02827580410019553
- Nilsson, M., Nordkvist, K., Jonzén, J., Lindgren, N., Axensten, P., Wallerman, J., et al. (2017). A nationwide forest attribute map of Sweden predicted using airborne laser scanning data and field data from the National Forest Inventory. *Remote Sens. Environ.* 194, 447–454. doi:10.1016/j.rse.2016.10.022
- Noordermeer, L., Bollandsås, O. M., Gobakken, T., and Næsset, E. (2018). Direct and indirect site index determination for Norway spruce and Scots pine using bitemporal airborne laser scanner data. *For. Ecol. Manag.* 428, 104–114. doi:10.1016/j.foreco.2018.06.041
- Perin, J., Hébert, J., Brostaux, Y., Lejeune, P., and Claessens, H. (2013). Modelling the top-height growth and site index of Norway spruce in Southern Belgium. *For. Ecol. Manag.* 298, 62–70. doi:10.1016/j.foreco.2013.03.009
- Pretzsch, H., Biber, P., Schütze, G., Uhl, E., and Rötzer, T. (2014). Forest stand growth dynamics in Central Europe have accelerated since 1870. *Nat. Commun.* 5 (1), 4967. doi:10.1038/ncomms5967
- Pretzsch, H. (2009). “Forest Dynamics, Growth, and Yield,” in *Forest dynamics, growth and yield: from measurement to model*. Editor H. Pretzsch (Germany: Springer), 1–39. doi:10.1007/978-3-540-88307-4\_1
- Rahimzadeh-Bajgiran, P., Hennigar, C., Weiskittel, A., and Lamb, S. (2020). Forest Potential Productivity Mapping by Linking Remote-Sensing-Derived Metrics to Site Variables. *Remote Sens.* 12 (12), 2056. Article 12. doi:10.3390/rs12122056
- Raulier, F., Lambert, M.-C., Pothier, D., and Ung, C.-H. (2003). Impact of dominant tree dynamics on site index curves. *For. Ecol. Manag.* 184 (1–3), 65–78. doi:10.1016/s0378-1127(03)00149-x
- Roussel, J.-R., Auty, D., Coops, N. C., Tompalski, P., Goodbody, T. R., Meador, A. S., et al. (2020). lidR: An R package for analysis of Airborne Laser Scanning (ALS) data. *Remote Sens. Environ.* 251, 112061. doi:10.1016/j.rse.2020.112061
- Schneider, F. D., Longo, M., Paul-Limoges, E., Scholl, V. M., Schmid, B., Morsdorf, F., et al. (2023). Remote Sensing-Based Forest Modeling Reveals Positive Effects of Functional Diversity on Productivity at Local Spatial Scale. *J. Geophys. Res. Biogeosciences* 128 (6), e2023JG007421. doi:10.1029/2023JG007421
- Shukla, P. R., Skea, J., Calvo Buendia, E., Masson-Delmotte, V., Pörtner, H. O., Roberts, D. C., et al. (2019). *IPCC, 2019: climate change and land: An IPCC special report on climate change, desertification, land degradation, sustainable land management, food security, and greenhouse gas fluxes in terrestrial ecosystems*.
- Smith, P., Bustamante, M., Ahammad, H., Clark, H., Dong, H., Elsiddig, E. A., et al. (2014). “Agriculture, forestry and other land use (AFOLU),” in *Climate change 2014: mitigation of climate change. Contribution of working group III to the fifth assessment report of the intergovernmental panel on climate change* (Cambridge: Cambridge University Press), 811–922.
- Socha, J., Hawrylo, P., Stereńczak, K., Miścicki, S., Tymińska-Czabańska, L., Młocik, W., et al. (2020a). Assessing the sensitivity of site index models developed using bi-temporal airborne laser scanning data to different top height estimates and grid cell sizes. *Int. J. Appl. Earth Observation Geoinformation* 91, 102129. doi:10.1016/j.jag.2020.102129
- Socha, J., Pierzchalski, M., Bałazy, R., and Cieślinski, M. (2017). Modelling top height growth and site index using repeated laser scanning data. *For. Ecol. Manag.* 406, 307–317. doi:10.1016/j.foreco.2017.09.039
- Socha, J., Solberg, S., Tymińska-Czabańska, L., Tompalski, P., and Vallet, P. (2021a). Height growth rate of Scots pine in Central Europe increased by 29% between 1900 and 2000 due to changes in site productivity. *For. Ecol. Manag.* 490, 119102. doi:10.1016/j.foreco.2021.119102
- Socha, J., and Tymińska-Czabańska, L. (2019). A method for the development of dynamic site index models using height–age data from temporal sample plots. *Forests* 10 (7), 542. doi:10.3390/f10070542
- Socha, J., Tymińska-Czabańska, L., Bronisz, K., Zięba, S., and Hawrylo, P. (2021b). Regional height growth models for Scots pine in Poland. *Sci. Rep.* 11 (1), 10330–10414. doi:10.1038/s41598-021-89826-9
- Socha, J., Tymińska-Czabańska, L., Grabska, E., and Orzel, S. (2020b). Site index models for main forest-forming tree species in Poland. *Forests* 11 (3), 301. doi:10.3390/f11030301
- Tompalski, P., Coops, N. C., White, J. C., Goodbody, T. R. H., Hennigar, C. R., Wulder, M. A., et al. (2021). Estimating Changes in Forest Attributes and Enhancing

Growth Projections: A Review of Existing Approaches and Future Directions Using Airborne 3D Point Cloud Data. *Curr. For. Rep.* 7 (1), 1–24. doi:10.1007/s40725-021-00135-w

Tompalski, P., Coops, N. C., White, J. C., and Wulder, M. A. (2015). Augmenting site index estimation with airborne laser scanning data. *For. Sci.* 61 (5), 861–873. doi:10.5849/forsci.14-175

Tukey, J. W. (1977). *Exploratory data analysis*.

Tymińska-Czabańska, L., Hawryło, P., Janiec, P., and Socha, J. (2022). Tree height, growth rate and stand density determined by ALS drive probability of Scots pine mortality. *Ecol. Indic.* 145, 109643. doi:10.1016/j.ecolind.2022.109643

Tymińska-Czabańska, L., Socha, J., Hawryło, P., Bałazy, R., Ciesielski, M., Grabska-Szwagrzyk, E., et al. (2021). Weather-sensitive height growth modelling of Norway spruce using repeated airborne laser scanning data. *Agric. For. Meteorology* 308, 108568. doi:10.1016/j.agrformet.2021.108568

Viet, H. D. X., Tymińska-Czabańska, L., and Socha, J. (2022). Drivers of site productivity for oak in Poland. *Dendrobiology* 88, 81–93. doi:10.12657/denbio.088.006

Wang, Y., Lehtomäki, M., Liang, X., Pyörälä, J., Kukko, A., Jaakkola, A., et al. (2019). Is field-measured tree height as reliable as believed—A comparison study of tree height estimates from field measurement, airborne laser scanning and terrestrial laser scanning in a boreal forest. *ISPRS J. Photogrammetry Remote Sens.* 147, 132–145. doi:10.1016/j.isprsjprs.2018.11.008

White, J. C., Coops, N. C., Wulder, M. A., Vastaranta, M., Hilker, T., and Tompalski, P. (2016). Remote sensing technologies for enhancing forest inventories: A review. *Can. J. Remote Sens.* 42 (5), 619–641. doi:10.1080/07038992.2016.1207484

Xu, D., Wang, H., Xu, W., Luan, Z., and Xu, X. (2021). LiDAR Applications to Estimate Forest Biomass at Individual Tree Scale: Opportunities, Challenges and Future Perspectives. *Forests* 12 (5), 550. Article 5. doi:10.3390/fl2050550

Zajączkowski, G., Jabłoński, M., Jabłoński, T., Małecka, M., Kowalska, A., Malachowska, J., et al. (2018). *Raport o stanie lasów w Polsce 2017. Państwowe gospodarstwo leśne lasy państwowe*. Warszawa: Centrum Informacyjne Lasów Państwowych.

Zielony, R., and Kliczkowska, A. (2012). Regionalizacja przyrodniczo-leśna Polski 2010. *Cent. Inf. Lasów Państwowych*.

# A low-cost alternative to LiDAR for site index models: applying repeated digital aerial photogrammetry data in the modelling of forest top height growth

Piotr Janiec  <sup>1,2,\*</sup>, Paweł Hawryło<sup>1</sup>, Luiza Tymińska-Czabańska<sup>1</sup>, Jakub Miszczyzyn<sup>1</sup>, Jarosław Socha<sup>1</sup>

<sup>1</sup>Department of Forest Resources Management, Faculty of Forestry, University of Agriculture in Krakow, Al. 29 Listopada 46, PL-31-425 Kraków, Poland

<sup>2</sup>Forest Management and Geodesy Bureau, Leśników 21, PL-05-090 Sekocin Stary, Poland

\*Corresponding author. Faculty of Forestry, Department of Forest Resources Management, University of Agriculture in Krakow, Al. 29 Listopada 46, PL-31-425 Kraków, Poland. E-mail: p.janiec@urk.edu.pl

## Abstract

Environmental and forest structural information derived from remote sensing data has been found suitable for modelling forest height growth and site index and therefore forest productivity assessment, with the advances in airborne laser scanning (ALS) playing a major role in this development. While there is growing interest in the use of ALS-derived point clouds, point clouds from high-resolution digital aerial photography (DAP) are also often used for mapping and estimating forest ecosystem properties due to their lower acquisition costs. In this study, we document the applicability of bi-temporal DAP data for developing top height (TH) growth models for Scots pine stands. Our results indicate that DAP data can function as an alternative to traditional TH measurements used in growth modelling when corrected based on a limited sample of field-measured reference TH values. As the correction cannot be constant for each DAP dataset due to the different parameters during data acquisition, we propose a straightforward method for the bias correction of DAP-derived TH estimates. By undertaking iterative random sampling, we were able to find the minimum number of reference measurements needed to calculate the TH correction in order to achieve the desired accuracy of the TH estimations based on DAP. Here, we used ALS data as the reference data; however, the ALS measurements can be replaced by any other reliable source of TH values. The presented method for determining TH can be used not only for site index and forest growth modelling but also in forest inventories.

**Keywords:** digital aerial photogrammetry; airborne laser scanning; point cloud; forestry; height growth

## Introduction

Site index model development is a fundamental task in forest management (Cieszewski and Strub 2007, Sharma et al. 2011). Top height (TH) growth models provide reliable estimates of forest growth and site index and are the most commonly used and widely accepted method for describing site productivity. In turn, reliable estimates of site productivity are essential for sustainable forest management, as site productivity is a key criterion for making site-specific decisions regarding species composition, silvicultural treatments, the determined allowable cut, rotation periods, and the forecasting of timber yield (Splechtn 2001, Pretzsch 2009). Bi-temporal, high-resolution remote sensing data can make important contributions to sustainable forest management in this context. Using such data, we can observe forest growth across spatially continuous areas and these data are hence considered a key source for the future development and improvement of dynamic forest models under the conditions of climate change (Gao et al. 2020). Such models can, e.g. be used to estimate terrestrial carbon stocks and fluctuations, which are crucial to the functioning of ecosystems on global and local scales (Skovsgaard and Vanclay 2008, Pretzsch 2009, Bontemps and Bouriaud 2014, Coops 2015).

The increasing availability of multi-temporal structural remote sensing data particularly enables the accurate estimation of height growth over large areas (Hauglin et al. 2021). Measuring the height of stands is important as TH at a given age is a fundamental measure of site productivity (Skovsgaard and Vanclay 2008, Bontemps and Bouriaud 2014, Coops 2015). In forest management, various types of data have been used for height growth modelling to enable the estimation of site productivity. Most commonly, growth trajectories obtained from stem analysis or repeated measurement data from permanent sample plots or temporary sample plots are used (Raulier et al. 2003, Socha and Tymińska-Czabańska 2019). However, collecting stem analysis and permanent sample plots data is time-consuming and expensive and typically constrained to local plots. Using stem analysis models can also lead to the overestimation of TH growth (Raulier et al. 2003, Marziliano et al. 2019) and stem analysis models do not include tree mortality and changes in social status in TH dynamics, due to the individual tree approach and the assumption that these trees are always dominant (Raulier et al. 2003). On the other hand, the use of temporary sample plots data may lead to the underestimation of a stand's TH growth (Raulier et al. 2003). In order to model representative site index curves

from this data source, the samples must be large and unbiased. Moreover, traditional tree height growth models constructed using longer time series of observations may not be suitable for measuring future fluctuations in tree growth due to ongoing climate change.

Over the last few decades, the use of remote sensing data has been a major factor in the improvement of forest inventories. In particular, airborne laser scanning (ALS) played a significant role in this revolution (Vauhkonen et al. 2014). ALS point clouds allow for the precise characterization of forest structure (Reutebuch et al. 2005) and are commonly used to measure forest TH increment (Hopkinson et al. 2008, Socha et al. 2020, Tymińska-Czabańska et al. 2021, 2022).

Aside from the growing interest in the use of ALS-derived point clouds, point clouds from high-resolution digital aerial photography (DAP) are also often used in forestry due to their lower acquisition costs (White et al. 2013, Fassnacht et al. 2016, Hawrylo et al. 2017, Igihaut et al. 2019, Tompalski et al. 2021). Recently, computer vision or photogrammetry techniques have been used to generate point clouds from aerial imagery. One of the main techniques used to generate point clouds from aerial imagery is structure from motion. Structure from motion uses the same techniques as traditional computer vision and photogrammetry, and is based on the identification of well-defined geometric features captured in multiple images from different angles to generate a 3D point cloud (Snavely et al. 2008). When applying aerial images, the photogrammetric 3D data can be complemented with spectral information representing the forest condition and species composition (Tuominen and Pekkarinen 2005, Franklin and Ahmed 2018).

DAP point clouds have proven useful for assessing tree stand characteristics such as the tree height (Guerra-Hernández et al. 2018), basal area (White et al. 2015), and timber volume (Straub et al. 2013, Hawrylo et al. 2017). Several recent studies compared forest stand inventories using DAP- and ALS-derived point clouds (Wallace et al. 2016, Hawrylo et al. 2017, Guerra-Hernández et al. 2018, Hartley et al. 2020, Mielcarek et al. 2020, Rodríguez-Vivancos et al. 2022). In all of these studies ALS-derived TH values are characterized by smaller errors than those derived from DAP. At the same time, most of the aforementioned studies report a very strong correlation between DAP, ALS, and field data.

Rennolls (1978) defined TH as the average of the heights of the 100 thickest trees per ha estimated for all non-empty 0.01 ha subplots and Hawrylo et al. (2024) adapted this method to ALS data. Recent studies indicate that stand height and, in particular, TH estimates derived from high-quality remote sensing data are more accurate than field measurements (Sibona et al. 2017, Wang et al. 2019, Jurjević et al. 2020, Hawrylo et al. 2024). These studies show that, ALS based TH estimates match the traditional measurements if the point cloud densities are  $>2$  points/m<sup>2</sup> (Hawrylo et al. 2024). It has furthermore been shown that bi-temporal ALS data can be successfully used to calibrate TH growth models (Tompalski et al. 2015, Socha et al. 2017, 2020, Tymińska-Czabańska et al. 2021). However, similar studies based on DAP data are still lacking. The ability to use DAP data for forest increment measurement and growth modelling would permit the widespread use of this technique across wide spatial and temporal scales by reducing acquisition costs, as compared with ALS data (Guerra-Hernández et al. 2018). In addition, the use of DAP data would enable the re-analysis of archived digital image datasets in retrospective studies.

Therefore, the aim of this study is to test the usefulness of DAP data for the calibration of TH growth models, using bi-temporal

DAP data from Scots pine stands. One challenge in this application of DAP data are biases induced by different acquisition settings of the image flights which need to be corrected. In our study, samples of ALS data were used as reference height values to correct the DAP data. However, our developed method is also intended to be applicable when ALS data are not available. In this case, the bias can also be determined based on field measurements. So as a second aim of our study, we developed a work-flow to determine the minimum number of field-measured heights that are needed to correct for the biases in the DAP data. The specific objectives of our study were as follows: (i) to compare the THs of pine stands calculated from the DAP and ALS point clouds, (ii) to propose a method for the correction of the systematic errors of the DAP-derived TH values, and (iii) to assess the adequacy of the height growth models based on DAP-derived TH observations.

## Materials and Methods

### Study area

The study area was selected based on the following criteria: dominance of Scots pine, availability of ALS and DAP data from two time periods for the same time frame. We chose to focus on Scots pine stands as they are one of the most ecologically and economically important tree species in Europe. In addition, high levels of mortality have been observed among Scots pine trees in central Europe in recent years, and stands characterized by accelerated growth have been particularly susceptible to mortality (Socha et al. 2023); as such, understanding the growth dynamics of this species is currently very important. The identified study area, which met the above criteria, covers 8000 ha and is located in the Piensk Forest District (Fig. 1). It is dominated by Scots pine with an area coverage of 80%, along with a small share of silver birch (9%), oak (2%), and black alder (2%). Stands age in the study area ranged from 1 to 205 years. Data related to the stand age and species composition were obtained from the Polish Forest Data Bank (<https://www.bdl.lasy.gov.pl/portal/>). These data are accurate to year and collected at stand level during the forest inventory. Stands  $>5$  years and with a proportion of Scots pine of  $>90\%$  were selected for the analysis.

### Data acquisition

#### 2015

ALS and DAP data were acquired in 2015 as part of the REMBIOFOR project ('Remote-sensing-based assessment of woody biomass and carbon storage in forests'). The ALS data were acquired on 24 August 2015 with the ALS positioning accuracy being better than 0.2 m (according to the contractor). The aerial photographs were acquired on 22 August 2015 using a Leica DMC II camera. The spatial resolution of the photographs was 0.25 m. The products were divided into two sets of photographs: CIR and RGB. The minimum image overlap was 80% along track and 40% across track.

We used the Agisoft PhotoScan Professional software package to generate airborne-image-based point clouds (IPCs). For data processing, we applied the workflow and software descriptions provided by Turner et al. (2013) and Dandois and Ellis (2013). The average point density of the generated IPC was 7.3 points/m<sup>2</sup> for ALS and 9 points/m<sup>2</sup> for DAP (Table 1).

#### 2021

We retrieved ALS and DAP data for the year 2021 from the GUGiK repository, which is freely available at <https://mapy.geoportali.gov.pl/>. The ALS data were acquired on 5 September 2021. The

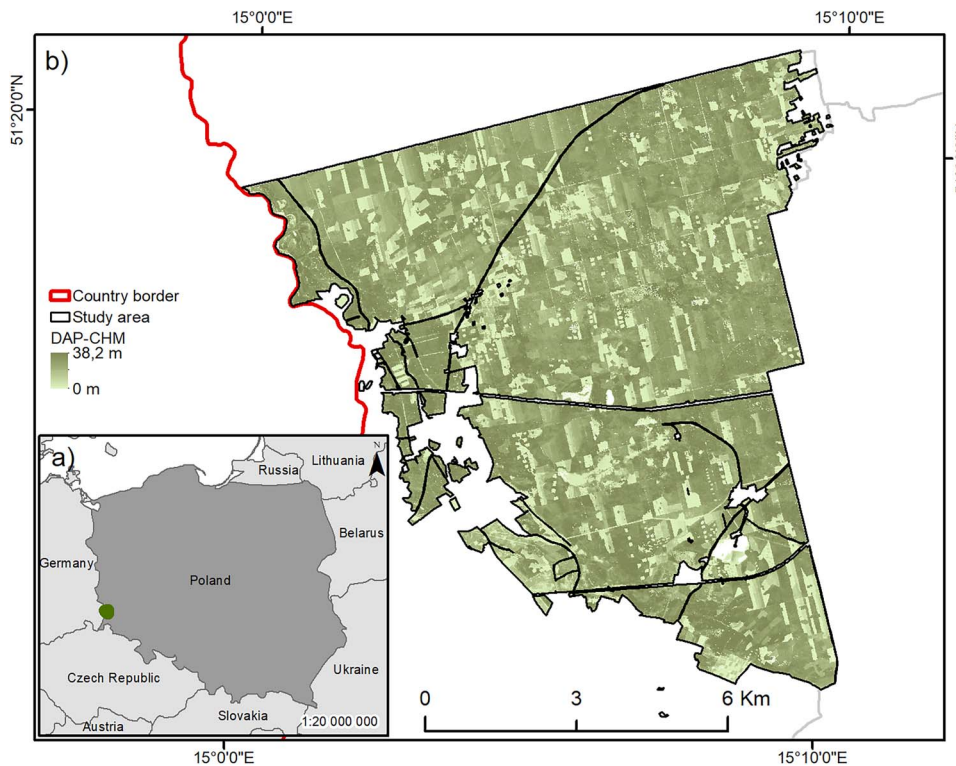


**Figure 1.** Study area: (a) location in Poland; (b) DAP-CHM: digital aerial photography canopy height model based on DAP-derived point clouds acquired in 2021.

**Table 1.** The DAP and ALS data parameters for the two acquisitions from 2015 and 2021.

| Data source | Acquisition year | Conditions | Point cloud density (points/m <sup>2</sup> ) | Positioning accuracy | Spatial resolution (m) |
|-------------|------------------|------------|--|----------------------|------------------------|
| ALS         | 2015             | Leaf on    | 7.3  | 0.2                  | -                      |
|             | 2021             | Leaf on    | 4  | 0.5                  | -                      |
| DAP         | 2015             | Leaf on    | 9  | -                    | 0.2                    |
|             | 2021             | Leaf on    | 7  | -                    | 0.25                   |

positional accuracy of the ALS was, at minimum, 0.5 m (according to the contractor). The aerial photographs were acquired on 9 October 2021 using a Leica DMC III camera. The spatial resolution of the photographs was 0.25 m. The data were split into two sets of photographs: CIR and RGB. The minimum image overlap was 60% along track and 25% across track. The external orientation parameters were obtained from the GUGIK repository for camera optimization and georeferencing. The data processing approach was the same as in 2015. The average point density of the generated IPC was 4 points/m<sup>2</sup> for ALS and 7 points/m<sup>2</sup> for DAP (Table 1).

## Preprocessing

We exported the DAP- and ALS-derived point clouds from each year to the LAS format. We processed the point clouds using the lidR package for R (Roussel et al. 2020) by first normalizing the point clouds by subtracting the elevation of the terrain (DTM, obtained from the GUGIK repository) from the corresponding DAP and ALS points collected in their respective years. We calculated canopy height models (CHMs) with a spatial resolution of 1.0 m with the use of the 'p2r' algorithm in the lidR package. In the next step, we performed individual tree detection using the 'locate\_trees' algorithm from the lidR package. We used the local

maximum filter (lmf) function with the following window size (ws):

$$ws = CHM \times 0.1 + 3 \quad (1)$$

## Determination of TH from repeated DAP and ALS data

The flowchart in Fig. 2 summarizes the whole methodology of the TH determination, DAP data correction estimation and TH growth modelling.

We calculated TH according to definition of Rennolls (1978) using the methodology described and tested by Socha et al. (2020) and Hawrylo et al. (2024). The effectiveness of this method has been proven in previous growth modelling studies (Socha et al. 2017, Tymińska-Czabańska et al. 2021, 2022).

TH was calculated for two sizes of grid cells: 10 × 10 m (TH<sub>10</sub> × 10) and 50 × 50 m (TH<sub>50</sub> × 50).

TH<sub>10</sub> × 10 was calculated based on ALS data and DAP data (TH<sub>DAP10 × 10</sub> and TH<sub>ALS10 × 10</sub>). The calculation of these THs consisted of selecting the highest individual treetop for the 10 × 10 m cells and treating them as the TH. TH values for the 10 × 10 m cells were calculated separately for 2015 and 2021 and used in further analysis to identify the bias of DAP data and correct TH from DAP.

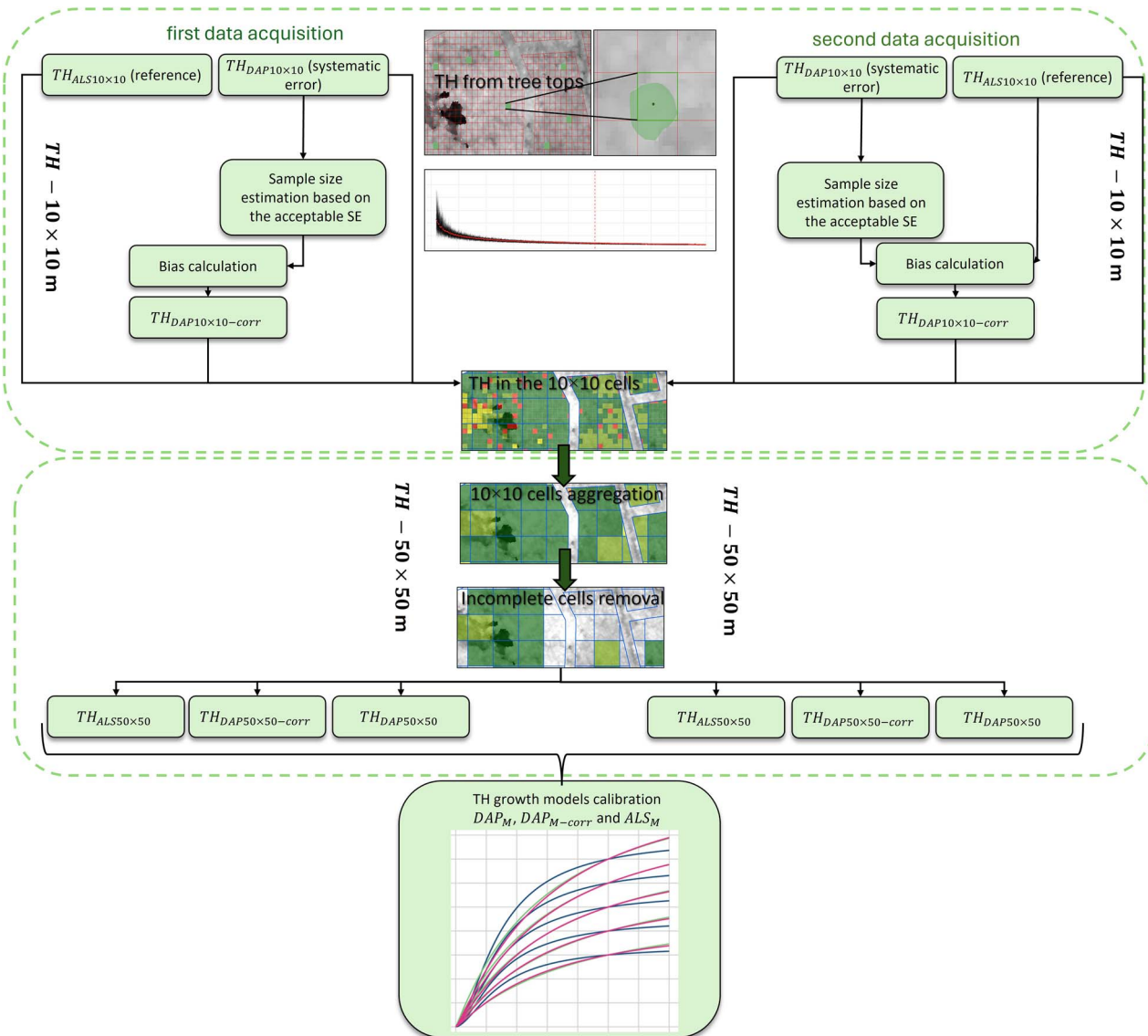


**Figure 2.** The flowchart of methods used in the study for the data treatment, correction assessment, and TH growth model calibration.

In a study by Socha et al. (2020), it was shown that, the use of  $50 \times 50 \text{ m}$  grid cells reduces the residuals of growth model fitting (Socha et al. 2020). Therefore, for model fitting we used  $TH_{50 \times 50}$  calculated according to the method described by Hawrylo et al. (2024). In this case TH was calculated for  $50 \times 50 \text{ m}$  grid cells as an average from non-empty  $10 \times 10 \text{ m}$  subcells. The  $10 \times 10 \text{ m}$  subcells with values less than two-third of the maximum height in the  $50 \times 50 \text{ m}$  grid were treated as empty in order to capture the height of the tallest trees. To avoid edge effects an internal 15 m buffers from the borders of individual stands, the forest trails and public roads were created. Only complete  $50 \times 50 \text{ m}$  grid cells (cells not clipped by buffer) were used to calculate the TH (Fig. 3). In this way, we obtained two types of TH for the  $50 \times 50 \text{ m}$  grid cells ( $TH_{DAP50 \times 50}$  and  $TH_{ALS50 \times 50}$ ). The  $TH_{DAP50 \times 50}$  and  $TH_{ALS50 \times 50}$  values were calculated separately for 2015 and 2021 and were used in further analysis to calibrate the TH growth models.

### Identification of the bias of TH calculated based on DAP data

While the TH values determined using ALS data are assumed to be accurate and unbiased (Wang et al. 2019, Jurjević et al. 2020, Hawrylo et al. 2024), TH values estimated using DAP data

could be systematically biased (Wallace et al. 2016, Hawrylo et al. 2017, Swinfield et al. 2019, Mielcarek et al. 2020). As such, we use  $TH_{ALS10 \times 10}$  data as a reference to investigate whether  $TH_{DAP10 \times 10}$  data are subject to systematic errors. To test for significant differences between  $TH_{DAP10 \times 10}$  and  $TH_{ALS10 \times 10}$ , indicating the presence of bias, we used a t-test for dependent samples. The occurrence of a systematic error in the TH calculated based on DAP data was checked separately for the years 2015 and 2021.

### Finding the minimum sample size for efficiently correcting the systematic bias of heights estimated using DAP data

While it is possible to use ALS data ( $TH_{ALS10 \times 10}$ ) as a reference to identify systematic errors in the calculation of TH from DAP data ( $TH_{DAP10 \times 10}$ ), our method is intended to be also applicable when ALS data are not available and bias must be determined based on field measurements in sample plots. For this it is important to know how many field sample plots need to be measured to correctly calculate the bias of the DAP data which will allow to correct for the bias. According to our assumption, the error of the TH calculation based on DAP data is systematic; therefore, in relation to the reference, the data should have the same distribution. Thus,

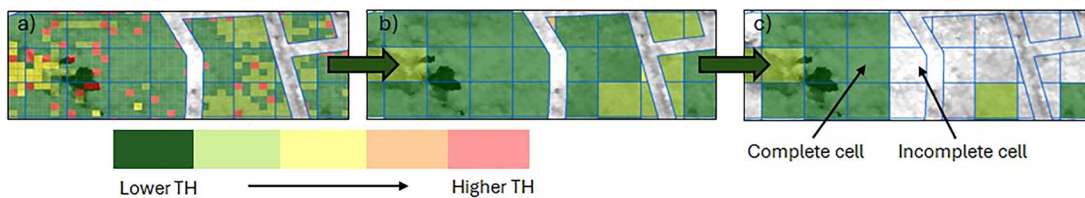


**Figure 3.** Top height calculations in  $50 \times 50$  grid cells: a) TH values in the  $10 \times 10$  cells; b) TH in the  $50 \times 50$  m grid cells, as an aggregation of  $10 \times 10$  m cells; c) removal of incomplete  $50 \times 50$  grid cells.

we determined the minimum sample size needed to estimate the TH with a specified standard error (SE; equation (2)):

$$SE = \frac{SD}{\sqrt{N}} \quad (2)$$

where SD is the standard deviation of  $TH_{DAP10 \times 10}$  calculated based on N observations (sample size).

We assumed the minimal sample size at which the mean SE falls  $<0.2$  is sufficient to determine the reference mean TH of the area. We adopted this value due to the accuracy of the height measuring instruments, which is  $\sim 0.2$  m (Stereńczak et al. 2019). We randomly sampled the  $TH_{DAP10 \times 10}$  across the entire study area. The samples were distributed evenly across the stand age classes (every 20 years), taking into account the number of stands in these classes. We conducted the sampling with different numbers of samples, ranging from 10 to 500, and calculated the SE for each sample size. We repeated the sampling 100 times for each possible sample size. Next, for each selected sample size, we calculated the mean SE of 100 iterations. The simulations used to find the best sample size were performed for each year (2015 and 2021) separately.

### Calculation of bias and corrections of DAP-derived TH

For each of the DAP datasets (2015 and 2021), the bias value with the minimum sample size found in the previous step was calculated (equation (3)):

$$\text{bias} = \frac{\sum_{i=1}^N (TH_{DAP10 \times 10} - TH_{ALS10 \times 10})}{N} \quad (3)$$

where  $TH_{DAP10 \times 10}$  and  $TH_{ALS10 \times 10}$  are the maximum heights of tree-tops in the grid obtained from DAP- and ALS-derived tree tops, respectively; N denotes the number of reference sample plots (sample size); and i is the summation index.

Next, to remove the systematic error from the TH calculated based on DAP data, we subtracted the correction value (bias) from  $TH_{DAP10 \times 10}$  values in each of the cells separately for the years 2015 and 2021. In this way, we obtained the corrected TH values calculated from the DAP data ( $TH_{DAP10 \times 10 - corr}$ ) for the years 2015 and 2021. Finally, the average of the corrected TH values for the  $10 \times 10$  grid cell ( $TH_{DAP10 \times 10 - corr}$ ) values were used to calculate the TH for the  $50 \times 50$  m grid cells for 2015 and 2021. Thus, we obtained corrected TH values from DAP in  $50 \times 50$  m grid cells ( $TH_{DAP50 \times 50 - corr}$ ), which were the basis for the development of the TH growth model.

### Calibration of the TH growth models using corrected DAP data

Pairs of TH-age data from 2015 and 2021 were used to calibrate the growth models. We calibrated three TH growth models

( $DAP_M$ ,  $DAP_{M-corr}$ , and  $ALS_M$ ) based on the TH values derived from  $TH_{DAP50 \times 50}$ ,  $TH_{DAP50 \times 50 - corr}$ , and  $TH_{ALS50 \times 50}$ . For the TH growth modelling, we applied the standard outlier elimination approach (Tukey 1977) as used by Socha et al. (2017). We calculated the outliers for each data type separately. For model calibration, we used the dynamic equation developed by Cieszewski (2001) with the use of the Generalized Algebraic Difference Approach (4):

$$TH = TH_1 \frac{T^{\beta_1} (T_1^{\beta_1} R + \beta_2)}{T_1^{\beta_1} (T^{\beta_1} R + \beta_2)} \quad (4)$$

where

$$R = Z_0 + \left( Z_0^2 + \frac{2\beta_2 TH_1}{T_1^{\beta_1}} \right)^{0.5} \quad (4.1)$$

$$Z_0 = TH_1 - \beta_3 \quad (4.2)$$

and  $\beta_1$ ,  $\beta_2$ , and  $\beta_3$  are the model parameters, TH denotes the top height at age T, and  $TH_1$  denotes the top height at age  $T_1$  and is assumed to represent unknown, local, site-specific parameters. The global parameters were simultaneously fitted with the use of nonlinear least-squares optimization and the Levenberg-Marquardt algorithm (Moré 2006) in the R environment (R Core Team 2013) using the glnls library (Joris 2023). This algorithm attempts to find a local minimum of the objective function by performing iterative steps in the direction of the solution, informed by the gradient of a first- or second-order Taylor approximation of the non-linear objective function (Moré 2006). As starting parameters, we chose  $\beta_1 = 1$ ,  $\beta_2 = 10\,000$ , and  $\beta_3 = 28$ , per Socha et al. (2017). For each model, we used the maximum number of iterations.

For each calibrated model, we calculated the mean absolute error (MAE, equation (5)), root mean squared error (RMSE, equation (6)), and adjusted coefficient of correlation ( $R_{adj}^2$ , equation (7)).

$$MAE(y, \hat{y}) = \frac{\sum_{i=0}^{N-1} |y_i - \hat{y}_i|}{N} \quad (5)$$

$$RMSE(y, \hat{y}) = \sqrt{\frac{\sum_{i=0}^{N-1} (y_i - \hat{y}_i)^2}{N}} \quad (6)$$

$$R_{adj}^2 = 1 - \frac{\sum_{i=0}^{N-1} (y_i - \hat{y}_i)^2}{\sum_{i=1}^N (y_i - \bar{y}_i)^2} \left( \frac{N-1}{N-p} \right) \quad (7)$$

where,  $y_i$  is the predicted value ( $TH_{DAP50 \times 50}$  or  $TH_{DAP50 \times 50 - corr}$ );  $\hat{y}_i$  is the reference value ( $TH_{ALS50 \times 50}$ ); i is the summation index; N is the number of cases,  $\bar{y}_i$  is the mean value of N cases; and p is the number of parameters in the model.

Finally, we compared the TH growth patterns of the developed models ( $DAP_M$ ,  $DAP_{M-corr}$  and  $ALS_M$ ) for the four selected site index values (20, 25, 30, 35) at a base age of 100 years.

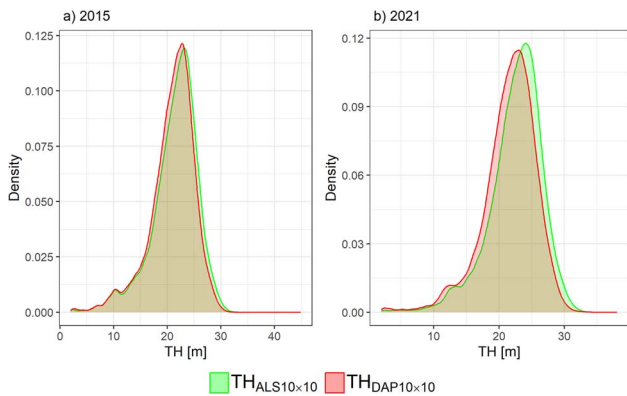


**Figure 4.**  $\text{TH}_{\text{ALS}10 \times 10}$  (green) and  $\text{TH}_{\text{DAP}10 \times 10}$  (red) height distribution for 2015 (a) and 2021 (b).

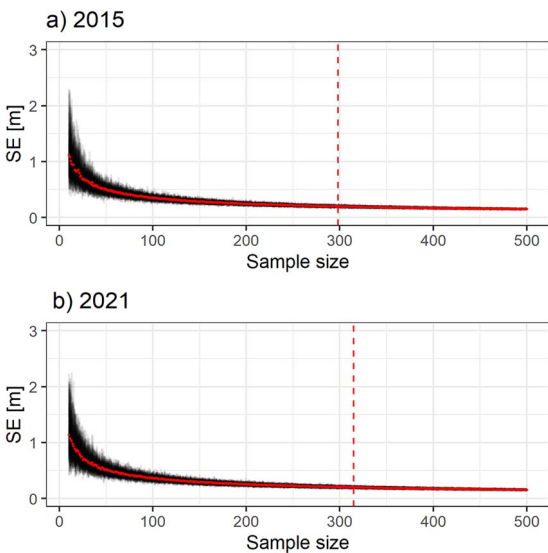


**Figure 5.** Dependence of SE value of the  $\text{TH}_{\text{DAP}10 \times 10}$  on the sample size in 2015 (a) and 2021 (b). The red dashed line indicates the number of sample size where the SE reaches 0.2 m.

## Results

### $\text{TH}_{\text{ALS}10 \times 10}$ and $\text{TH}_{\text{DAP}10 \times 10}$ data height distributions

The t-test showed significant differences between the average TH calculated using DAP and ALS data in 2015 and 2021 ( $P < 0.001$ ).

As expected, we observed a similar height distribution of  $\text{TH}_{\text{DAP}10 \times 10}$  and  $\text{TH}_{\text{ALS}10 \times 10}$  for both of the analysed years of data acquisition (Fig. 4). The  $\text{TH}_{\text{ALS}10 \times 10}$  data were slightly shifted towards higher values. This shift is particularly evident for the year 2021. In 2015, the difference between the TH distributions was lower. The distributions of data in the analysed years indicate that it is possible to apply TH correction to the DAP data using a constant correction value.

### Correction of $\text{TH}_{\text{DAP}10 \times 10}$ observations and calculation of $\text{TH}_{\text{DAP}50 \times 50}$

Using the iterative random sampling of  $\text{TH}_{\text{DAP}10 \times 10}$ , we estimated the sample size for which the SE reached an assumed value of 0.2 m (Fig. 5). The sample size required to achieve the assumed margin of error was 298 in 2015 and 315 in 2021 (Fig. 5). However, the most significant decrease in SE was observed up to a sample size of  $\sim 150$  (Fig. 5).

Based on the selected sample size we estimated the bias, which was treated in further analysis as a correction value. The bias in 2015, estimated on 298 randomly selected  $\text{TH}_{\text{ALS}10 \times 10}$  was  $-0.50$  m (Table 2). The bias in 2021, based on 315 randomly selected  $10 \times 10$  grid cells'  $\text{TH}_{\text{ALS}10 \times 10}$  values, was  $-0.94$  m (Table 2).

For the 2015 data, the post-correction bias of  $\text{TH}_{\text{DAP}10 \times 10 - \text{corr}}$  decreased to  $-0.01$  m and the average  $\text{TH}_{\text{DAP}10 \times 10 - \text{corr}}$  and  $\text{TH}_{\text{ALS}10 \times 10}$  values were not significantly different ( $P = 0.5909$ ). For the 2021 data, the average post-correction bias decreased to  $-0.06$  m, but, despite the notable decrease in the t-statistic from 88.3 to 5.44, the differences between the average  $\text{TH}_{\text{DAP}10 \times 10 - \text{corr}}$  and  $\text{TH}_{\text{ALS}10 \times 10}$  remained significant ( $P < 0.0001$ ).

The values of  $\text{TH}_{\text{DAP}50 \times 50}$  were directly compared with  $\text{TH}_{\text{DAP}50 \times 50}$  (Fig. 6). Significant differences between  $\text{TH}_{\text{DAP}50 \times 50}$  and  $\text{TH}_{\text{DAP}50 \times 50}$  values were visible, especially for 2021. However, after correction, the TH bias was removed for both years.

## Top height growth models

By fitting the parameters of the growth function equation (4) to the TH-age data pairs obtained for 2015 and 2021, where TH was determined in three ways ( $\text{TH}_{\text{DAP}50 \times 50}$ ,  $\text{TH}_{\text{DAP}50 \times 50 - \text{corr}}$ , and  $\text{TH}_{\text{ALS}50 \times 50}$ ), three growth models were developed ( $\text{DAP}_M$ ,  $\text{DAP}_{M-\text{corr}}$  and  $\text{ALS}_M$ , Table 3).  $\text{DAP}_M$  was characterized by the highest MAE, RMSE, and lowest  $R^2_{\text{adj}}$ .  $\text{ALS}_M$  was characterized by the best accuracy; however, the  $\text{DAP}_{M-\text{cor}}$  model had almost the same fitting statistics as the  $\text{ALS}_M$  model. According to the t-test of the modelled TH, we observed significant differences between  $\text{DAP}_M$  and  $\text{DAP}_{M-\text{corr}}$  ( $P$ -value  $< 0.0001$ ).  $\text{DAP}_M$  was characterized by a significant difference in comparison to  $\text{ALS}_M$  ( $P$ -value  $< 0.0001$ ). However, there were no significant difference between  $\text{DAP}_{M-\text{corr}}$  and  $\text{ALS}_M$  ( $P$ -value = 0.5695).

TH growth models calibrated based on  $\text{TH}_{\text{DAP}50 \times 50}$  and  $\text{TH}_{\text{ALS}50 \times 50}$  data were characterized by different TH growth patterns (Fig. 6). Differences in the obtained TH growth patterns of the  $\text{DAP}_M$  result directly from the different biases of  $\text{TH}_{\text{DAP}50 \times 50}$  in 2015 and 2021. The growth patterns of  $\text{DAP}_{M-\text{cor}}$  are very similar to  $\text{ALS}_M$  (Fig. 7).

## Discussion

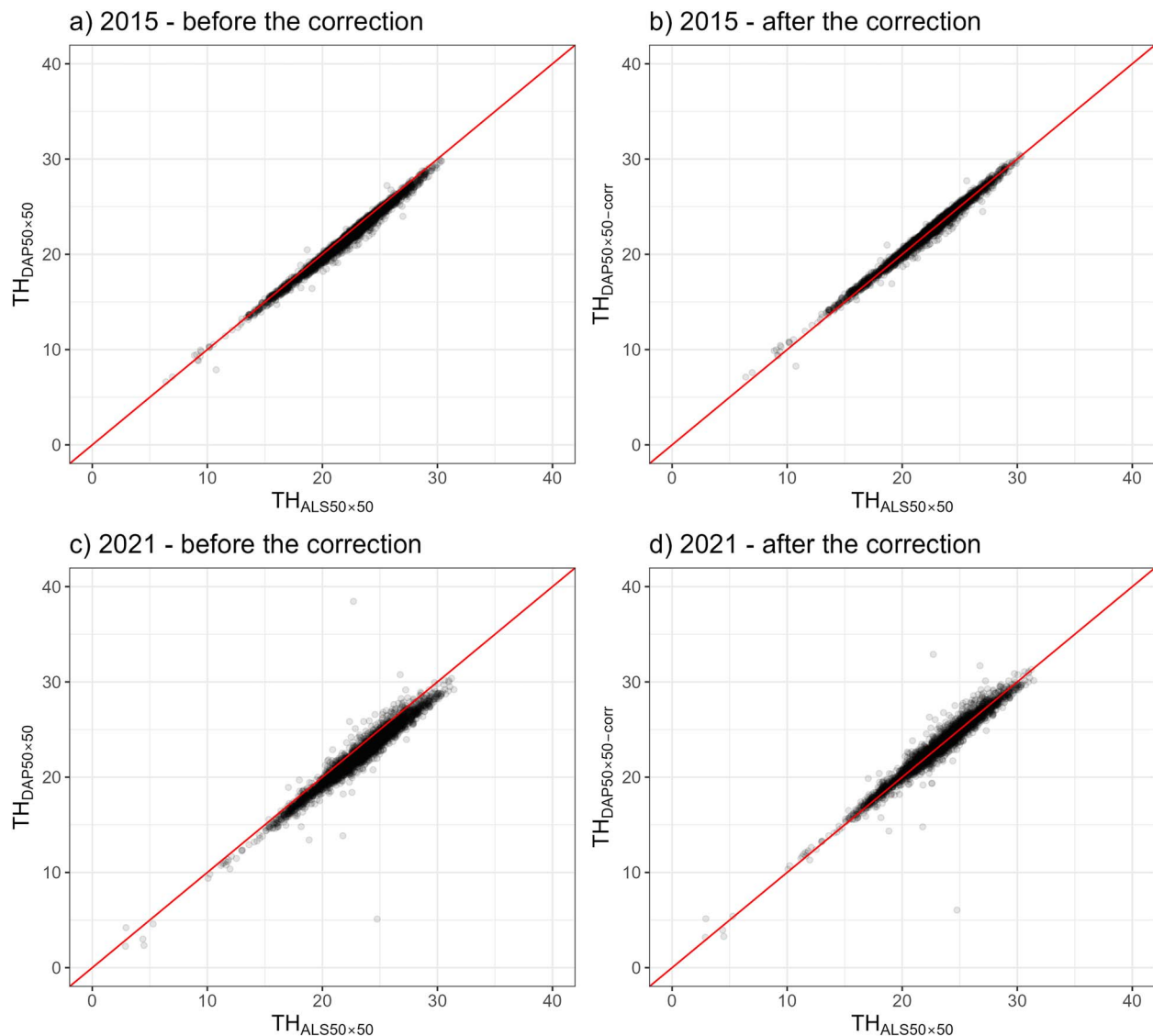
In this study, we demonstrate the utility of DAP-derived point clouds for the development of local TH growth models. Recognizing the systematic errors in TH values derived from DAP data, we developed a straightforward method for correcting these errors. In our analyses, we used ALS data to correct the TH bias calculated from DAP data, but the developed approach can also be based on field measurement data from, e.g.  $10 \times 10$  m plots if precise co-registration between field and remote sensing data can be ensured. In addition, we proposed a simple approach to determine the sample size needed to accurately carry out the correction of DAP-derived TH values. After correction, the TH values determined using DAP data were used to develop a TH growth model for Scots pine. The developed model has almost the same fit statistics as the reference model developed using ALS data, as well as similar predictive abilities. Our study shows that DAP data can provide a robust basis for developing TH growth models and can be widely used at local and regional scales, significantly reducing acquisition costs compared with ALS data.

### DAP-derived TH bias

We found a bias in the TH values estimated using DAP point clouds that was specific to the year of acquisition. In this regard, our research is in line with other studies that have found that the

**Table 2.** Comparison of the mean top height values determined by DAP ( $\text{TH}_{\text{DAP}10 \times 10}$ ) and ALS ( $\text{TH}_{\text{ALS}10 \times 10}$ ) for the years of data acquisition using the t-test.

| Acquisition year | Sample size | Correction            | Mean $\text{TH}_{\text{ALS}10 \times 10}$ | Mean $\text{TH}_{\text{DAP}10 \times 10}$ | Bias (m) | t-value | P-value  |
|------------------|-------------|-----------------------|---|---|----------|---------|----------|
| 2015             | 298         | Before the correction | 20.23                                     | 19.72                                     | -0.50    | 43.42   | < 0.0001 |
|                  |             | After the correction  |   | 20.22                                     | -0.01    | 0.54    | 0.5909   |
| 2021             | 315         | Before the correction | 21.22                                     | 20.23                                     | -0.94    | 88.3    | < 0.0001 |
|                  |             | After the correction  |   | 21.16                                     | -0.06    | 5.44    | <0.0001  |

**Figure 6.** Relationship of  $\text{TH}_{\text{DAP}50 \times 50}$  on  $\text{TH}_{\text{ALS}50 \times 50}$  before (a) and after (b) the correction in 2015; before (c) and after (d) the correction in 2021.**Table 3.** Parameters and fit statistics of the TH growth models developed using DAP-derived TH ( $\text{DAP}_M$ ), corrected DAP-derived TH ( $\text{DAP}_{M-\text{corr}}$ ), and ALS-derived TH ( $\text{ALS}_M$ ).

| Model                        | Model parameters |           |            | Fit statistics |           |                      |
|------------------------------|------------------|-----------|------------|----------------|-----------|----------------------|
|                              | $\beta_1$        | $\beta_2$ | $\beta_3$  | *MAE (m)       | *RMSE (m) | * $R^2_{\text{adj}}$ |
| $\text{ALS}_M$               | 1.054            | 16161.264 | -51.455    | 0.258          | 0.778     | 0.931                |
| $\text{DAP}_M$               | 1.639            | 1.134e+09 | -2.241e+06 | 0.445          | 0.853     | 0.929                |
| $\text{DAP}_{M-\text{corr}}$ | 1.168            | 3.083e+07 | -1.317e+05 | 0.269          | 0.795     | 0.928                |

\*MAE-mean absolute error, RMSE-root mean square error,  $R^2_{\text{adj}}$  – adjusted coefficient of determination.

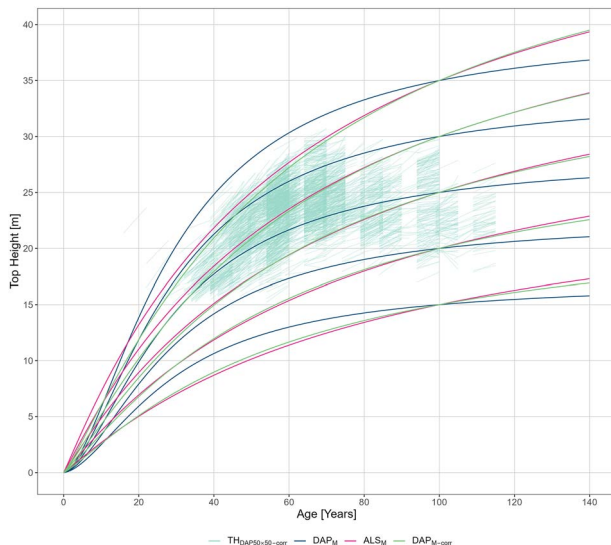


**Figure 7.** Comparison of the growth patterns of TH growth models for Scots pine fitted to TH estimated using DAP data ( $DAP_M$ ), corrected DAP data ( $DAP_{M\_corr}$ ), and TH estimates using ALS data ( $ALSM$ ). The growth curves were drawn for the five selected site index values (15, 20, 25, 30, 35) at a base age of 100 years. The thin green lines indicate the observed changes in the corrected top height determined from the DAP data for  $50 \times 50$  m grid cells ( $TH_{DAP50 \times 50\_corr}$ ) over the period 2015–2021.

TH values obtained from DAP data are systematically underestimated (Wallace et al. 2016, Hawrylo et al. 2017, Swinfield et al. 2019, Mielcarek et al. 2020). According to Socha et al. (2017), ALS-derived TH measurements can function as a good alternative to data from permanent sample plots or stem analysis data. Therefore, we here used ALS data from the years of DAP data acquisition (2015, 2021) as a reference to calculate the systematic error (bias) of the DAP-derived TH. We attribute the variation in the bias of TH estimated using DAP data to different weather conditions on the DAP data acquisition dates which are likely to have resulted in differing illumination conditions affecting the image-matching process (Holopainen et al. 2015). Consequently, there is a high probability of obtaining different accuracies for separate DAP campaigns. Furthermore, the aerial photographs available to us were obtained using different cameras and different flight parameters that are likely to also impact the obtained DAP parameters and TH estimation accuracy. For this reason, the bias required for the correction of TH values derived from DAP data should be determined separately for each DAP data acquisition. A strong linear correlation and similar data distribution of reference and DAP-derived heights is the prerequisite for assuming that correction is feasible (Jensen and Mathews 2016). A similar solution was applied in a tropical forest by Swinfield et al. (2019), who showed that the accuracy of the TH calculation improved significantly after the correction of bias.

### Estimation of TH correction derived from DAP

In order to make our approach applicable when ALS data are not available, we propose an alternative solution to calculating the bias of the DAP data based on field measured top-height from forest inventory plots. To estimate the bias of the TH values determined using DAP data using field data, it is necessary to calculate the minimum sample size required to adequately determine the correction. We used iterative sampling to assess how the sample size affects the SE of the  $TH_{DAP10 \times 10}$  without the correction. We took 0.2 as the SE threshold for achieving a

sufficient accuracy, although we recognize that the sample size may vary depending on the DAP data. In addition, the SE can be affected by unbalanced sampling of the data, especially uneven distribution of data across age classes. In this study, sampling was carried out in such a way that the samples were evenly distributed by age classes. However, the number of sample plots required to achieve the target accuracy for a given dataset may also depend on other factors, such as the species composition and topography, which could be further considered in the sample size selection and calculation.

DAP data are typically more widely available than ALS data and we showed that DAP data can perform similarly well as ALS data if our bias-correction procedure is applied (Wallace et al. 2016, Mielcarek et al. 2020). Our bias correction method requires reference data. However, the strength of our approach lies in its flexibility regarding the source of these reference data. Not only ALS data but also field measurement and potentially UAV data can be used. If repeated data acquisitions are available or are planned, our approach enables also the integration of data from various sources, including field sample plots, DAP, ALS, and UAV data, facilitating the modelling of TH growth through the developed TH time series (Tompalski et al. 2015).

In our study we used ALS data as the reference, but ALS may often not be available. Contrarily, field sample plots are often established during regular forest inventories and are therefore readily available in many forests. If the available sample plots are temporally not matching the DAP acquisition dates, it may in some cases also be possible to collect a limited number of additional field plots temporally close to planned DAP overflight dates. Thus, with a relatively small amount of field work, it should be possible to estimate the correction necessary to eliminate the bias of TH estimated using DAP data at the forest district level.

### Top height growth models

After correcting the bias in TH calculated based on DAP data, we used the TH calculated for subcells of  $10 \times 10$  m to calculate the TH in  $50 \times 50$  m grid cells and calibrate the growth model. The model developed on uncorrected DAP data ( $DAP_M$ ) differed substantially from the reference model ( $ALSM$ ). This was caused by various systematic errors in the DAP-derived TH values for both 2015 and 2021. However, after correction, the model's ( $DAP_{M\_corr}$ ) accuracy increased substantially. The MAE and RMSE of the model after correction approached the accuracy of the reference ALS model. Therefore, our research exemplifies the potential for developing a TH growth model based on point cloud data derived from DAP.

Our approach was tested in Scots pine monocultures. In the future, it will be necessary to investigate the possibility of applying the correction to more diverse stands composed of different species. Mielcarek et al. (2020) highlighted differences in DAP-derived TH values between coniferous and deciduous species. Swinfield et al. (2019) claim that canopy gaps and the canopy density may also affect the DAP results. DAP-derived TH is more accurate for more open and fragmented tree stands (Zahawi et al. 2015, Jensen and Mathews 2016) and young plantations (Zarco-Tejada et al. 2014). Therefore, future research should focus on whether it is possible to calculate the DAP TH bias correction for large areas without a more sophisticated model or extensive field work. One promising option to further improve the efficiency may be to replace field height measurements with either strip or spot surveys from a drone equipped with a LiDAR sensor.

Besides the straightforward approach suggested here, more complex models could also be used for DAP TH bias correction.

Recently, machine learning approaches have been tested for the prediction of stand properties with the use of DAP data (Li et al. 2018, Viljanen et al. 2018, Zhang et al. 2021). The implementation of machine learning methods may also make it possible to introduce DAP-derived TH growth models across larger areas. Machine learning models could potentially also be trained to correct for biases between DAP heights and reference heights, considering also the characteristics of the point cloud and the camera and flight parameters. However, training data from field measured TH on sample plots or TH determined for part of the area by ALS will still be required. In comparison, our presented approach seems much simpler and easier to implement. A comparison between our method and such more complex machine learning-based approaches is worth considering.

A very important advantage of using DAP data as compared with ALS data is the low cost of data acquisition (Hawrylo et al. 2017). Photogrammetric flights can be flown at higher heights than ALS, and the aircraft can fly faster, allowing information to be collected over the same area in a much shorter time than with ALS (Goodbody et al. 2019). In some countries, DAP data are collected regularly at relatively short intervals (Gobakken et al. 2015), therefore DAP has the potential to be a reliable, cost-effective data source for the modelling of TH growth. However, one key limitation is that free access to DAP data at national level is still challenging in some countries. Furthermore, even in countries where data are accessible, the quality of the data often varies over time and space. Therefore, DAP data collection campaigns should be coordinated nationally to ensure consistent data quality.

In addition to its use in the calibration of height growth models, the developed DAP-derived TH correction approach can be used to estimate TH for many other applications, such as site productivity estimation, biomass determination, and forest monitoring. This is particularly relevant in an era of dynamic changes in forest ecosystems under the effects of climate change and anthropopression.

## Conclusions

In this study, we demonstrated the applicability of DAP data to the development of TH growth models for Scots pine. Our results show that DAP-derived TH increment could be an alternative to TH increment estimations based on field measurements or ALS data. The TH determined using the DAP data in our study showed a significant systematic error specific to the given date of acquisition. However, we here presented an approach to eliminate this problem by applying a bias correction based on a limited number of TH measurements from either ALS or field data. The corrected multi-temporal DAP data then allow for the accurate estimation of TH growth and the development of TH growth models. Developing growth models and monitoring changes in forest growth dynamics is essential in an era of changing climatic conditions. The increasing availability of DAP data facilitates the effective modelling of forest TH growth, which is crucial for estimating wood and biomass production and carbon sequestration.

## Acknowledgements

We thank the anonymous reviewers whose feedback helped to improve and clarify this manuscript.

## Conflict of interest

The authors declare no conflicts of interest.

## Funding

This research was funded by the General Directorate of State Forests in Poland under the project 'Rozbudowa metody inwentaryzacji urządzeniowej stanu lasu z wykorzystaniem efektów projektu REMBIOFOR' (Extension of the forest inventory method using the results of the REMBIOFOR project), contract no. EO.271.3.12.2019.

## Data availability

Data and code are available on request.

## References

- Bontemps J-D, Bouriaud O. Predictive approaches to forest site productivity: recent trends, challenges and future perspectives *Forestry*. 2014;**87**:109–28. <https://doi.org/10.1093/forestry/cpt034>.
- Cieszewski CJ. Three methods of deriving advanced dynamic site equations demonstrated on inland Douglas-fir site curves. *Canadian Journal of Forest Research*, 2001;**31**(1):165–173. <https://doi.org/10.1139/x00-132>.
- Cieszewski CJ, Strub M. Parameter estimation of base-age invariant site index models: which data structure to use?—a discussion *Forest Sci.* 2007;**53**:552–5.
- Computing R. R: A Language and Environment for Statistical Computing. Vienna: R Core Team, 2013.
- Coops NC. Characterizing forest growth and productivity using remotely sensed data *Current Forest Rep.* 2015;**1**:195–205. <https://doi.org/10.1007/s40725-015-0020-x>.
- Dandois JP, Ellis EC. High spatial resolution three-dimensional mapping of vegetation spectral dynamics using computer vision. *Remote Sensing of Environment*, 2013;**136**:259–276. <https://doi.org/10.1016/j.rse.2013.04.005>.
- Fassnacht FE, Latifi H, Stereńczak K. et al. Review of studies on tree species classification from remotely sensed data. *Remote Sensing of Environment*, 2016;**186**:64–87. <https://doi.org/10.1016/j.rse.2016.08.013>.
- Franklin SE, Ahmed OS. Deciduous tree species classification using object-based analysis and machine learning with unmanned aerial vehicle multispectral data *Int J Remote Sens.* 2018;**39**:5236–45.
- Gao Y, Skutsch M, Panque-Gálvez J. et al. Remote sensing of forest degradation: a review *Environ Res Lett.* 2020;**15**:103001. <https://doi.org/10.1088/1748-9326/aba047>.
- Gobakken T, Bollandsås OM, Næsset E. Comparing biophysical forest characteristics estimated from photogrammetric matching of aerial images and airborne laser scanning data *Scand J Forest Res.* 2015;**30**:73–86. <https://doi.org/10.1080/02827581.2014.961954>.
- Goodbody TRH, Coops NC, White JC. Digital aerial photogrammetry for updating area-based Forest inventories: a review of opportunities, challenges, and future directions *Curr Forestry Rep.* 2019;**5**:55–75. <https://doi.org/10.1007/s40725-019-00087-2>.
- Guerra-Hernández J, Cosenza DN, Rodriguez LCE. et al. Comparison of ALS-and UAV (SfM)-derived high-density point clouds for individual tree detection in eucalyptus plantations *Int J Remote Sens.* 2018;**39**:5211–35.
- Hartley RJ, Leonardo EM, Massam P. et al. An assessment of high-density UAV point clouds for the measurement of young forestry trials *Remote Sens (Basel)*. 2020;**12**:4039.
- Hauglin M, Rahlf J, Schumacher J. et al. Large scale mapping of forest attributes using heterogeneous sets of airborne laser scanning and National Forest Inventory data *For Ecosyst.* 2021;**8**:1–15.

- Hawryło P, Socha J, Wężyk P. et al. How to adequately determine the top height of forest stands based on airborne laser scanning point clouds? *For Ecol Manage*. 2024;551:121528. <https://doi.org/10.1016/j.foreco.2023.121528>.
- Hawryło P, Tompalski P, Wężyk P. Area-based estimation of growing stock volume in scots pine stands using ALS and airborne image-based point clouds *Forestry*. 2017;90:686–96. <https://doi.org/10.1093/forestry/cpx026>.
- Hopkinson C, Chasmer L, Hall RJ. The uncertainty in conifer plantation growth prediction from multi-temporal lidar datasets *Remote Sens Environ*. 2008;112:1168–80. <https://doi.org/10.1016/j.rse.2007.07.020>.
- Holopainen M, Vastaranta M, Karjalainen M. et al. Forest inventory attribute estimation using airborne laser scanning, aerial stereoscopy, radargrammetry and interferometry—Finnish experiences of the 3D techniques. 2015. <https://doi.org/10.5194/isprsannals-II-3-W4-63-2015>.
- Iglhaut J, Cabo C, Puliti S. et al. Structure from motion photogrammetry in forestry: a review *Current Forestry Rep*. 2019;5:155–68. <https://doi.org/10.1007/s40725-019-00094-3>.
- Jensen JLR, Mathews AJ. Assessment of image-based point cloud products to generate a bare earth surface and estimate canopy heights in a woodland ecosystem *Remote Sens (Basel)*. 2016;8:Article 1. <https://doi.org/10.3390/rs8010050>.
- Joris, C. (2023). Gslnls: GSL nonlinear least-squares fitting. <https://CRAN.R-project.org/package=gslnls>.
- Jurjević L, Liang X, Gašparović M. et al. Is field-measured tree height as reliable as believed – part II, a comparison study of tree height estimates from conventional field measurement and low-cost close-range remote sensing in a deciduous forest *ISPRS J Photogrammet Remote Sens*. 2020;169:227–41. <https://doi.org/10.1016/j.isprsjprs.2020.09.014>.
- Li D, Gu X, Pang Y. et al. Estimation of Forest aboveground biomass and leaf area index based on digital aerial photograph data in Northeast China Forests. 2018;9:Article 5. <https://doi.org/10.3390/f9050275>.
- Marziliano PA, Tognetti R, Lombardi F. Is tree age or tree size reducing height increment in *Abies alba* mill. At its southernmost distribution limit? *Ann Forest Sci*. 2019;76:Article 1. <https://doi.org/10.1007/s13595-019-0803-5>.
- Mielcarek M, Kamińska A, Stereńczak K. Digital aerial photogrammetry (DAP) and airborne laser scanning (ALS) as sources of information about tree height: comparisons of the accuracy of remote sensing methods for tree height estimation *Remote Sens (Basel)*. 2020;12:Article 11. <https://doi.org/10.3390/rs12111808>.
- Moré JJ. The Levenberg-Marquardt algorithm: Implementation and theory. In: *Numerical Analysis: Proceedings of the Biennial Conference Held at Dundee June 28–July 1, 1977*, Springer, Berlin, Heidelberg, 2006, 105–16. <https://doi.org/10.1007/BFb0067700>.
- Pretzsch H. Forest dynamics, growth, and yield. In: Pretzsch H, (ed.). *Forest Dynamics, Growth and Yield: From Measurement to Model*. Springer, Berlin, Heidelberg, 2009, 1–39. [https://doi.org/10.1007/978-3-540-88307-4\\_1](https://doi.org/10.1007/978-3-540-88307-4_1).
- Raulier F, Lambert M-C, Pothier D. et al. Impact of dominant tree dynamics on site index curves *For Ecol Manage*. 2003;184:65–78.
- Rennolls K. ‘Top height’: its definition and estimation *Commonw For Rev*. 1978;57:215–9.
- Reutzbuch SE, Andersen H-E, McGaughey RJ. Light detection and ranging (LIDAR): an emerging tool for multiple resource inventory *J Forestry*. 2005;103:286–92. <https://doi.org/10.1093/jof/103.6.286>.
- Rodríguez-Vivancos A, Manzanera JA, Martín-Fernández S. et al. Analysis of structure from motion and airborne laser scanning features for the evaluation of forest structure *Eur J For Res*. 2022;141:447–65. <https://doi.org/10.1007/s10342-022-01447-7>.
- Roussel J-R, Auty D, Coops NC. et al. Lid R: an R package for analysis of airborne laser scanning (ALS) data *Remote Sens Environ*. 2020;251:112061.
- Sharma RP, Brunner A, Eid T. et al. Modelling dominant height growth from national forest inventory individual tree data with short time series and large age errors *For Ecol Manage*. 2011;262:2162–75.
- Sibona E, Vitali A, Meloni F. et al. Direct measurement of tree height provides different results on the assessment of LiDAR accuracy *Forests*. 2017;8:Article 1. <https://doi.org/10.3390/f8010007>.
- Skovsgaard JP, Vanclay JK. Forest site productivity: a review of the evolution of dendrometric concepts for even-aged stands *Forestry*. 2008;81:13–31.
- Snavely N, Seitz SM, Szeliski R. Modeling the world from internet photo collections *Int J Comput Vis*. 2008;80:189–210.
- Socha J, Hawryło P, Stereńczak K. et al. Assessing the sensitivity of site index models developed using bi-temporal airborne laser scanning data to different top height estimates and grid cell sizes *Int J Appl Earth Observ Geoinform*. 2020;91:102129. <https://doi.org/10.1016/j.jag.2020.102129>.
- Socha J, Pierzchalski M, Bałazy R. et al. Modelling top height growth and site index using repeated laser scanning data *For Ecol Manage*. 2017;406:307–17.
- Socha J, Tymińska-Czabańska L. A method for the development of dynamic site index models using height-age data from temporal sample plots *Forests*. 2019;10:542.
- Socha J, Hawryło P, Tymińska-Czabańska L. et al. Higher site productivity and stand age enhance forest susceptibility to drought-induced mortality. *Agricultural and Forest Meteorology*, 2023;341:109680. <https://doi.org/10.1016/j.agrformet.2023.109680>.
- Splechtn BE. Height growth and site index models for Pacific silver fir in southwestern British Columbia *J Ecosyst Manage*. 2001;1:2–14. <https://doi.org/10.22230/jem.2001v1n1a214>.
- Stereńczak K, Mielcarek M, Wertz B. et al. Factors influencing the accuracy of ground-based tree-height measurements for major European tree species *J Environ Manage*. 2019;231:1284–92. <https://doi.org/10.1016/j.jenvman.2018.09.100>.
- Straub C, Stepper C, Seitz R. et al. Potential of UltraCamX stereo images for estimating timber volume and basal area at the plot level in mixed European forests *Can J For Res*. 2013;43:731–41. <https://doi.org/10.1139/cjfr-2013-0125>.
- Swinfield T, Lindsell JA, Williams JV. et al. Accurate measurement of tropical forest canopy heights and aboveground carbon using structure from motion *Remote Sens (Basel)*. 2019;11:Article 8. <https://doi.org/10.3390/rs11080928>.
- Tompalski P, Coops NC, White JC. et al. Estimating changes in forest attributes and enhancing growth projections: a review of existing approaches and future directions using airborne 3D point cloud data *Curr Forestry Rep*. 2021;7:1–24.
- Tompalski P, Coops NC, White JC. et al. Augmenting site index estimation with airborne laser scanning data *Forest Sci*. 2015;61:861–73.
- Tuominen S, Pekkarinen A. Performance of different spectral and textural aerial photograph features in multi-source forest inventory *Remote Sens Environ*. 2005;94:256–68. <https://doi.org/10.1016/j.rse.2004.10.001>.
- Turner D, Lucieer A, Wallace L. Direct georeferencing of ultra-highresolution UAV imagery. *IEEE Transactions on Geoscience and Remote Sensing*, 2013;52(5):2738–2745. <https://doi.org/10.1109/TGRS.2013.2265295>.

- Tukey JW. *Exploratory Data Analysis*. Addison-Wesley. 1977. [https://doi.org/10.1007/978-0-387-32833-1\\_136](https://doi.org/10.1007/978-0-387-32833-1_136).
- Tymińska-Czabańska L, Hawryło P, Socha J. Assessment of the effect of stand density on the height growth of scots pine using repeated ALS data. *Int J Appl Earth Observ Geoinform.* 2022;108:102763.
- Tymińska-Czabańska L, Socha J, Hawryło P, et al. Weather-sensitive height growth modelling of Norway spruce using repeated airborne laser scanning data. *Agric For Meteorol.* 2021;308:108568.
- Vauhkonen J, Maltamo M, McRoberts RE, et al. Introduction to forestry applications of airborne laser scanning. In: Maltamo M, Næsset E, Vauhkonen J, (eds.). *Forestry Applications of Airborne Laser Scanning: Concepts and Case Studies*. Netherlands: Springer, 2014, 1–16. [https://doi.org/10.1007/978-94-017-8663-8\\_1](https://doi.org/10.1007/978-94-017-8663-8_1).
- Viljanen N, Honkavaara E, Näsi R, et al. A novel machine learning method for estimating biomass of grass swards using a photogrammetric canopy height model, images and vegetation indices captured by a drone. *Agri.* 2018;8:Article 5. <https://doi.org/10.3390/agriculture8050070>.
- Wallace L, Lucieer A, Malenovský Z, et al. Assessment of Forest structure using two UAV techniques: a comparison of airborne laser scanning and structure from motion (SfM) point clouds. *Forests.* 2016;7:Article 3. <https://doi.org/10.3390/f7030062>.
- Wang Y, Lehtomäki M, Liang X, et al. Is field-measured tree height as reliable as believed—a comparison study of tree height estimates from field measurement, airborne laser scanning and terrestrial laser scanning in a boreal forest. *ISPRS J Photogramm Remote Sens.* 2019;147:132–45.
- White JC, Stepper C, Tompalski P, et al. Comparing ALS and image-based point cloud metrics and modelled forest inventory attributes in a complex coastal Forest environment. *Forests.* 2015;6:Article 10. <https://doi.org/10.3390/f6103704>.
- White JC, Wulder MA, Vastaranta M, et al. The utility of image-based point clouds for forest inventory: a comparison with airborne laser scanning. *Forests.* 2013;4:Article 3. <https://doi.org/10.3390/f4030518>.
- Zahawi RA, Dandois JP, Holl KD, et al. Using lightweight unmanned aerial vehicles to monitor tropical forest recovery. *Biol Conserv.* 2015;186:287–95. <https://doi.org/10.1016/j.biocon.2015.03.031>.
- Zarco-Tejada PJ, Diaz-Varela R, Angileri V, et al. Tree height quantification using very high resolution imagery acquired from an unmanned aerial vehicle (UAV) and automatic 3D photo-reconstruction methods. *Eur J Agron.* 2014;55:89–99. <https://doi.org/10.1016/j.eja.2014.01.004>.
- Zhang H, Bauters M, Boeckx P, et al. Mapping canopy heights in dense tropical forests using low-cost UAV-derived photogrammetric point clouds and machine learning approaches. *Remote Sens (Basel).* 2021;13:3777.



# Digital aerial photogrammetry as a spatial and temporal extension of ALS in forest height growth modeling

Piotr Janiec<sup>a,b</sup>, Paweł Hawryło<sup>a</sup>, Luiza Tymińska-Czabańska<sup>a</sup>, Marcin Polak<sup>a</sup> and Jarosław Socha<sup>a</sup>

<sup>a</sup>Department of Forest Resources Management, Faculty of Forestry, University of Agriculture in Krakow, Kraków, Poland; <sup>b</sup>Forest Management and Geodesy Bureau, Sekocin Stary, Poland

## ABSTRACT

Forest height is the key variable measured within the frame of forest monitoring and, at the same time, the most important input variable in forest growth modeling. In particular, top height (TH), a fundamental stand attribute that affects biomass allocation and carbon storage. In this study, we demonstrated the potential of digital aerial photogrammetry (DAP) data in TH growth modeling. We used DAP-derived TH corrected by using reference TH values calculated based on airborne laser scanning (ALS) data. The novelty of this approach lies in the fact that we corrected DAP-based TH measurement using reference from different years. In the developed approach, the ALS-derived TH is updated to the year of DAP data collection using a TH growth model, so that it can be used as a reference for the correction of the DAP-derived TH. We showed that the effectiveness of TH updating is almost independent of the growth model used, indicating that this parameter can be updated using models that are not adapted to local growth conditions. We then showed that the TH derived from the DAP data corrected by using the proposed approach is useful for developing appropriate local TH growth models.

## ARTICLE HISTORY

Received 8 May 2024  
Accepted 11 October 2024

## KEYWORDS

DAP; airborne laser scanning; LiDAR; top height; growth models; remote sensing

## 1. Introduction

We are currently witnessing rapid changes in forest ecosystem dynamics, particularly in terms of growth and productivity (Mensah et al. 2021; Pretzsch et al. 2014). Such changes have a profound impact on forest growth resilience, and efforts in forest management are required to preserve forests and help them adapt to climate change (Pretzsch 2009). Under changing growth conditions, the ability to monitor forest parameters in near real time becomes increasingly important (Achim et al. 2022). Growth models that account for local site conditions and actual growth patterns are also becoming progressively more relevant for sustainable forest management (Achim et al. 2022; Blanco Vaca and Wong 2023; Bontemps and Bouriaud 2014). The unprecedented number of new forest data that are being acquired with remote sensing technologies opens up new opportunities for the development of forest growth models that overcome previous data availability limitations (Tompalski et al. 2021). Therefore, in an era of observable environmental change, it seems

**CONTACT** Piotr Janiec  [piotrjaniec2@gmail.com](mailto:piotrjaniec2@gmail.com)  Department of Forest Resources Management, Faculty of Forestry, University of Agriculture in Krakow, Al. 29 Listopada 46, 31–425 Kraków, Poland; Forest Management and Geodesy Bureau, Sekocin Stary, Poland

© 2024 The Author(s). Published by Informa UK Limited, trading as Taylor & Francis Group  
This is an Open Access article distributed under the terms of the Creative Commons Attribution License (<http://creativecommons.org/licenses/by/4.0/>), which permits unrestricted use, distribution, and reproduction in any medium, provided the original work is properly cited. The terms on which this article has been published allow the posting of the Accepted Manuscript in a repository by the author(s) or with their consent.

necessary to combine traditional methods for monitoring and modeling forest growth by using field measurements with remote sensing data to adequately respond to emerging challenges.

Forest height is one of the key variables measured in forest monitoring and, at the same time, the most important input variable in forest growth modeling (António et al. 2007; Bastin et al. 2018; Bi et al. 2010; Sharma, Amateis, and Burkhart 2002; Vanninen et al. 1996). In particular, top height (TH), a fundamental morphological stand attribute that affects biomass allocation and carbon storage, gives a direct indication of forest growth (Zhou et al. 2019) and is also one of the parameters that can be relatively precisely measured and monitored by using remote sensing data (Hawrylo et al. 2024; Janiec et al. 2023; Jurjević et al. 2020; Tymińska-Czabańska et al. 2021; Tymińska-Czabańska, Hawrylo, and Socha 2022; Wang et al. 2019). TH is one of the primary variables used to determine site productivity in site index (SI) approaches (Zhou et al. 2019). Accurate assessments of site productivity are critical for sustainable forest management, as site productivity plays a vital role in making informed decisions about species composition, silvicultural practices, allowable harvest levels, rotation lengths, and timber yield projections (Pretzsch 2009). The accuracy of the determination of SIs is affected by the accuracy of the determination of stand age and TH and the adequacy of the SI model. To date, field measurements from sample plots and stem analysis have been used to develop SI models (Socha and Tymińska-Czabańska 2019). However, with both sample plots (SP) and stem analysis (SA) data, it is difficult to cover the full range of site conditions and forest growth variability due to the time-consuming and costly nature of the measurements. As a result, the models developed from SP and SA data often do not adequately reflect local growth patterns (Marziliano, Tognetti, and Lombardi 2019; Socha and Tymińska-Czabańska 2019). In the context of rapidly changing site conditions, an additional and particularly important limitation of SP inventory data and growth reconstruction data from SA is that the models developed based on them reflect long-term growth patterns that may differ significantly from currently observed increments (Mensah et al. 2021). This problem can be solved with the use of remote sensing products, in particular airborne laser scanning (ALS) and airborne digital aerial photogrammetry (DAP) data (Guerra-Hernández et al. 2018).

In recent years, bi-temporal ALS data have been used in height growth modeling, with satisfactory results (Socha et al. 2017; Socha et al. 2020; Tompalski et al. 2015; Tymińska-Czabańska et al. 2021). However, there is still a limited number of multi-temporal ALS data available for areas of interest. DAP data have demonstrated their utility in assessing various forest stand attributes, including tree height (Guerra-Hernández et al. 2018), basal area (White et al. 2015), and timber volume (Hawrylo, Tompalski, and Węzyk 2017; Straub et al. 2013). Recent research has focused on comparing forest stand inventories derived from DAP and airborne laser scanning (ALS) point clouds (Guerra-Hernández et al. 2018; Hartley et al. 2020; Hawrylo, Tompalski, and Węzyk 2017; Mielcarek, Kamińska, and Stereńczak 2020; Prado et al. 2022; Wallace et al. 2016). The studies consistently find that ALS-derived top height (TH) values have smaller errors compared to those obtained from DAP. Nevertheless, these studies often report a strong correlation between DAP, ALS and field data. A much more accessible but much less common source of stand height data for modeling is represented by multi-temporal DAP data. DAP point clouds can be a relatively easily accessible and less expensive source of data for the calibration of growth models. The DAP data can be acquired using low-cost drones during the forest inventory. Archival DAP data is much more widely available than LiDAR data. Its use allows backward modeling and the construction of much longer time series. The Structure for Motion technique allows for straightforward point cloud delivery without having to impose strict homogeneity by overlapping images, positioning and calibrating the camera (Iglhaut et al. 2019). This technique is less expensive than ALS data acquisition and, in particular, provides more widely available multi-temporal DAP data. However, these data represent only the upper forest canopy (White et al. 2013). Studies comparing stand height determination methods based on ALS and DAP data have shown that ALS data are characterized by a smaller error (Guerra-Hernández et al. 2018; Hartley et al. 2020; Hawrylo, Tompalski, and Węzyk 2017; Mielcarek, Kamińska, and Stereńczak 2020). Stand height values determined with DAP have systematic acquisition-specific errors and are, at the same time, highly correlated with actual stand height values (Jensen and Mathews 2016). If

reference data from field measurements or ALS data are available for the study area for the years of DAP data collection, it is possible to directly determine the bias in DAP stand height (TH) determination and perform correction. In such a case, the systematic error is determined separately for each DAP acquisition year by calculating the difference between the average TH calculated with DAP and the reference TH determined from sample plot measurements or by using ALS data. A limitation of this DAP data correction method is that its application requires ALS or ground survey data to be available for the year in which the DAP data were collected; while DAP data are generally readily available, this is less often true for ALS data or reference ground survey data for a specific forest district. Thus, it is often difficult to apply this method, and the enormous potential of using DAP data remains limited. Therefore, the aim of this research study was to develop a method to correct DAP data based on ALS data or data from sample plot measurements referring to a different year from the year of DAP data collection. The fact that not only ALS data but also field measurement data can be used as a reference makes the developed approach flexible.

In order to verify the assumptions of the proposed approach, we established two sub-objectives in which we verified the following assumptions: (1) We aimed to verify the suitability of different TH growth models to update the TH determined for the year of ALS acquisition (or field measurements) according to the reference TH for the year of DAP data acquisition. We assumed that for the very short time between the ALS data acquisition or field measurements and the DAP data acquisition, the errors in the determination of the TH increment are negligible compared with the corrected TH and that the selection of TH growth model used for updating this parameter has no effect on the accuracy of the calculated correction. (2) We aimed to determine whether the TH values obtained by using the DAP data corrected with the proposed approach were useful for developing appropriate local TH growth models.

## 2. Methods

### 2.1. Study area description

The study area comprised Scots pine (*Pinus sylvestris*) stands in Milicz Forest District (Figure 1). The entire study area covered nearly 23,600 ha, of which Scots pine stands cover nearly 6,400 ha. The area is partly located in Natural Forest Regions III and V, based on the Polish natural forest regionalization system (Zielony and Kliczkowska 2012). The stands in the study area were predominantly Scots pine (75%), with a share of oak (10%), beech (6%), black alder (5%), and silver birch (2%). The age of the Scots pine stands varied between 1 and 160 years; however, in the analysis, we excluded tree stands younger than 10 and older than 120 years. We also excluded tree stands with a share of Scots pine lower than 80%. It is probable that the young stands observed at the time of the initial measurement exhibited a markedly different age and height structure compared to the second data acquisition. Consequently, we excluded these stands from the subsequent analyses, as they are characterized by high variability and the presence of outliers, which may have a detrimental effect on the calibration of the models. The ALS data from two periods (2012 and 2019) covered only the southern part of the study area (Figure 1), while the DAP data from two other periods (2013 and 2020) covered the entire study area.

### 2.2. Data acquisition

Information on species composition and stand age was obtained from the National Forest Information System and Forest Data Bank (<https://www.bdl.lasy.gov.pl/portal/>). We acquired the DAP and ALS data from the official repository of the Head Office of Geodesy and Cartography (GUGiK) in Poland (<https://www.geoportal.gov.pl/>).

The acquired airborne DAP data referred to the years 2013 and 2020 (Table 1), where the RGB photos were characterized by 0.25 m spatial resolution and minimum image overlaps of 60% along

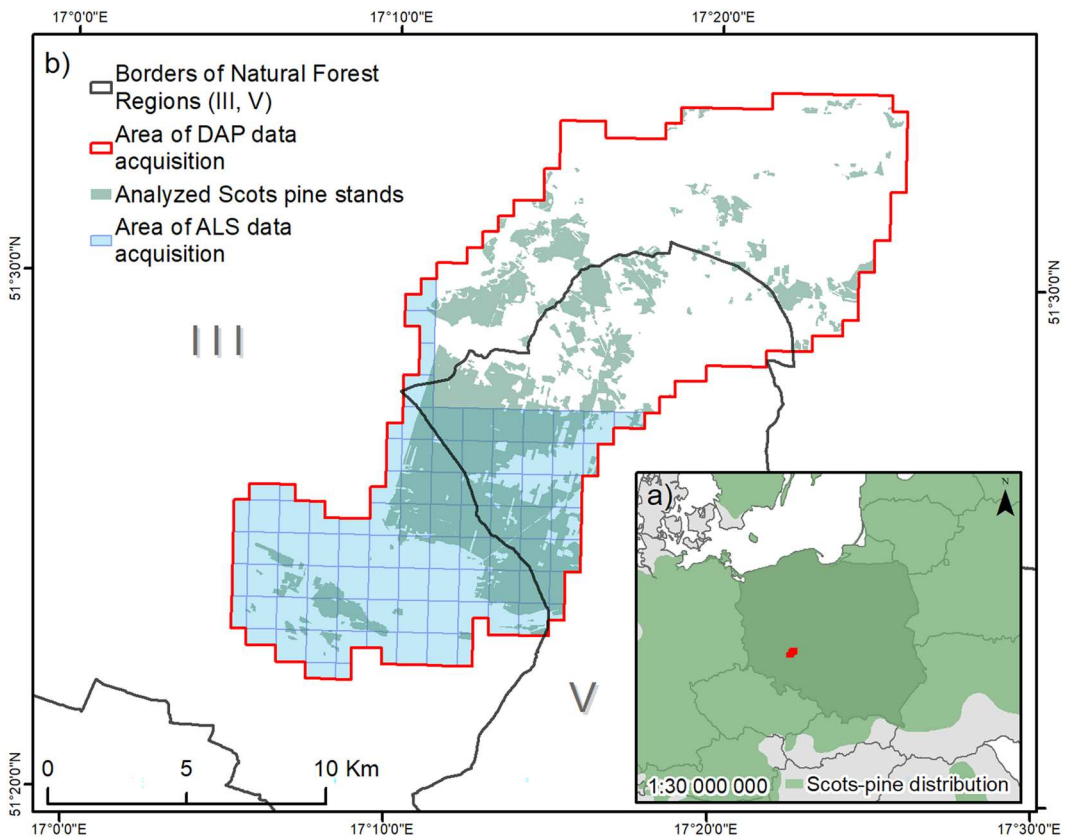


**Figure 1.** Study area location in Poland (a) and in Milicz Forest District, western Poland (b).

the track and 25% across the track. We selected 100 and 108 images for 2013 and 2020, respectively, within a buffer of 2 km from the study area. Both datasets were acquired under leaf-off conditions. Airborne image-based point clouds were generated using the computer vision DAP approach (Turner, Lucieer, and Watson 2012) and the Agisoft PhotoScan Professional software package. A detailed description of the workflow and software can be found in Turner, Lucieer, and Wallace (2013) and Dandois and Ellis (2013). We used high accuracy parameter for the photo alignment, with 1.000 key point limit per Mpx and 10.000 tie point limit. The point cloud was generated with high quality and mild depth filtering. For aerotriangulation, for the 2020 photos, the external orientation parameters were obtained from the GUGiK, while for the 2013 photos, we used ground control points (GCPs) created both manually and based on the orthophotomap and digital terrain model (DTM) for that year. We generated 15 GCPs for this year. The average density values of the acquired point clouds were 4.3 and 4.5 points/m<sup>2</sup> for 2013 and 2020, respectively (Table 1).

The ALS data referred to the years 2012 and 2019 and were acquired under leaf-off conditions (Table 1). The mean density of both point clouds was 4 points/m<sup>2</sup>, and the ALS positioning accuracy was 0.15 m (according to the provider). Both point clouds were already classified by the data providers.

**Table 1.** DAP (digital aerial photogrammetry) and ALS (airborne laser scanning) data acquisition parameters.

| Type of Data | Acquisition Year | Density [points/m <sup>2</sup> ] | Positioning Accuracy [m] | Spatial Resolution of Images [m] |
|--------------|------------------|----------------------------------|--------------------------|----------------------------------|
| DAP          | 2013             | 4.3                              | -                        | 0.25                             |
|              | 2020             | 4.5                              | -                        | 0.25                             |
| ALS          | 2012             | 4                                | 0.15                     | -                                |
|              | 2019             | 4                                | 0.15                     | -                                |

### 2.3. Determination of TH based on ALS and DAP for years of data acquisition

We performed point cloud processing by using the lidR package in the R environment (Roussel et al. 2020). In the first step, we normalized the point clouds. For ALS data normalization, we used the normalize\_height function and the knnidw algorithm with its default parameters. In the case of the DAP data, we normalized them by subtracting the ALS-derived DTM from each DAP point, where the DTM, with a spatial resolution of 1 m, was derived from the GUGiK (2012). In the next step, we calculated the canopy height models (CHMs) for the years 2012 and 2019 for the ALS data and for the years 2013 and 2020 for the DAP data. All CHMs were created with a spatial resolution of 1 m. For this purpose, we used the ‘p2r’ algorithm with a subcircle size of 0.3 m.

Defining TH as the average height of the 100 thickest trees per 1 ha without taking into account their location is inappropriate, as it depends on the size of the sample plot (or stand). Therefore, to determine the top height, we used the definition proposed by Rennolls (1978), according to which this parameter should be calculated as the average height of non-empty 0.01 ha subplots. In order to obtain the TH of the analyzed pine stands according to this definition, we applied the method for calculating this parameter recommended by Hawryło et al. (2024). TH calculated with this method is hardly sensitive to changes as a result of silvicultural treatments (Hawryło et al. 2024). By following the methodology verified in previous TH growth modeling studies (Socha et al. 2017; Socha et al. 2020; Tymińska-Czabańska et al. 2021; Tymińska-Czabańska, Hawryło, and Socha 2022), all Scots pine stands in the study area were divided into  $50 \times 50$  m grid cells, obtained with the aggregation of 25  $10 \times 10$  m subcells (Figure 2 a). For this purpose, for each year of acquisition, the TH was calculated for the  $50 \times 50$  m grid cells as the average of the 25 maximum CHM values of the  $10 \times 10$  m subcells. In the calculation of the averages, the cells of the  $10 \times 10$  m grid with maximum CHM values lower than 2/3 of the TH of the  $50 \times 50$  m grid cells, which were considered empty, were removed to capture only the heights of the tallest trees (Figure 2 b). In order to eliminate the counting of trees from neighboring stands in each stand, an internal buffer of 15 m in width was used, and the  $50 \times 50$  m grid cells that fell completely within the stand without entering the buffer boundaries were included in the calculations (Figure 2 c). This method for determining heights was applied to both the DAP and ALS data for individual acquisition years. The TH values calculated for the  $50 \times 50$  m grid cells were treated as single observations in the modeling.

### 2.4. Updating of TH determined from ALS to year of DAP data acquisition

Previous studies have shown that TH determined from point clouds extracted from DAP data is subject to systematic acquisition-specific errors (Hawryło, Tompalski, and Węzyk 2017; Mielcarek,

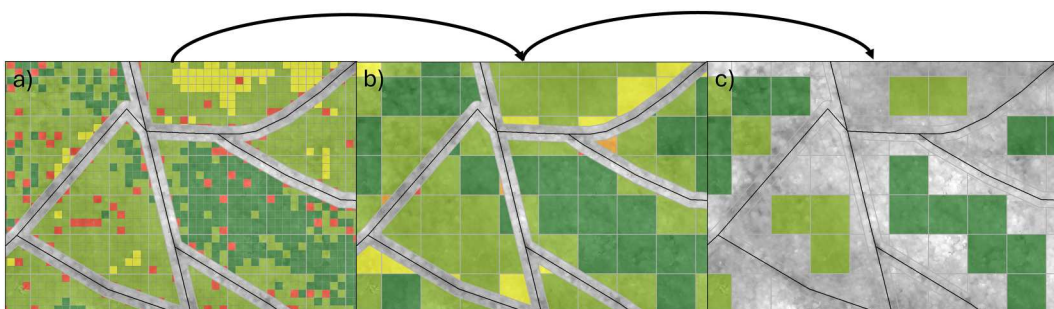


**Figure 2.** General workflow of top height (TH) estimation. Canopy height model (CHM) values from green (lower values) to red (higher values) in (a)  $10 \times 10$  subcells and (b)  $50 \times 50$  m grid cells, resulting from aggregation of 25  $10 \times 10$  m subcells; c) internal buffer of 15 m in width and removal of incomplete  $50 \times 50$  grid cells. The black lines refers to the stands boundaries.

Kamińska, and Stereńczak 2020; Swinfield et al. 2019; Wallace et al. 2016). It is therefore necessary to identify the bias of TH<sub>DAP</sub> and correct it by using reference TH values; the latter can be determined with ALS data (TH<sub>ALS</sub>), which often have higher accuracy than data from traditional field surveys (Hawryło et al. 2024; Wang et al. 2019). A limitation of this DAP data correction method is that its use requires the availability of ALS data for the year in which the DAP data were collected, which can limit the great potential of using DAP data. We therefore developed a method to update TH<sub>ALS</sub> collected in any year according to the TH of the year of DAP data acquisition (Figure 3). The TH updated in this way was used as a reference (TH<sub>ref</sub>) for TH<sub>DAP</sub> correction (TH<sub>DAPcorr</sub>).

In the developed approach, the data for estimating the TH<sub>ref</sub> of the year of DAP data acquisition are calculated by using the TH<sub>ALS</sub> calculated for the year of ALS data acquisition, which is updated by using any TH growth model up to the year of DAP data acquisition (Figure 3). This is performed by calculating the TH increment for the period representing the difference between the year of ALS data acquisition and the year of DAP data acquisition calculated by using the TH growth model. The TH estimated using the ALS data is then updated to the year of DAP data acquisition by using the TH increment (Figure 3). The updated TH is then used as the reference value (TH<sub>ref</sub>) of the year of DAP data acquisition.

We assumed that for a relatively short time between ALS and DAP data acquisition, the errors in the determination of the TH increment performed by using different models is negligible compared with the value of the corrected TH. Therefore, the result of updating TH<sub>ALS</sub> to that of the year of DAP data acquisition should not depend on the TH growth model used to estimate the TH increment. To verify this assumption, we used 3 TH growth models (Table 2, equation 1) to calculate the TH increment required to estimate the TH<sub>ref</sub> of the years of DAP data acquisition – 2013 and 2020. For this purpose, we applied the TH growth model for Scots pine in Poland (M1) and the regional TH growth models for Natural Forest Regions III (M2) and V (M3), in which the study area was located.

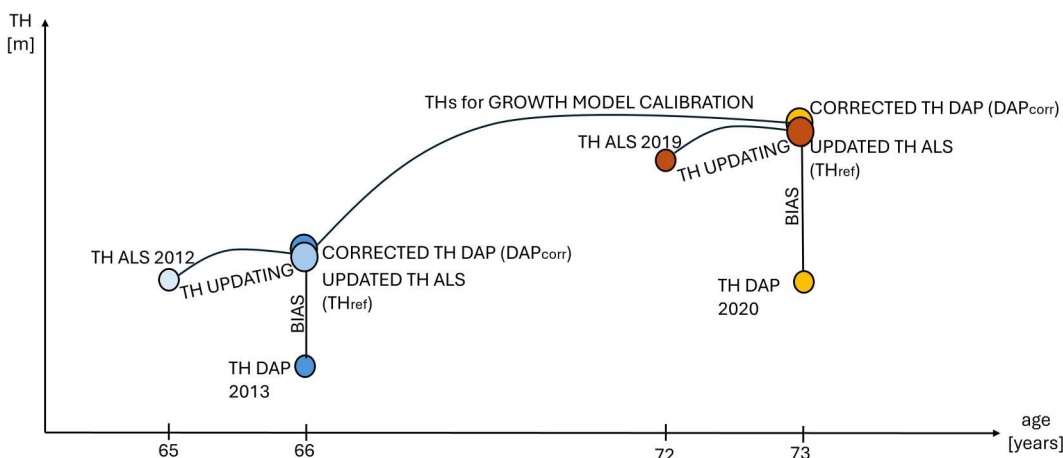


**Figure 3.** Graphic description of top height (TH) updating and use of updated TH for TH DAP correction.

**Table 2.** Parameters of models used for updating top height (TH) obtained from ALS data according to DAP data acquisition year (Socha et al. 2021).

| Model | Spatial Scope of Model    | $\beta_1$ | $\beta_2$ | $\beta_3$ |
|-------|---------------------------|-----------|-----------|-----------|
| M1    | Poland                    | 1.363     | 5920.904  | 30.443    |
| M2    | Natural Forest Region III | 1.26398   | 37741.1   | -14.6078  |
| M3    | Natural Forest Region V   | 1.39      | 3325.004  | 36.6838   |

The general form of the TH growth models used to calculate the TH increment used to update TH ALS according to that of the year of DAP data acquisition is described by [equation 1](#):

$$TH = TH_1 \frac{T_1^{\beta_1} R + \beta_2}{T_1^{\beta_1} (T^{\beta_1} R + \beta_2)} \quad (1)$$

where

$$R = Z_0 + \left( Z_0^2 + \frac{2\beta_2 TH_1}{T_1^{\beta_1}} \right)^{0.5} \quad (1.1)$$

$$Z_0 = TH_1 - \beta_3 \quad (1.2)$$

and  $\beta_1$ ,  $\beta_2$ , and  $\beta_3$  are model parameters ([Table 2](#)); TH is the top height at age T; and  $TH_1$  is the top height at age  $T_1$ . R is an expression describing the growth rate, while  $Z_0$  is an adjustment expression.

By using the stand age (T) and  $TH_{ALS}$  defined for each  $50 \times 50$  m grid cell for 2012 and 2019, based on the 3 selected TH growth models ([Table 2](#)),  $TH_{ref}$  was calculated for the DAP data acquisition years 2013 and 2020, respectively. In this way, 3 reference TH values were obtained ( $TH_{ref1}$ ,  $TH_{ref2}$ , and  $TH_{ref3}$ ). In order to test Assumption 1, which states that the result of the updated TH does not significantly depend on the growth model used, the  $TH_{ref}$  values obtained with the 3 models were compared by using ANOVA. In further analyses, the reference values obtained with the 3 models ( $TH_{ref1}$ ,  $TH_{ref2}$ , and  $TH_{ref3}$ ) calculated in this way for 2013 and 2020 provided a reference for the DAP data acquired in those years.

The reference data were then used to investigate whether  $TH_{DAP}$  was subject to systematic error. A t-test for the dependent variables was performed in order to verify the existence of significant differences between  $TH_{DAP}$  and the 3  $TH_{ref}$  values ( $TH_{ref1}$ ,  $TH_{ref2}$ , and  $TH_{ref3}$ ), which would have indicated the presence of bias.

Then, for the 2013 and 2020 acquisition years, the bias of  $TH_{DAP}$  was calculated as the average difference between  $TH_{DAP}$  and  $TH_{ref1}$ ,  $TH_{ref2}$ , and  $TH_{ref3}$  of each  $50 \times 50$  m grid cell. These differences were calculated by using  $50 \times 50$  m grid cells from the ALS data acquisition area ([Figure 1](#)). Next, the average DAP bias calculated separately for each  $TH_{ref}$  ( $TH_{ref1}$ ,  $TH_{ref2}$ , and  $TH_{ref3}$ ) and the years 2013 and 2020 for the ALS data acquisition area was summed to the  $TH_{DAP}$  calculated for each  $50 \times 50$  m grid cell within the DAP data acquisition area ([Figure 1](#)). In this way, we obtained 3 corrected TH values ( $TH_{DAPcorr1}$ ,  $TH_{DAPcorr2}$ , and  $TH_{DAPcorr3}$ ) for each of the DAP data acquisition years (2013 and 2020) ([Figure 4](#)).

## 2.5. Evaluation of effectiveness of TH DAP correction method

The evaluation of the TH correction method was carried out for the area with ALS data availability by comparing the corrected TH values ( $TH_{DAPcorr1}$ ,  $TH_{DAPcorr2}$ , and  $TH_{DAPcorr3}$ ) with the respective  $TH_{ref}$  values ( $TH_{ref1}$ ,  $TH_{ref2}$ , and  $TH_{ref3}$ ). The TH errors were characterized by using the MAE ([equation 2](#)) and RMSE ([equation 3](#)):

$$RMSE(y, \hat{y}) = \sqrt{\frac{\sum_{i=0}^{N-1} (y_i - \hat{y}_i)^2}{N}} \quad (2)$$

$$MAE(y, \hat{y}) = \frac{\sum_{i=0}^{N-1} |y_i - \hat{y}_i|}{N} \quad (3)$$

where  $y_i$  is the measured value,  $\hat{y}_i$  is the predicted value, i is the summation index, N is the number of cases,  $\bar{y}_i$  is the mean volume of N cases, and p is the number of parameters in the model.

The statistical difference between corrected and reference TH values was tested by using Student's t-test for dependent variables.

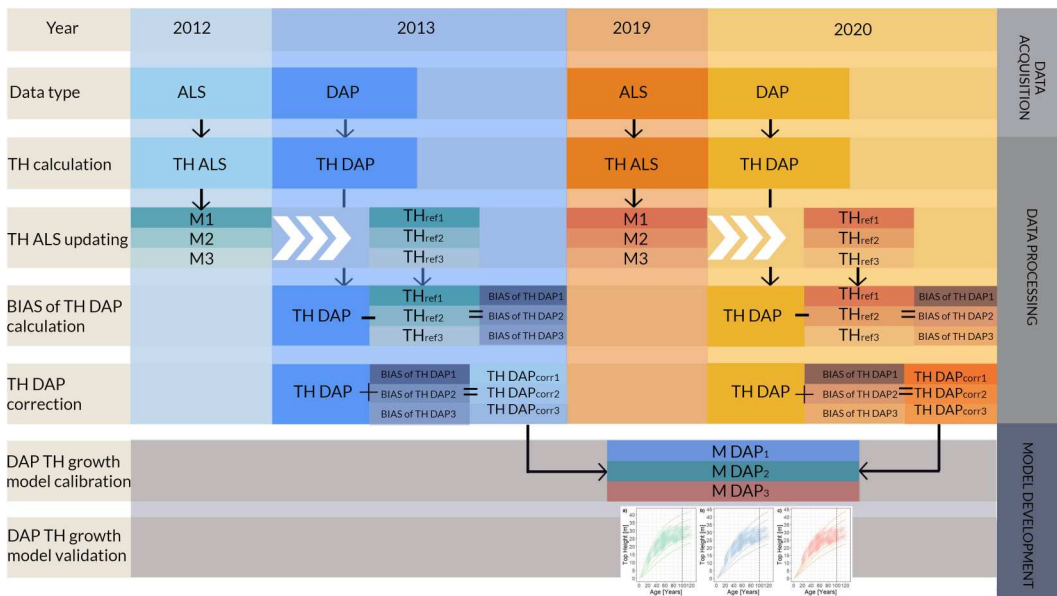


**Figure 4.** Flowchart of methods used for DAP model calibration.

## 2.6. Use of corrected DAP TH for calibration of local TH growth model

In the next stage of the analyses, the TH DAP values ( $\text{TH DAP}_{\text{corr}1}$ ,  $\text{TH DAP}_{\text{corr}2}$ , and  $\text{TH DAP}_{\text{corr}3}$ ) determined for 2013 and 2020 were used to calibrate the TH growth models. Prior to calibration, a standard method for eliminating TH outliers (Tukey 1977) was employed, as it has been shown to be effective in previous TH growth modeling studies (Janiec et al. 2023; Socha et al. 2017; Tymińska-Czabańska, Hawryło, and Socha 2022). The outliers were calculated and removed from 20-year age classes for both 2013 and 2020.

Two pairs of age (T) and TH values ( $T_{2013}$  and  $\text{TH DAP}_{\text{corr}(1-3)2013}$ , and  $T_{2020}$  and  $\text{TH DAP}_{\text{corr}(1-3)2020}$ ) calculated for 2013 and 2020 for each grid cell were used to calibrate the parameters of the growth function (Equation 1). In this way, 3 models were developed ( $M_{\text{DAP}1}$ ,  $M_{\text{DAP}2}$ , and  $M_{\text{DAP}3}$ ).

To obtain the fitting model parameters, we used nonlinear least-squares optimization and the Levenberg – Marquardt algorithm (Moré 1978), while for model fitting, we used the gsnls library in the R environment (Core Team 2021).

## 2.7. Model evaluation

The following goodness-of-fit statistics were used to compare the models developed ( $M_{\text{DAP}1}$ ,  $M_{\text{DAP}2}$ , and  $M_{\text{DAP}3}$ ):

- Mean absolute error (MAE; equation 2);
- Root-mean-squared error (RMSE; equation 3);
- Adjusted coefficient of determination ( $R^2_{\text{adj}}$ ), calculated as follows:

$$R^2_{\text{adj}} = 1 - \frac{\sum_{i=0}^{N-1} (y_i - \hat{y}_i)^2}{\sum_{i=1}^N (y_i - \bar{y}_i)^2} \left( \frac{N-1}{N-p} \right) \quad (4)$$

where  $y_i$  is the measured value,  $\hat{y}_i$  is the predicted value,  $i$  is the summation index,  $N$  is the number of cases,  $\bar{y}_i$  is the mean volume of  $N$  cases, and  $p$  is the number of parameters in the model. As reference, we used the TH values estimated by using the updated ALS TH.

Next, we evaluated the developed models ( $M_{DAP1}$ ,  $M_{DAP2}$ , and  $M_{DAP3}$ ) in order to verify Assumption 2. To assess the appropriateness of the developed models, we compared them with the reference model for Scots pine in Poland ( $M1$ ) and the regional TH growth models for Natural Forest Regions III ( $M2$ ) and V ( $M3$ ).

The flowchart in Figure 4 provides a summary of the above-described methodology, which consists of the following steps: 1. TH calculation based on the ALS and DAP data in the analysed years 2. TH ALS updating, based on the growth models 3. BIAS of TH DAP calculation 4. TH DAP correction 5. DAP TH growth model calibration 6. DAP TH growth model validation.

### 3. Results

#### 3.1. Comparison of $TH_{ref}$ values obtained with three growth models

In order to test Assumption 1, which states that the result of the updated TH does not depend on the growth model used, we compared three  $TH_{ref}$  values ( $TH_{ref1}$ ,  $TH_{ref2}$ , and  $TH_{ref3}$ ) calculated with the three different models ( $M1$ - $M3$ ) by using ANOVA and found no significant differences for either the year 2013 ( $p = 0.931$ ) or the year 2020 ( $p = 0.893$ ).

#### 3.2. Comparison of reference TH and TH derived from DAP and bias identification

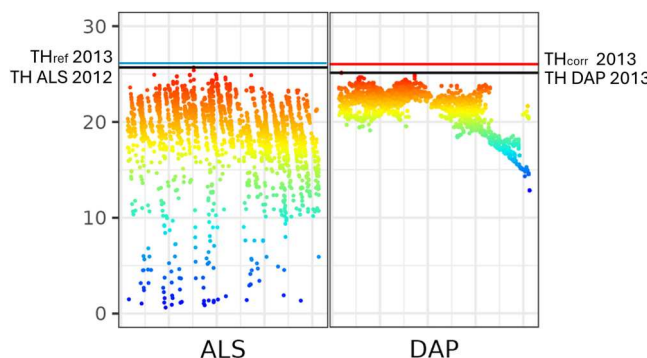
The bias, RMSE, and MAE of the DAP-derived TH differed substantially between 2013 and 2020 (Table 3). Moreover DAP-derived TH differed substantially from all reference TH values ( $TH_{ref1}$ ,  $TH_{ref2}$ , and  $TH_{ref3}$ ). This allowed us to estimate the correction values of the DAP data (Table 3).

#### 3.3. Evaluation of effectiveness of proposed method for DAP-derived TH correction

The average DAP bias (correction values) obtained with the use of the three growth models was added to TH DAP for the years 2013 and 2020 (Figure 5). The corrected DAP-derived TH ( $TH_{DAPcorr1}$ ,  $TH_{DAPcorr2}$ , and  $TH_{DAPcorr3}$ ) were characterized by substantially lower bias, RMSE,

**Table 3.** Characteristics of bias of DAP-derived top height (TH) in comparison with reference TH obtained by using 3 growth models ( $M1$ - $M3$ ).

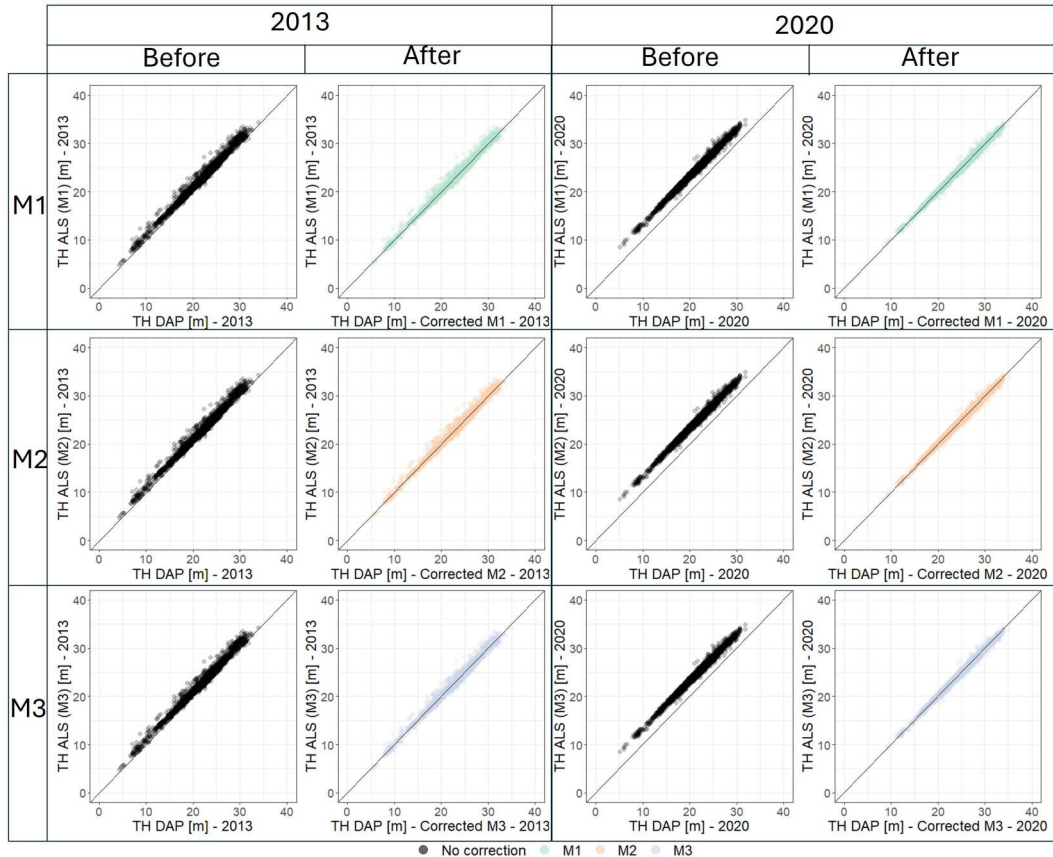
| Reference TH | 2013     |          |         |         | 2020     |          |         |         |
|--------------|----------|----------|---------|---------|----------|----------|---------|---------|
|              | Bias [m] | RMSE [m] | MAE [m] | p-Value | Bias [m] | RMSE [m] | MAE [m] | p-Value |
| THref1       | 0.900    | 1.160    | 0.936   | <0.01   | 3.212    | 3.240    | 3.210   | <0.01   |
| THref2       | 0.940    | 1.190    | 0.974   | <0.01   | 3.255    | 3.280    | 3.250   | <0.01   |
| THref3       | 0.905    | 1.160    | 0.940   | <0.01   | 3.216    | 3.240    | 3.210   | <0.01   |



**Figure 5.** Example of application of DAP-derived top height (TH) correction for 2013 using  $TH_{ref}$  obtained from updating ALS-derived TH for 2012 ( $TH_{ALS2012}$ ).

**Table 4.** Characteristics of accuracy of estimation of corrected DAP-derived top height (TH).

| Corrected TH            | 2013     |          |         |         | 2020     |          |         |         |
|-------------------------|----------|----------|---------|---------|----------|----------|---------|---------|
|                         | Bias [m] | RMSE [m] | MAE [m] | p-Value | Bias [m] | RMSE [m] | MAE [m] | p-Value |
| TH DAP <sub>corr1</sub> | 0.014    | 0.707    | 0.403   | 0.905   | -0.002   | 0.407    | 0.313   | 0.981   |
| TH DAP <sub>corr2</sub> | 0.014    | 0.710    | 0.405   | 0.902   | -0.002   | 0.410    | 0.315   | 0.985   |
| TH DAP <sub>corr3</sub> | 0.014    | 0.706    | 0.402   | 0.906   | -0.002   | 0.406    | 0.312   | 0.980   |

**Figure 6.** Comparison of DAP-derived top height (TH) values for 2013 and 2020 before and after correction with ALS-derived TH values updated with three TH growth models (M1, M2, and M3).

and MAE (Table 4) than the corresponding values before correction (Table 3, Figure 6). Moreover, after correction, the DAP-derived TH (TH DAP<sub>corr1</sub>, TH DAP<sub>corr2</sub>, and TH DAP<sub>corr3</sub>) did not differ significantly from the reference TH (TH<sub>ref1</sub>, TH<sub>ref2</sub>, and TH<sub>ref3</sub>, respectively). We found that with respect to the corrected DAP-derived TH values for 2013, those for 2020 were characterized by smaller bias compared with the reference data. We did not observe significant differences in the bias, RMSE, and MAE of the corrected TH (TH DAP<sub>corr1</sub>, TH DAP<sub>corr2</sub>, and TH DAP<sub>corr3</sub>) for either 2013 or 2020 ( $p > 0.05$ ). Moreover, for both years, these values were not significantly different from the reference TH ALS (TH<sub>ref1</sub>, TH<sub>ref2</sub>, and TH<sub>ref3</sub>) ( $p > 0.05$ ; Table 4).

### 3.4. Model development

The three corrected DAP-derived TH values (TH DAP<sub>corr1</sub>, TH DAP<sub>corr2</sub>, and TH DAP<sub>corr3</sub>) for 2013 and 2020 were used for the calibration of the TH growth models (M<sub>DAP1</sub>, M<sub>DAP2</sub>, and

**Table 5.** Parameter fit characteristics and accuracy of top height (TH) growth models ( $M_{DAP1}$ ,  $M_{DAP2}$ , and  $M_{DAP3}$ ) developed using corrected DAP-derived TH.

|            | Parameter | Value  | Standard Error | t-Value | p-Value | RMSE [m] | MAE [m] | R2    |
|------------|-----------|--------|----------------|---------|---------|----------|---------|-------|
| $M_{DAP1}$ | $\beta_1$ | 1.3    | 0.02           | 78.14   | <0.01   | 0.343    | 0.276   | 0.995 |
|            | $\beta_2$ | 9338.7 | 1308.84        | 7.14    | <0.01   |          |         |       |
|            | $\beta_3$ | 25.9   | 3.17           | 8.18    | <0.01   |          |         |       |
| $M_{DAP2}$ | $\beta_1$ | 1.3    | 0.02           | 78.04   | <0.01   | 0.343    | 0.276   | 0.995 |
|            | $\beta_2$ | 9259.7 | 1302.58        | 7.11    | <0.01   |          |         |       |
|            | $\beta_3$ | 26.2   | 3.18           | 8.23    | <0.01   |          |         |       |
| $M_{DAP3}$ | $\beta_1$ | 1.3    | 0.02           | 78.13   | <0.01   | 0.344    | 0.277   | 0.995 |
|            | $\beta_2$ | 9341.5 | 1309.53        | 7.13    | <0.01   |          |         |       |
|            | $\beta_3$ | 25.9   | 3.18           | 8.14    | <0.01   |          |         |       |

$M_{DAP3}$ , respectively) (Table 5), which were developed based on the DAP-derived corrected TH ( $M_{DAP1}$ ,  $M_{DAP2}$ , and  $M_{DAP3}$ , respectively) and had almost identical parameters and goodness-of-fit statistics. The growth trajectories plotted for these models were identical (Figure 7d).

The developed DAP models were characterized by good data fit (Figure 7, Table 5); the modeled TH growth trajectories did not differ substantially from the corrected TH measurements across the entire height distribution.

The growth trajectories of the three compared models were identical (Figure 7 d), so only model  $M_{DAP1}$  was used for direct comparison with the reference models (M1-M3) (Figure 8). The trajectories of the compared TH growth models were more or less similar depending on site productivity. For the least productive sites, with a site index at a base age of 100 years equal to 20 m, the TH model growth trajectories were very similar (Figure 8). The largest differences were observed for the sites with the highest productivity (site index = 40 m). It is worth noting, however, that the

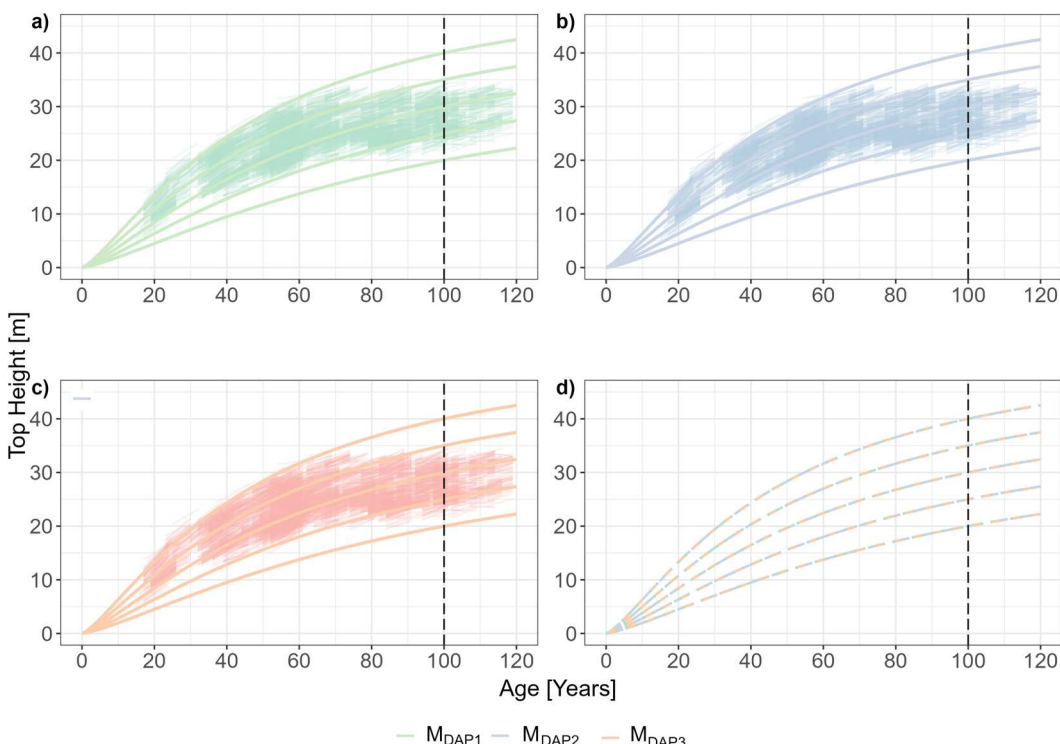


**Figure 7.** Trajectories of top height growth plotted with 3 models, i.e. (a)  $M_{DAP1}$ , (b)  $M_{DAP2}$ , and (c)  $M_{DAP3}$ , which were developed by using top height (TH) change data (thin dashes) obtained from corrected DAP-derived TH values, and their direct comparison (d).

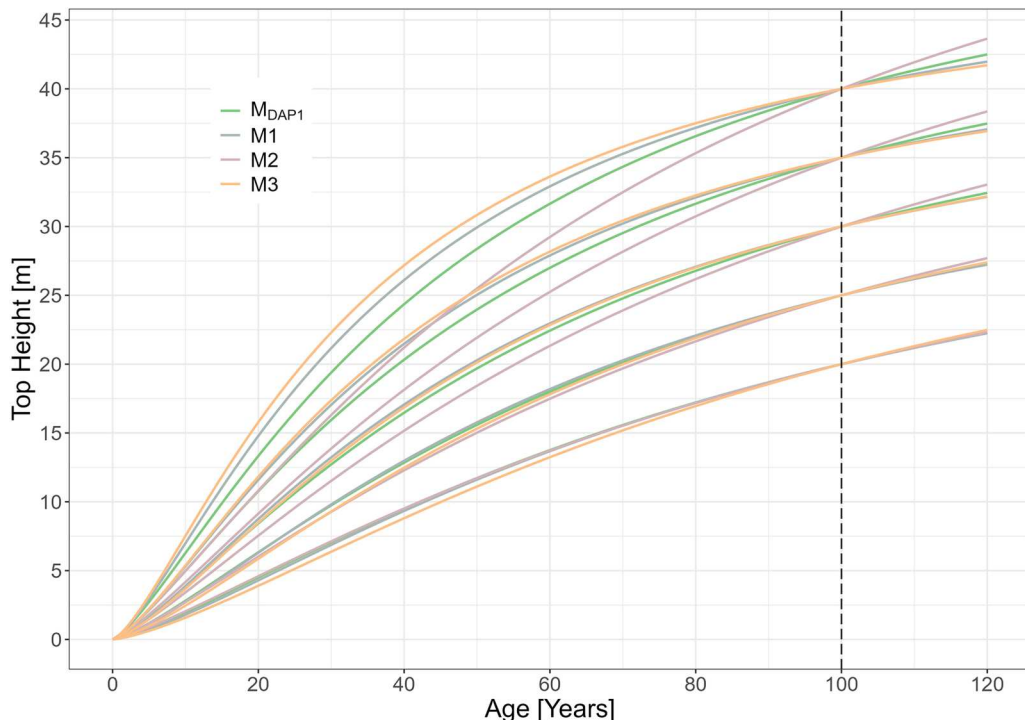


**Figure 8.** Top height (TH) growth models calibrated with corrected DAP data ( $M_{DAP}$ ) and SA (stem analysis; M1, M2, and M3) based on Socha et al. (2021).

trajectories plotted on the basis of the models developed by using the corrected DAP-derived TH presented an averaged TH growth rate compared with the growth rates reflected by the models for Poland (M1), Natural Forest Region III (M2), and Natural Forest Region V (M3). This indicates the adequacy of the models developed on the basis of the DAP-derived TH values.

## Discussion

In this study, we developed a new method to utilize DAP data in TH growth modeling whereby DAP-derived TH is corrected by using reference ALS-derived TH. The novelty of this approach lies in the fact that the reference data can be collected in a incremental period different from the DAP data. The approach developed assumes that the ALS-derived TH is updated according to the year of DAP data collection, so that it can be used as a reference for the DAP-derived TH. We tested the suitability of different TH growth models for updating the ALS-derived TH to the year of DAP data collection. The effectiveness of this TH update is almost independent of the growth model used. Therefore the TH updating can also be performed by using models not adapted to local growth conditions. Next, we showed that the TH obtained from the DAP data corrected by using the proposed technique is useful for developing appropriate local TH growth models.

The developed method increases the potential for using DAP data to determine TH and stand growth. Moreover, we showed that TH underestimation is specific to the DAP image acquisition time. Similarly, the systematic bias of the DAP-derived forest stand height has been widely documented in the literature (Mielcarek, Kamińska, and Stereńczak 2020; Swinfield et al. 2019; Wallace et al. 2016). Our analysis results show that when performing increment determination and then growth modeling with DAP-derived TH, differences in the systematic TH error due to different acquisition times represent a significant problem. The TH estimated on the basis of DAP data

from 2020 was characterized by significantly larger underestimation than that for 2013. This effect may be related to a different type of image aerotriangulation method. Moreover, the differences can also be justifiable by the different light or weather conditions at the time of measurement and different camera parameters (Holopainen et al. 2015).

Therefore, for eliminating the systematic error, correction specific to each DAP data acquisition year is necessary; however, in turn, this requires acquiring reference data to determine the bias. While DAP data are generally widely available for many acquisition dates, obtaining reference data for the same period is challenging.

We solved the above issue by establishing a method to calculate reference TH values for the year of DAP data acquisition based on the values acquired in other years, which are updated by using a TH growth model (workflow). As our analysis results show, any model can be used to update TH. In our case, we updated ALS data, but in the same way, we could update data from field measurements such as sample plots. Recent studies have demonstrated that TH estimates derived from high-quality remote sensing data are more accurate than conventional field measurements (Hawrylo et al. 2024; Jurjević et al. 2020; Sibona et al., 2017; Wang et al. 2019). TH estimates based on the ALS point cloud are appropriate, under the condition that the point cloud density exceeds 2 points/m<sup>2</sup> (Hawrylo et al. 2024). The ALS data we used in our study meet this condition. If the time between ALS data acquisition or field measurements and DAP data acquisition is relatively short, the errors in the determination of the TH increment are negligible compared with the updated TH height values. Some increase in error can be expected as the temporal difference between the data used to determine the reference TH and the DAP data increases. The updated TH values provide a reliable reference to correct the DAP-derived TH by extracting bias. Correcting DAP-derived TH eliminates bias and makes the DAP-derived TH fully reliable. This finding is in line with the work by Swinfield et al. (2019), who applied TH correction in the case of a tropical forest. Our approach allows for eliminating extensive fieldwork during the inventory process. These results represent another example of the usefulness of employing DAP data in the forest inventory process previously documented by other researchers (Hawrylo, Tompalski, and Węzyk 2017; Tompalski et al. 2018; White et al. 2015).

The flexibility of the developed approach lies in the fact that not only ALS data but also field measurement data or UAV data can be used as a reference. Our approach allows for multi-source data fusion (sample plot, DAP, ALS, and UAV data), which in turn allows for TH growth modeling to be performed by using the developed TH time series (Tompalski et al. 2018). In Poland, multi-temporal DAP data are available for the whole country; however, this data coverage is not homogenous in time. The time gap between field data collection and image acquisition is very important, according to Price et al. (2020), with smaller gaps resulting in significantly better model performance despite smaller samples. The time lag is especially important when modeling over large areas, for which it is hard to capture data over short periods (Stepper, Straub, and Pretzsch 2015). By updating TH with growth models, we showed that this parameter can be determined for any period.

With our DAP and ALS data fusion approach, it is possible to observe growth patterns over shorter periods and thus take into consideration other factors that have an impact on forest growth. Specifically, stand height growth dynamics depend on multiple factors, which often change over short periods and are site-specific (Tymińska-Czabańska et al. 2021); they can be affected not only by weather conditions but also forest management treatments (Skovsgaard and Vanclay 2008; Tymińska-Czabańska, Hawrylo, and Socha 2022). By using multi-source data fusion, we can capture an appropriate, site-specific picture of TH growth. The advantage of using DAP images lies in the significantly lower acquisition costs compared with ALS images (Hawrylo, Tompalski, and Węzyk 2017). However, it should be noted that processing DAP data from large areas can be computationally demanding (Goodbody, Coops, and White 2019).

The variable accuracy of DAP data was highlighted in a study by Holopainen et al. (2015). For stands with a complex structure, the use of DAP data may lead to larger errors in height

determination. Therefore, the suitability of our method for this use case needs to be verified. Another limitation is that access to DAP data at national level is still a challenge. Campaigns should be coordinated nationally to obtain consistent data with the same parameters. In the future the space-borne sensors could be an alternative for the aerial data on a national level. However space-borne sensors are not accurate enough yet to calibrate local growth models. Products such as GEDI or ICESat-2 have a very high potential for global research. However, we need the accuracy of the TH estimate to be as close as possible to the actual value. A recent study comparing LiDAR and space-borne laser scanning shows that the RMSE of space-borne laser scanning is 6.10 m (Li et al. 2024). Another study compared ICESat-2, GEDI and high resolution LiDAR and shows height estimates, with RMSE and MAE of 7.49 and 4.64 m (ICESat-2) and 6.52 and 4.08 m (GEDI) for 98th percentile relative heights (Yu et al. 2024). This type of error can have a very significant impact on the accuracy of a model.

Accurate DAP growth models can support management decisions, such as thinning and harvesting schedules, to optimize forest productivity. Enhanced predictions of forest growth also enable long-term planning and helping managers to develop adaptive management strategies. In addition to the use of DAP data in modeling stand growth and productivity, their large availability for TH determination can be very useful for quantifying wood volume and biomass (Bontemps and Bouriaud 2014; Pretzsch 2009; Saarela et al. 2020; Weiskittel, Crookston, and Radtke 2011). In particular, developing local growth models and performing large-scale TH determination from DAP data allow for a more efficient and accurate assessment of the capacity of forests to sequester CO<sub>2</sub>, which is one of the challenges in modern forestry (Shukla et al. 2019; Smith et al. 2014).

## Conclusions

In this study, we demonstrated the high potential of DAP data in TH growth modeling by establishing a method whereby DAP-derived TH is corrected using reference ALS-derived TH. The novelty of this approach lies in the fact that the reference data can be collected in a different period from that of the DAP data. The developed approach assumes that the ALS-derived TH is updated to the year of DAP data collection by using a TH growth model, so that it can be used as a reference for the DAP-derived TH. We showed that the effectiveness of TH updating is independent of the growth model used, indicating that this parameter can be updated by using models that are not adapted to local growth conditions. We then showed that the TH derived from DAP data corrected by using the proposed approach is useful for developing appropriate local TH growth models. Therefore, the developed approach increases the potential for using DAP data to determine TH and stand growth, opening up new possibilities for the flexible and straightforward use of DAP data in forest management and growth modeling. In addition, the wide availability of DAP data for TH determination is conducive for quantifying wood volumes, biomass, and carbon sequestration.

## Acknowledgements

We thank the anonymous reviewers whose feedback helped to improve and clarify this manuscript.

## Data availability statement

Data available on request from the authors.

## Disclosure statement

No potential conflict of interest was reported by the author(s).

## Funding

This research was funded by General Directorate of State Forests in Poland under the project 'Rozbudowa metody inwentaryzacji urządzeniowej stanu lasu z wykorzystaniem efektów projektu REMBIOFOR' [Extension of the forest inventory method using the results of the REMBIOFOR project], contract no. EO.271.3.12.2019.

## References

- Achim, Alexis, Guillaume Moreau, Nicholas C Coops, Jodi N Axelson, Julie Barrette, Steve Bédard, Kenneth E Byrne, et al. 2022. "The Changing Culture of Silviculture." *Forestry: An International Journal of Forest Research* 95 (2): 143–152. <https://doi.org/10.1093/forestry/cpab047>.
- António, Nuno, Margarida Tomé, José Tomé, Paula Soares, and Luís Fontes. 2007. "Effect of Tree, Stand, and Site Variables on the Allometry of Eucalyptus Globulus Tree Biomass." *Canadian Journal of Forest Research* 37 (5): 895–906. <https://doi.org/10.1139/X06-276>.
- Bastin, Jean-François, Ervan Rutishauser, James R. Kellner, Sassan Saatchi, Raphael Pélassier, Bruno Hérault, Ferry Slik, et al. 2018. "Pan-Tropical Prediction of Forest Structure from the Largest Trees." *Global Ecology and Biogeography* 27 (11): 1366–1383. <https://doi.org/10.1111/geb.12803>.
- Bi, Huiquan, Yushan Long, John Turner, Yuancai Lei, Peter Snowdon, Yun Li, Richard Harper, Ayalsew Zerihun, and Fabiano Ximenes. 2010. "Additive Prediction of Aboveground Biomass for Pinus Radiata (D. Don) Plantations." *Forest Ecology and Management* 259 (12): 2301–2314. <https://doi.org/10.1016/j.foreco.2010.03.003>.
- Blanco Vaca, Juan Antonio, and Yueh-Hsin Lo Wong. 2023. "Latest Trends in Modelling Forest Ecosystems: New Approaches or Just New Methods?." *Current Forestry Reports* 9: 219–229. <https://doi.org/10.1007/s40725-023-00189-y>.
- Bontemps, Jean-Daniel, and Olivier Bouriaud. 2014. "Predictive Approaches to Forest Site Productivity: Recent Trends, Challenges and Future Perspectives." *Forestry* 87 (1): Oxford University Press: 109–128. <https://doi.org/10.1093/forestry/cpt034>.
- Core Team, R. 2021. *R: A Language and Environment for Statistical Computing [Computer Software]*. Vienna, Austria: R Foundation for Statistical Computing.
- Dandois, Jonathan P., and Erle C. Ellis. 2013. "High Spatial Resolution Three-Dimensional Mapping of Vegetation Spectral Dynamics Using Computer Vision." *Remote Sensing of Environment* 136:Elsevier: 259–276. <https://doi.org/10.1016/j.rse.2013.04.005>.
- Goodbody, Tristan R. H., Nicholas C. Coops, and Joanne C. White. 2019. "Digital Aerial Photogrammetry for Updating Area-Based Forest Inventories: A Review of Opportunities, Challenges, and Future Directions." *Current Forestry Reports* 5 (2): 55–75. <https://doi.org/10.1007/s40725-019-00087-2>.
- Guerra-Hernández, Juan, Diogo N. Cosenza, Luiz Carlos Estraviz Rodriguez, Margarida Silva, Margarida Tomé, Ramón A. Díaz-Varela, and Eduardo González-Ferreiro. 2018. "Comparison of ALS-and UAV (SfM)-Derived High-Density Point Clouds for Individual Tree Detection in Eucalyptus Plantations." *International Journal of Remote Sensing* 39 (15–16): Taylor & Francis: 5211–5235. <https://doi.org/10.1080/01431161.2018.1486519>.
- Hartley, Robin JL, Ellen Mae Leonardo, Peter Massam, Michael S. Watt, Honey Jane Estarija, Liam Wright, Nathanael Melia, and Grant D. Pearse. 2020. "An Assessment of High-Density UAV Point Clouds for the Measurement of Young Forestry Trials." *Remote Sensing* 12 (24): MDPI: 4039. <https://doi.org/10.3390/rs12244039>.
- Hawrylo, Paweł, Jarosław Socha, Piotr Wężyk, Wojciech Ochał, Wojciech Krawczyk, Jakub Miszczyk, and Luiza Tymińska-Czabańska. 2024. "How to Adequately Determine the Top Height of Forest Stands Based on Airborne Laser Scanning Point Clouds?" *Forest Ecology and Management* 551 (January): 121528. <https://doi.org/10.1016/j.foreco.2023.121528>.
- Hawrylo, Paweł, Piotr Tompalski, and Piotr Wężyk. 2017. "Area-Based Estimation of Growing Stock Volume in Scots Pine Stands Using ALS and Airborne Image-Based Point Clouds." *Forestry: An International Journal of Forest Research* 90 (5): 686–696. <https://doi.org/10.1093/forestry/cpx026>.
- Holopainen, M., M. Vastaranta, M. Karjalainen, K. Karila, S. Kaasalainen, E. Honkavaara, and J. Hyppä. 2015. "Forest Inventory Attribute Estimation Using Airborne Laser Scanning, Aerial Stereophotogrammetry, Radargrammetry and Interferometry-Finnish Experiences of the 3D Techniques." *ISPRS Annals of the Photogrammetry, Remote Sensing and Spatial Information Sciences* 2:63–69. <https://doi.org/10.5194/isprsaannals-II-3-W4-63-2015>.
- Iglhaut, Jakob, Carlos Cabo, Stefano Puliti, Livia Piermattei, James O'Connor, and Jacqueline Rosette. 2019. "Structure from Motion Photogrammetry in Forestry: A Review." *Current Forestry Reports* 5 (3): 155–168. <https://doi.org/10.1007/s40725-019-00094-3>.
- Janiec, Piotr, Luiza Tymińska-Czabańska, Paweł Hawrylo, and Jarosław Socha. 2023. "Development of Regional Height Growth Model for Scots Pine Using Repeated Airborne Laser Scanning Data." *Frontiers in Environmental Science* 11), <https://www.frontiersin.org/articles/10.3389/fenvs.2023.1260725>.
- Jensen, Jennifer L. R., and Adam J. Mathews. 2016. "Assessment of Image-Based Point Cloud Products to Generate a Bare Earth Surface and Estimate Canopy Heights in a Woodland Ecosystem." *Remote Sensing* 8 (1): Multidisciplinary Digital Publishing Institute: 50. <https://doi.org/10.3390/rs8010050>.

- Jurjević, Luka, Xinlian Liang, Mateo Gašparović, and Ivan Balenović. 2020. "Is Field-Measured Tree Height as Reliable as Believed – Part II, A Comparison Study of Tree Height Estimates from Conventional Field Measurement and Low-Cost Close-Range Remote Sensing in a Deciduous Forest." *ISPRS Journal of Photogrammetry and Remote Sensing* 169 (November): 227–241. <https://doi.org/10.1016/j.isprsjprs.2020.09.014>.
- Li, Hantao, Xiaoxuan Li, Tomomichi Kato, Masato Hayashi, Junjie Fu, and Takuwa Hiroshima. 2024. "Accuracy Assessment of GEDI Terrain Elevation, Canopy Height, and Aboveground Biomass Density Estimates in Japanese Artificial Forests." *Science of Remote Sensing* 10 (December): 100144. <https://doi.org/10.1016/j.srs.2024.100144>.
- Marziliano, Pasquale A., Roberto Tognetti, and Fabio Lombardi. 2019. "Is Tree Age or Tree Size Reducing Height Increment in Abies Alba Mill. at Its Southernmost Distribution Limit?" *Annals of Forest Science* 76 (1): BioMed Central: 1–12. <https://doi.org/10.1007/s13595-018-0784-9>.
- Mensah, Alex Appiah, Emma Holmström, Hans Petersson, Kenneth Nyström, Euan G. Mason, and Urban Nilsson. 2021. "The Millennium Shift: Investigating the Relationship Between Environment and Growth Trends of Norway Spruce and Scots Pine in Northern Europe." *Forest Ecology and Management* 481:Elsevier: 118727. <https://doi.org/10.1016/j.foreco.2020.118727>.
- Mielcarek, Miłosz, Agnieszka Kamińska, and Krzysztof Stereńczak. 2020. "Digital Aerial Photogrammetry (DAP) and Airborne Laser Scanning (ALS) as Sources of Information About Tree Height: Comparisons of the Accuracy of Remote Sensing Methods for Tree Height Estimation." *Remote Sensing* 12 (11): Multidisciplinary Digital Publishing Institute: 1808. <https://doi.org/10.3390/rs12111808>.
- Moré, J. J.. 1978. "The Levenberg-Marquardt algorithm: implementation and theory." In *Numerical analysis. Lecture Notes in Mathematics*. Vol. 630, edited by G. A. Watson, 105–116. Berlin, Heidelberg: Springer. <https://doi.org/10.1007/BFb0067700>.
- Prado, Diego Rodriguez de, Aitor Vázquez Veloso, Yun Fan Quian, Irene Ruano, Felipe Bravo, and Celia Herrero de Aza. 2022. "Can Mixed Forests Sequester More CO<sub>2</sub> Than Pure Forests in Future Climate Scenarios? A Case Study of Pinus Sylvestris Combinations in Spain." *European Journal of Forest Research*, Springer Berlin Heidelberg. <https://doi.org/10.1007/s10342-022-01507-y>.
- Pretzsch, Hans. 2009. "Forest Dynamics, Growth, and Yield." In *Forest Dynamics, Growth and Yield: From Measurement to Model*, edited by Hans Pretzsch, 1–39. Berlin, Heidelberg: Springer. [https://doi.org/10.1007/978-3-540-88307-4\\_1](https://doi.org/10.1007/978-3-540-88307-4_1).
- Pretzsch, Hans, Peter Biber, Gerhard Schütze, Enno Uhl, and Thomas Rötzer. 2014. "Forest Stand Growth Dynamics in Central Europe Have Accelerated Since 1870." *Nature Communications* 5 (1): Nature Publishing Group UK London: 4967. <https://doi.org/10.1038/ncomms5967>.
- Price, Bronwyn, Lars T. Waser, Zuyuan Wang, Mauro Marty, Christian Ginzler, and Florian Zellweger. 2020. "Predicting Biomass Dynamics at the National Extent from Digital Aerial Photogrammetry." *International Journal of Applied Earth Observation and Geoinformation* 90 (August): 102116. <https://doi.org/10.1016/j.jag.2020.102116>.
- Rennolls, Keith. 1978. "'Top Height'; Its Definition and Estimation." *The Commonwealth Forestry Review* 57 (3 (173)): Commonwealth Forestry Association: 215–219. <https://www.jstor.org/stable/42607466>.
- Roussel, Jean-Romain, David Auty, Nicholas C. Coops, Piotr Tompalski, Tristan RH Goodbody, Andrew Sánchez Meador, Jean-François Bourdon, Florian De Boissieu, and Alexis Achim. 2020. "lidR: An R Package for Analysis of Airborne Laser Scanning (ALS) Data." *Remote Sensing of Environment* 251, Elsevier: 112061. <https://doi.org/10.1016/j.rse.2020.112061>.
- Saarela, Svetlana, André Wästlund, Emma Holmström, Alex Appiah Mensah, Sören Holm, Mats Nilsson, Jonas Fridman, and Göran Ståhl. 2020. "Mapping Aboveground Biomass and Its Prediction Uncertainty Using LiDAR and Field Data, Accounting for Tree-Level Allometric and LiDAR Model Errors." *Forest Ecosystems* 7 (1): 43. <https://doi.org/10.1186/s40663-020-00245-0>.
- Sharma, Mahadev, Ralph L. Amateis, and Harold E. Burkhardt. 2002. "Top Height Definition and Its Effect on Site Index Determination in Thinned and Unthinned Loblolly Pine Plantations." *Forest Ecology and Management* 168:163–175. [https://doi.org/10.1016/S0378-1127\(01\)00737-X](https://doi.org/10.1016/S0378-1127(01)00737-X).
- Shukla, Priyadarshi R., Jim Skea, E. Calvo Buendia, Valérie Masson-Delmotte, Hans Otto Pörtner, D. C. Roberts, Panmao Zhai, Raphael Slade, Sarah Connors, and Renée Van Diemen. 2019. "IPCC, 2019: Climate Change and Land: An IPCC Special Report on Climate Change, Desertification, Land Degradation, Sustainable Land Management, Food Security, and Greenhouse Gas Fluxes in Terrestrial Ecosystems." *Intergovernmental Panel on Climate Change (IPCC)*.
- Sibona, E., A. Vitali, F. Meloni, L. Caffo, A. Dotta, E. Lingua, R. Motta, and M. Garbarino. 2017. "Direct measurement of tree height provides different results on the assessment of LiDAR accuracy." *Forests* 8 (1): 7. <https://doi.org/10.3390/f8010007>.
- Skovsgaard, J. P., and Jerome K. Vanclay. 2008. "Forest Site Productivity: A Review of the Evolution of Dendrometric Concepts for Even-Aged Stands." *Forestry: An International Journal of Forest Research* 81 (1): Oxford University Press: 13–31. <https://doi.org/10.1093/forestry/cpm041>.

- Smith, Pete, Mercedes Bustamante, Helal Ahammad, Harry Clark, Hongmin Dong, Elnour A. Elsiddig, Helmut Haberl, Richard Harper, Joanna House, and Mostafa Jafari. 2014. "Agriculture, Forestry and Other Land Use (AFOLU)." In *Climate Change 2014: Mitigation of Climate Change. Contribution of Working Group III to the Fifth Assessment Report of the Intergovernmental Panel on Climate Change*, 811–922. Cambridge: Cambridge University Press.
- Socha, Jarosław, Paweł Hawryło, Krzysztof Stereńczak, Stanisław Miścicki, Luiza Tymińska-Czabańska, Wojciech Młoczek, and Piotr Gruba. 2020. "Assessing the Sensitivity of Site Index Models Developed Using Bi-Temporal Airborne Laser Scanning Data to Different Top Height Estimates and Grid Cell Sizes." *International Journal of Applied Earth Observation and Geoinformation* 91 (September): 102129. <https://doi.org/10.1016/j.jag.2020.102129>.
- Socha, Jarosław, Marcin Pierzchalski, Radomir Bałazy, and Mariusz Ciesielski. 2017. "Modelling Top Height Growth and Site Index Using Repeated Laser Scanning Data." *Forest Ecology and Management* 406:Elsevier: 307–317. <https://doi.org/10.1016/j.foreco.2017.09.039>.
- Socha, Jarosław, and Luiza Tymińska-Czabańska. 2019. "A Method for the Development of Dynamic Site Index Models Using Height-Age Data from Temporal Sample Plots." *Forests* 10 (7): MDPI: 542. <https://doi.org/10.3390/f10070542>.
- Socha, Jarosław, Luiza Tymińska-Czabańska, Karol Bronisz, Stanisław Zięba, and Paweł Hawryło. 2021. "Regional Height Growth Models for Scots Pine in Poland." *Scientific Reports* 11 (1): Springer: 1–14. <https://doi.org/10.1038/s41598-020-79139-8>.
- Stepper, Christoph, Christoph Straub, and Hans Pretzsch. 2015. "Assessing Height Changes in a Highly Structured Forest Using Regularly Acquired Aerial Image Data." *Forestry: An International Journal of Forest Research* 88 (3): 304–316. <https://doi.org/10.1093/forestry/cpu050>.
- Straub, Christoph, Christoph Stepper, Rudolf Seitz, and Lars T. Waser. 2013. "Potential of UltraCamX Stereo Images for Estimating Timber Volume and Basal Area at the Plot Level in Mixed European Forests." *Canadian Journal of Forest Research* 43 (8): NRC Research Press: 731–741. <https://doi.org/10.1139/cjfr-2013-0125>.
- Swinfield, Tom, Jeremy A. Lindsell, Jonathan V. Williams, Rhett D. Harrison, Habibi Agustiono, Elva Gemita, Carola B. Schönlieb, and David A. Coomes. 2019. "Accurate Measurement of Tropical Forest Canopy Heights and Aboveground Carbon Using Structure from Motion." *Remote Sensing* 11 (8): Multidisciplinary Digital Publishing Institute: 928. <https://doi.org/10.3390/rs11080928>.
- Tompalski, Piotr, Nicholas C. Coops, Peter L. Marshall, Joanne C. White, Michael A. Wulder, and Todd Bailey. 2018. "Combining Multi-Date Airborne Laser Scanning and Digital Aerial Photogrammetric Data for Forest Growth and Yield Modelling." *Remote Sensing* 10 (2): Multidisciplinary Digital Publishing Institute: 347. <https://doi.org/10.3390/rs10020347>.
- Tompalski, Piotr, Nicholas C. Coops, Joanne C. White, Tristan RH Goodbody, Chris R. Hennigar, Michael A. Wulder, Jarosław Socha, and Murray E. Woods. 2021. "Estimating Changes in Forest Attributes and Enhancing Growth Projections: A Review of Existing Approaches and Future Directions Using Airborne 3D Point Cloud Data." *Current Forestry Reports* 7 (1): Springer: 1–24. <https://doi.org/10.1007/s40725-021-00135-w>.
- Tompalski, Piotr, Nicholas C. Coops, Joanne C. White, and Michael A. Wulder. 2015. "Augmenting Site Index Estimation with Airborne Laser Scanning Data." *Forest Science* 61 (5): Oxford University Press Oxford, UK: 861–873. <https://doi.org/10.5849/forsci.14-175>.
- Tukey, J. W. 1977. *Exploratory Data Analysis*. Reading, MA: Addison-Wesley.
- Turner, Darren, Arko Lucieer, and Luke Wallace. 2013. "Direct Georeferencing of Ultrahigh-Resolution UAV Imagery." *IEEE Transactions on Geoscience and Remote Sensing* 52 (5): IEEE: 2738–2745. <https://doi.org/10.1109/TGRS.2013.2265295>.
- Turner, Darren, Arko Lucieer, and Christopher Watson. 2012. "An Automated Technique for Generating Georectified Mosaics from Ultra-High Resolution Unmanned Aerial Vehicle (UAV) Imagery, Based on Structure from Motion (SfM) Point Clouds." *Remote Sensing* 4 (5): Molecular Diversity Preservation International: 1392–1410. <https://doi.org/10.3390/rs4051392>.
- Tymińska-Czabańska, Luiza, Paweł Hawryło, and Jarosław Socha. 2022. "Assessment of the Effect of Stand Density on the Height Growth of Scots Pine Using Repeated ALS Data." *International Journal of Applied Earth Observation and Geoinformation* 108:Elsevier: 102763. <https://doi.org/10.1016/j.jag.2022.102763>.
- Tymińska-Czabańska, Luiza, Jarosław Socha, Paweł Hawryło, Radomir Bałazy, Mariusz Ciesielski, Ewa Grabska-Szwagrzyk, and Paweł Netzel. 2021. "Weather-Sensitive Height Growth Modelling of Norway Spruce Using Repeated Airborne Laser Scanning Data." *Agricultural and Forest Meteorology* 308:Elsevier: 108568. <https://doi.org/10.1016/j.agrformet.2021.108568>.
- Vanninen, Petteri, Hanna Ylitalo, Risto Sievänen, and Annikki Mäkelä. 1996. "Effects of Age and Site Quality on the Distribution of Biomass in Scots Pine (*Pinus Sylvestris L.*)."*Trees* 10 (4): 231–238. <https://doi.org/10.1007/BF02185674>.
- Wallace, Luke, Arko Lucieer, Zbyněk Malenovský, Darren Turner, and Petr Vopěnka. 2016. "Assessment of Forest Structure Using Two UAV Techniques: A Comparison of Airborne Laser Scanning and Structure from Motion (SfM) Point Clouds." *Forests* 7 (3): Multidisciplinary Digital Publishing Institute: 62. <https://doi.org/10.3390/f7030062>.

- Wang, Yunsheng, Matti Lehtomäki, Xinlian Liang, Jiri Pyörälä, Antero Kukko, Anttoni Jaakkola, Jingbin Liu, Ziyi Feng, Ruizhi Chen, and Juha Hyppä. 2019. "Is Field-Measured Tree Height as Reliable as Believed—A Comparison Study of Tree Height Estimates from Field Measurement, Airborne Laser Scanning and Terrestrial Laser Scanning in a Boreal Forest." *ISPRS Journal of Photogrammetry and Remote Sensing* 147:Elsevier: 132–145. <https://doi.org/10.1016/j.isprsjprs.2018.11.008>.
- Weiskittel, Aaron R., Nicholas L. Crookston, and Philip J. Radtke. 2011. "Linking Climate, Gross Primary Productivity, and Site Index Across Forests of the Western United States." *Canadian Journal of Forest Research* 41 (8): 1710–1721. <https://doi.org/10.1139/x11-086>.
- White, Joanne C., Christoph Stepper, Piotr Tompalski, Nicholas C. Coops, and Michael A. Wulder. 2015. "Comparing ALS and Image-Based Point Cloud Metrics and Modelled Forest Inventory Attributes in a Complex Coastal Forest Environment." *Forests* 6 (10): Multidisciplinary Digital Publishing Institute: 3704–3732. <https://doi.org/10.3390/f6103704>.
- White, Joanne C., Michael A. Wulder, Mikko Vastaranta, Nicholas C. Coops, Doug Pitt, and Murray Woods. 2013. "The Utility of Image-Based Point Clouds for Forest Inventory: A Comparison with Airborne Laser Scanning." *Forests* 4 (3): Multidisciplinary Digital Publishing Institute: 518–536. <https://doi.org/10.3390/f4030518>.
- Yu, Qiuyan, Michael G. Ryan, Wenjie Ji, Lara Prihodko, Julius Y. Anchang, Njoki Kahiu, Abid Nazir, Jingyu Dai, and Niall P. Hanan. 2024. "Assessing Canopy Height Measurements from ICESat-2 and GEDI Orbiting LiDAR Across Six Different Biomes with G-LiHT LiDAR." *Environmental Research: Ecology* 3 (2): IOP Publishing: 025001. <https://doi.org/10.1088/2752-664X/ad39f2>.
- Zhou, Mengli, Xiangdong Lei, Guangshuang Duan, Jun Lu, and Huiru Zhang. 2019. "The Effect of the Calculation Method, Plot Size, and Stand Density on the Top Height Estimation in Natural Spruce-Fir-Broadleaf Mixed Forests." *Forest Ecology and Management* 453 (December): 117574. <https://doi.org/10.1016/j.foreco.2019.117574>.
- Zielony, Roman, and Anna Kliczkowska. 2012. *Regionalizacja Przyrodniczo-Lleśna Polski* 2010. Centrum Informacyjne Lasów Państwowych.

## Oświadczenie udziałów procentowych w publikacji

Janiec, P., Tymińska-Czabańska, L., Hawryło, P., & Socha, J. (2023). Development of regional height growth model for Scots pine using repeated airborne laser scanning data. *Frontiers in Environmental Science*, 11, 1260725. <https://doi.org/10.3389/fenvs.2023.1260725>

1. Piotr Janiec 70%
2. Luiza Tymińska-Czabańska 10%
3. Paweł Hawryło 10%
4. Jarosław Socha 10%

## Oświadczenie udziałów procentowych w publikacji

Janiec, P., Hawryło, P., Tymińska-Czabańska, L., Miszczyżyn, J., & Socha, J. (2024). A low-cost alternative to LiDAR for site index models: applying repeated digital aerial photogrammetry data in the modelling of forest top height growth. *Forestry: An International Journal of Forest Research*, cpae047. <https://doi.org/10.1093/forestry/cpae047>

- |                             |     |
|-----------------------------|-----|
| 1. Piotr Janiec             | 70% |
| 2. Paweł Hawryło            | 10% |
| 3. Luiza Tymińska-Czabańska | 5%  |
| 4. Jakub Miszczyżyn         | 5%  |
| 5. Jarosław Socha           | 10% |

## Oświadczenie udziałów procentowych w publikacji

Janiec, P., Hawryło, P., Tymińska-Czabańska, L., Polak, M., & Socha, J. (2024). Digital aerial photogrammetry as a spatial and temporal extension of ALS in forest height growth modeling. International Journal of Digital Earth, 17(1), 2418879.  
<https://doi.org/10.1080/17538947.2024.2418879>

1. Piotr Janiec 70%
2. Paweł Hawryło 5%
3. Luiza Tymińska-Czabańska 10%
4. Marcin Polak 5%
5. Jarosław Socha 10%